

UC Berkeley

UC Berkeley Electronic Theses and Dissertations

Title

Functional Brain Network Organization Supporting Executive Control Processing

Permalink

<https://escholarship.org/uc/item/3q57d3n2>

Author

Gallen, Courtney Leigh

Publication Date

2016

Peer reviewed|Thesis/dissertation

Functional Brain Network Organization Supporting Executive Control Processing

by

Courtney Leigh Gallen

A dissertation submitted in partial satisfaction of the

requirements for the degree of

Doctor of Philosophy

in

Neuroscience

in the

Graduate Division

of the

University of California, Berkeley

Committee in charge:

Professor Mark D'Esposito, Chair

Professor William Jagust

Professor Michael Silver

Professor William Satariano

Summer 2016

Abstract

Functional Brain Network Organization Supporting Executive Control Processing

by

Courtney Leigh Gallen

Doctor of Philosophy in Neuroscience

University of California, Berkeley

Professor Mark D'Esposito, Chair

Executive control comprises a set of neural processes that are critical for goal-directed behaviors, such as attention and working memory. Such complex behaviors likely rely on the flexible communication within and between brain sub-networks, or modules. In this thesis, I present several projects that use graph theoretical methods to describe the brain as a complex network and examine the role of brain network organization in supporting aspects of executive control processing. Across these projects, I use a variety of methods, such as functional magnetic resonance imaging (fMRI), functional connectivity, and cognitive training.

The first chapter of this thesis examines the influence of attention demands on brain network organization. Here, I show that brain network modules become more integrated during the processing of relevant stimuli compared with the processing of irrelevant distractors during a working memory N-back task. The strength of this reconfiguration is related to faster task performance, suggesting its importance in executive control.

The second chapter of this thesis examines the influence of aging on reconfiguration of brain networks due to executive control (i.e., N-back load) demands. Here, I demonstrate that older adults exhibit changes in brain network organization at lower levels of demand compared with young adults. Further, brain network reconfiguration from a task-free 'resting-state' to an N-back task is related to better task performance and greater structural connectivity of a core frontal-posterior white matter tract.

The final two chapters of this thesis examine how brain network organization can predict gains in executive control processing after cognitive interventions. The first project shows that the extent of segregation of brain network modules (i.e., higher network modularity) is predictive of greater training-related cognitive gains in older adults. The second project extends this predictive framework to healthy young adults.

In sum, these projects demonstrate that brain networks flexibly reconfigure depending on executive control demands and that aspects of brain networks are predictive of training-related gains of executive control. These findings provide insight into how properties of large-scale brain networks allow for executive control processing.

Table of Contents

CHAPTER 1	1
CHAPTER 2	4
2.1 ABSTRACT	4
2.2 INTRODUCTION	4
2.3 MATERIALS AND METHODS	6
2.4 RESULTS	10
2.5 DISCUSSION	17
CHAPTER 3	19
3.1 ABSTRACT	19
3.2 INTRODUCTION	19
3.3 MATERIALS AND METHODS	20
3.4 RESULTS	26
3.5 DISCUSSION	33
3.6 SUPPLEMENTAL MATERIAL	39
CHAPTER 4	41
4.1 ABSTRACT	41
4.2 INTRODUCTION	41
4.3 MATERIALS AND METHODS	42
4.4 RESULTS	44
4.5 DISCUSSION	50
CHAPTER 5	52
5.1 ABSTRACT	52
5.2 INTRODUCTION	52
5.3 MATERIALS AND METHODS	54
5.4 RESULTS	60
5.5 DISCUSSION	67
CHAPTER 6	71
REFERENCES	73

Acknowledgements

This work would not have been possible without the support of the D'Esposito lab, especially from my graduate adviser, Mark D'Esposito, who been an amazing mentor over the past five years. I'd also like to thank my officemates past and present, Elizabeth Lorenc, Caterina Gratton, and Maxwell Bertolero, for making the lab an even more fun workplace. My collaborators on these projects, especially Pauline Baniqued, Gary Turner, Areeba Adnan, and the group at the UT Dallas Center for BrainHealth, have also provided invaluable guidance on these projects. I'd also like to thank the other members of my dissertation committee, Bill Jagust, Michael Silver, and Bill Satariano, for helping me grow as a scientist. Finally, I'd like to thank my friends and family, especially my dad, brother, and Kevin Mann, for their incredible encouragement during my time at Berkeley.

Chapter 1

INTRODUCTION

Aspects of executive control processing, such as attention and working memory, are critical for guiding goal-directed behavior. It is thought that these and other complex behaviors rely on communication between groups of brain regions or brain sub-networks (Mattar et al., 2015; Medaglia et al., 2015). Graph theoretical tools can be used to describe the brain as a complex network that is comprised of such sub-networks, or modules. Analyses of structural MRI and resting-state fMRI data have found that the brain exhibits a modular organization (Sporns and Betzel, 2015), where highly modular networks have dense connections within, and sparse connections between, modules (Newman and Girvan, 2004). It is thought that this type of network organization allows for segregated processing of specialized behaviors within modules and integrated processing of complex behaviors across modules (Meunier et al., 2009b).

While functional brain networks exhibit modular organization during task-free resting-states, there is growing evidence that this type of organization is flexible and reconfigures due to varying executive control demands (Kitzbichler et al., 2011; Stanley et al., 2014; Liang et al., 2015; Vatansever et al., 2015; Wen et al., 2015). Specifically, higher working memory demands (e.g., increasing N-back load) are associated with increased connectivity between network modules, thus decreasing their segregation or the 'modularity' of the network. Further, participants exhibiting greater network reconfiguration with increasing demands perform faster (Kitzbichler et al., 2011; Vatansever et al., 2015). This pattern of reconfiguration due to varying executive control demands has been interpreted to represent the formation of a global neuronal 'workspace' (Dehaene et al., 1998) in which greater cognitive effort is supported by increased communication between network modules.

However, the majority of these previous studies have examined reconfiguration that occurs across entire task blocks with varying cognitive demands and has not examined more rapid changes in network properties that can occur on an individual-trial basis due to changing task goals. The first project in this dissertation examined changes in network properties that occur during an N-back task with intervening distracting stimuli (Gallen et al., in preparation). I found that brain networks exhibit decreased modularity selectively to relevant stimuli compared to distractors. Moreover, the extent of this reconfiguration was related to faster task performance. These results suggest that brain networks can flexibly adopt a less modular, 'workspace', organization to guide behavior, depending on changing attention demands during working memory.

In addition to reconfiguration due to cognitive demands, there is evidence that aging is associated with changes in the modular organization of the brain. Several studies of structural and functional brain networks have shown that older adults have less modular brain networks than young adults (Meunier et al., 2009a; Chen et al., 2011b; Onoda and Yamaguchi, 2013; Chan et al., 2014; Geerligs et al., 2014a), which is thought to reflect decreased segregation, or integrity, of brain network modules in aging. Despite this, the

majority of these studies have examined age-related changes in network properties in the absence of a task. As aging is associated with declines in executive control properties like working memory (Park et al., 2002; Grady, 2008; 2012), it is important to also examine how brain networks reconfigure during cognitive processing in older adults. The second project in this dissertation examined how aging alters the reconfiguration of brain networks due to working memory demands (Gallen et al., 2016). I found that, while young adults exhibit network reconfiguration between a task-free resting state and the most demanding N-back condition, older adults also exhibited this pattern of reconfiguration at lower levels of demand. In older adults, network reconfiguration was related to greater connectivity of a frontal-posterior white matter tract and faster task performance, suggesting that it is important for supporting executive processing in aging.

While aging is associated with declines in various aspects of cognition, there is also evidence that these declines are not immutable. Previous studies have shown that interventions aimed to improve aspects of executive control processing can enhance functioning and underlying functional connectivity between brain regions in older adults (Chapman et al., 2015; Cao et al., 2016). However, while there is often variability in training responses across individuals, relatively few studies have examined neural predictors of training-related gains in older adults. One previous study in patients with traumatic brain injury (TBI) found that individuals with more modular brain networks during a task-free resting-state exhibited greater training-related gains in aspects of executive control processing (Arnemann et al., 2015). In the final two projects in this dissertation, I examined whether this predictive framework could be extended to healthy populations, namely older and young adults. In the first of these projects (**Ch. 4**), I found that older adults who had more modular brain networks exhibited greater training-related gains in aspects of strategic reasoning, particularly in sub-networks thought to mediate 'associative' functions compared with those involved in sensory-motor processing (Gallen et al., submitted). In the second project (**Ch. 5**), we found a similar relationship between pre-training network modularity and training-related gains in attention in a group of young adults (Baniqued, Gallen et al., in preparation). The findings of these two projects suggest that brain network modularity may be a unifying biomarker that can predict training-related outcomes across a variety of interventions and populations.

Together, these projects provide evidence for the importance of functional brain network organization in successful executive control processing. Reconfiguration of brain networks due to varying cognitive demands supports behavioral performance in both young and older adults. Further, properties of brain networks during a task-free resting-state can be used to index gains in executive control after cognitive interventions. The results of these studies add to evidence that examination of functional brain networks is critical for understanding complex behavior.

Dissertation Outline

- Ch. 2: Effects of attention on brain network organization during working memory (Gallen et al., in preparation)
- Ch. 3: Reconfiguration of brain networks to support executive control in aging (Gallen et al., 2016)
- Ch. 4: Brain network predictors of training-related cognitive gains in older adults (Gallen et al., submitted)
- Ch. 5: Brain network predictors of training-related cognitive gains in young adults (Baniqued, Gallen et al., in preparation)

Chapter 2

INFLUENCE OF SELECTIVE ATTENTION ON BRAIN NETWORK RECONFIGURATION DURING WORKING MEMORY

2.1 Abstract

Selective attention underlies our ability to attend relevant stimuli while ignoring irrelevant stimuli, a critical process for prioritizing information in working memory. Prior work has shown that visual cortical areas are modulated by attention demands during working memory; however, it is not yet understood how large-scale brain networks reconfigure between the processing of relevant versus irrelevant information in the service of working memory. Here, we investigated the effects of selective attention on brain network structure during working memory performance. Using task-related functional connectivity and graph theoretical measures, we quantified changes in network modularity, a measure of the integrity of modular network organization, that occurred depending on task conditions. Network modularity was reduced while subjects were engaged in a 1-back condition with varying attention demands compared to a baseline condition. Further, during the 1-back trials, network modularity was selectively reduced during the processing of relevant stimuli compared to irrelevant stimuli. This effect was strongest in default mode and visual sub-networks or modules. Finally, greater changes in network modularity between processing relevant versus irrelevant stimuli were related to more rapid task performance for relevant stimuli. These results suggest that brain networks reconfigure while attending relevant stimuli to adopt a more globally distributed organization in which there is greater communication between modules. More integration between network modules for attended stimuli supports better working memory performance.

2.2 Introduction

Goal-directed behavior is critical for guiding our actions within the capacity limitations of the brain. Selective attention enables us to focus on relevant information in the environment while ignoring distracting information, and it influences the perception and maintenance of information in working memory. Not surprisingly, a large body of work suggests that selective attention and working memory are intimately related (Gazzaley and Nobre, 2012). Varying selective attention demands have been shown to influence the activity of sensory cortical regions important for stimulus processing. Stimulus-selective regions show increased activity when attending relevant information and decreased activity when ignoring irrelevant information (Gazzaley et al., 2005a; Gazzaley, 2011). These effects are not thought to be a property of sensory regions per se, but are instead guided by top-down modulatory connections from prefrontal and parietal control areas. Using task-based functional connectivity analyses (Rissman et al., 2004), regions of prefrontal cortex have been shown to be more connected to

scene-selective sensory regions when scenes were attended and less connected when scenes were ignored during the encoding phase of a working memory task (Gazzaley et al., 2007). Further work has aimed to characterize the connectivity changes between brain sub-networks and sensory regions depending on task goals. Visual regions were more connected with prefrontal and parietal cortex during the processing of relevant stimuli and were more connected to regions of the default mode network during the processing of irrelevant stimuli (Chadick and Gazzaley, 2011), suggesting that sensory regions are differentially connected with brain sub-networks depending on task goals. In line with this work, it is thought that the effects of attention on goal-directed behavior, such as working memory, emerge from the interactions between multiple brain regions or distributed brain networks (Buschman and Kastner, 2015). However, the interactions among large-scale brain networks during varying attention demands during working memory have not been fully examined.

Communication among brain sub-networks can be quantified with graph theoretical tools that model the brain as a complex network comprised of separable sub-networks or modules. Modular network organization is thought to be important for guiding behavior in that it enables local processing within modules for more specialized functions and global processing between modules for more complex functions (Meunier et al., 2009b; 2010). The integrity of modular network organization can be quantified with a modularity metric—highly modular networks have dense connections within modules and sparser connections between modules.

Neuroimaging studies have shown that the brain exhibits a modular organization in terms of both structural connections and functional connections measured during task-free resting states (Sporns and Betzel, 2015). There has also been a recent effort to examine how this modular organization changes during task performance, particularly working memory tasks. Work using N-back tasks has shown that the modular network structure of the brain is affected by increasing task demands (i.e., N-back load) (Kitzbichler et al., 2011; Braun et al., 2015; Vatansever et al., 2015; Wen et al., 2015). In more demanding N-back conditions, brain networks exhibit decreased modularity, which is thought to reflect increased integration between network modules to support increased cognitive demands (Kitzbichler et al., 2011; Vatansever et al., 2015; Wen et al., 2015). Other task-based fMRI studies have also highlighted the behavioral importance of network modularity, such as auditory perception (Sadaghiani et al., 2015) and visual awareness (Godwin et al., 2015).

Building on this previous work, we here sought to use task-related functional connectivity analyses (Rissman et al., 2004) to investigate how the modular organization of the brain changes with varying attention during working memory performance. Using a 1-back task with high selective attention demands and a comparison 0-back condition, we first examined how brain modularity is altered with task condition. We next examined how modularity fluctuates throughout the duration of a task condition depending on whether the stimuli are relevant or irrelevant. Finally, we examined how the reconfiguration of modularity with differing task goals is related to performance.

2.3 Materials and Methods

2.3.1 Participants

75 healthy young adults (49 females; age range = 18-38, three subjects over 30 years old) recruited for six separate studies were included in this analysis. Participants were screened to exclude those with any history of neurologic or psychiatric disorders, or, for Study 3, abnormal or infrequent menstrual cycles or use of a hormonal birth control. Informed consent was obtained from participants in accordance with the Committee for the Protection of Human Subjects at the University of California, Berkeley.

We included participants with a minimum of four blocks for each cognitive task condition (see below). This resulted in 26 subjects from Study 1, 10 subjects from Study 2, 11 subjects from Study 3, 15 subjects from Study 4, 5 subjects from Study 5, and 8 subjects from Study 6.

2.3.2 Cognitive task

The cognitive task performed during fMRI scanning was an N-back task for faces and scenes that consisted of either 16 (N = 17 participants) or 20 (N = 58 participants) blocks lasting approximately two minutes each (Figure 2.1). Separate analyses using this cognitive task have been previously published for Studies 1-4 (Lee and D'Esposito, 2012; Cohen et al., 2014). Each task block contained 20 trials of consecutively presented face and scene stimuli (10 of each) during which participants were instructed to either attend to and remember images from the relevant stimulus category, while ignoring images from the irrelevant category, or to attend both categories. Each stimulus was presented for 600 ms, with a 2.4, 4.4, or 6.4 s jittered delay (randomly ordered) between each stimulus presentation. The four conditions varied working memory and selective attention demands and were referred to as: 'Categorize,' 'Select Scenes,' 'Select Faces,' and 'Select Both.' As we were interested in the processing of relevant and irrelevant stimuli, we focused on analyzing data from the Select Scenes and Select Faces conditions and included data from Categorize as a baseline comparison condition. Data from the Select Both condition was not included in our task-related functional connectivity analyses.

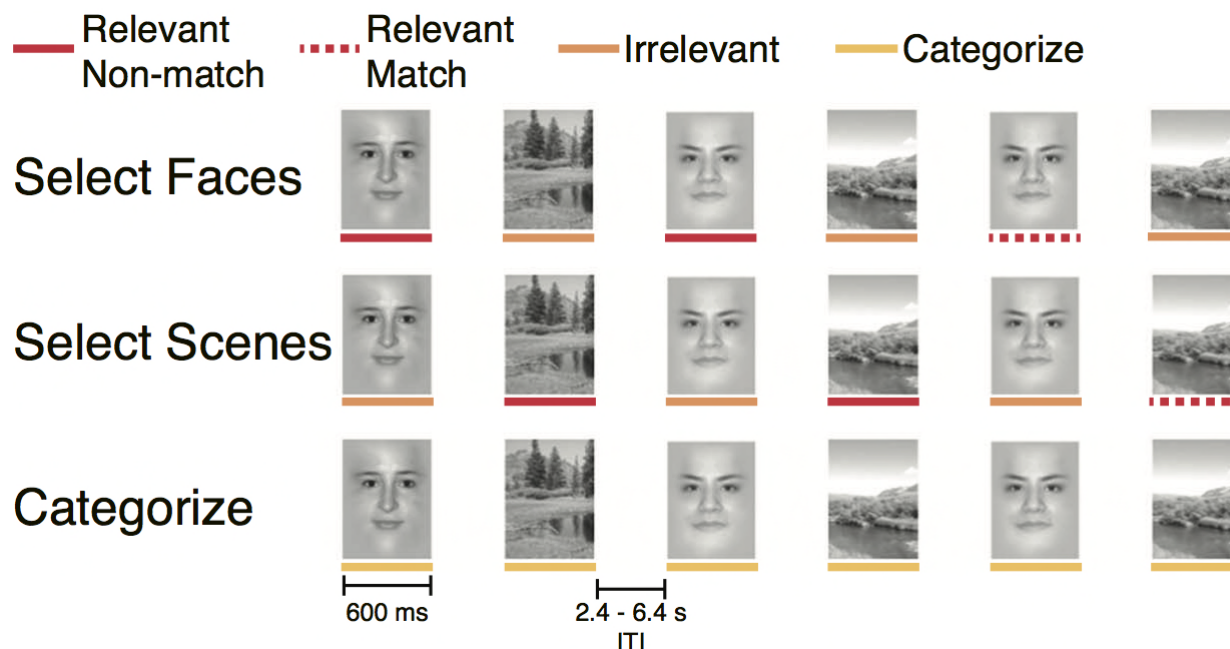


Figure 2.1. Experimental design for the cognitive task. Each task condition consisted of 20 sequentially presented stimuli (10 faces and 10 scenes). Colored lines under the stimuli are presented for illustrative purposes and were not present during performance of the cognitive task. Dashed red lines highlight 1-back matches for the relevant stimulus condition.

In Categorize blocks, participants indicated with a button press whether the current image was a face or a scene, with no attempt to remember the image. In Select Scenes blocks, participants were instructed to selectively attend to and remember images from the relevant category (scenes) and ignore images from the irrelevant category (faces). In Select Faces blocks, participants were instructed to selectively attend to and remember images from the relevant category (faces) and ignore images from the irrelevant category (scenes). In Select Scenes and Faces blocks, participants indicated if the currently attended image matched the previous image in the same category; participants responded to all ignored items with the ‘no-match’ button. Finally, in Select Both blocks, participants were instructed to attend to and maintain both the face and scene stimuli. If the current image matched the previous image of the same category, participants pressed the ‘match’ button. Participants completed four or five blocks of each condition during the scanning session, yielding a maximum of 40 or 50 face and scene stimuli for each task condition.

2.3.3 MRI acquisition and preprocessing

Imaging data were collected on 3T Siemens Trio scanners at the University of California, San Francisco Neuroscience Brain Imaging Center (Study 3) or the University of California, Berkeley Brain Imaging Center (all other studies). T1-weighted structural and T2*-weighted echo planar images (EPis) were collected with a 12-channel head coil for all studies.

Functional data were collected using GRAPPA with acceleration factor 2 for Studies 3, 4, 6, and two subjects in Study 5 (TE = 27 ms) and no parallel imaging for Study 2 (TE = 32 ms), Study 1 (TE = 24 ms), and three subjects in Study 5 (TE = 24 ms). All studies used 18 5 mm axial slices with a 0.5 mm gap (interleaved slices for Studies 2, 3, 4, 6, and two subjects in Study 5; descending slices for Study 1 and three subjects in Study 5). All studies collected functional volumes with TR = 1000 ms and a 3.5 mm² in-plane resolution. Four or five 114-volume runs of each of the four task conditions were collected, yielding a total of 30.4 or 38 minutes of task data. A high-resolution axial MP-RAGE T1-weighted sequence was used to acquire structural images for all studies (TR = 2300 ms, TE = 2.98 ms, FA = 9°, 1 mm³ voxels).

Standard preprocessing of EPI data was carried out with AFNI and FSL. EPI volumes were slice-time and motion corrected, co-registered to the T1-weighted structural image, and warped to the MNI template space using FSL's non-linear registration. Intensity spikes were removed and interpolated with AFNI after slice-time and motion correction. Functional data were resampled to 2 mm isotropic voxels, combining motion correction and atlas transformation in a single interpolation. MNI-warped functional data were spatially smoothed with a 6 mm full width at half maximum Gaussian kernel and scaled so that each voxel's run mean was equal to 100.

2.3.4 Task-related functional connectivity analyses

We first parcellated the brain into a set of 264 atlas regions (Power et al., 2011). To calculate the task-related functional connectivity between each pair of ROIs for specific conditions, we implemented a beta-series correlation analysis (Rissman et al., 2004). For each subject, we modeled stimulus onsets for trials in which correct responses were made for all task conditions (i.e., face and scene stimuli for Categorize, Select Scenes, Select Faces, and Select Both). These regressors were created by convolving a double gamma function with the onset times for each trial type. We also separately modeled incorrect or missed trials. Motion parameters and run means and linear trends were included as nuisance regressors.

This resulted in a parameter estimate, or beta value, for each trial. Beta values were averaged across all voxels within each ROI and concatenated for each condition of interest to create a 'beta-series' for each ROI. For examining effects of attention condition, we created beta-series from combined scene and face trials for Categorize, Select Scenes, and Select Faces conditions. This resulted in three beta series, one for each task condition. For examining effects of stimulus relevance, we created separate beta series for scene and face trials for Categorize (categorized scenes and categorized faces), Select Scenes (relevant scenes and irrelevant faces), and Select Faces (relevant faces and irrelevant scenes) conditions. This resulted in six beta series: a face and scene beta series for each of the three task conditions. Finally, task-related functional connectivity matrices were created for each participant and condition of interest by correlating the beta series between each pair of ROIs using Pearson's correlation coefficient and applying a Fisher z-transform. ROIs were excluded from subsequent analyses if they were missing EPI coverage due to incomplete sampling of the whole brain during fMRI scanning in 90% or more voxels from the original 81-voxel

ROI across scanning runs in any subject. A total of 193 ROIs were included in the final network analyses.

2.3.5 Module-based network metrics

The 193 x 193 functional connectivity matrices were binarized to create adjacency matrices that indicate the presence or absence of a connection between a pair of regions. Matrices were binarized over a range of connection density thresholds, where thresholding of the matrices was achieved by matching the number of network connections across subjects (here, the top 2-10% of all possible connections in the network in 2% increments). Each of these thresholded matrices was used to create unweighted, undirected whole-brain graphs (defined as a set of nodes or ROIs and the edges or connections between them) with which network metrics were examined. Network metrics were created separately for each connection threshold and are presented as the average across connection density thresholds.

We first quantified Newman's modularity, a global network measure that compares the number of connections within to the number of connections between modules (Newman and Girvan, 2004). Modularity will be 1 if all connections fall within modules and it will be 0 if there are no more connections within modules than would be expected by chance. We assigned each node to one module according to the modular partition identified with these nodes in Power et al. (2011). We then quantified global network modularity for each subject and condition of interest. We also examined the contribution of each module to global modularity, which is the sum of the modularity across network modules.

We investigated the robustness of our findings by equating the number of beta values in each beta-series across conditions within subjects by randomly selecting a subset of beta values for conditions with higher accuracy (see Table 2.1). Finally, we examined the reliability of our findings by using a spectral algorithm (Newman, 2006) to identify the most optimal modular partition (i.e., maximal modularity) for each subject and condition separately, rather than imposing the Power et al. (2011) modular partition across all graphs.

2.3.6 Statistical analysis

Accuracy (percent correct trials) and reaction times (average reaction time for correct trials) on the task were assessed with separate repeated-measures ANOVAs with within-subject factors of Relevance (Categorize, Irrelevant, Relevant) and Stimulus (Faces, Scenes). The effect of attention condition on network properties was assessed with a repeated measures ANOVA with a within-subject factor of task Condition (Categorize, Select Faces, Select Scenes). The effect of relevance on network properties was assessed with a repeated measures ANOVA with within-subject factors of Relevance (Categorize, Irrelevant, Relevant) and Stimulus (Faces, Scenes).

We also examined the behavioral correlates of changes in network organization, focusing on reaction time, in line with previous work (Kitzbichler et al., 2011; Vatansever

et al., 2015). We first calculated the reaction time for relevant stimuli (average of relevant face and relevant scene RTs) and the change in network modularity between (1) relevant and irrelevant and (2) relevant and categorized stimuli. We then performed Pearson's correlations between reaction time and the change in modularity.

2.4 Results

2.4.1 Task performance

Both accuracy and reaction times (RTs) were influenced by relevance and stimulus type (Table 2.1). An ANOVA with within-subject factors of Relevance (Categorize, Irrelevant, Relevant) and Stimulus (Scenes, Faces) on accuracy and RTs showed main effects of Relevance (accuracy: $F = 15.346$, $p < 0.001$; RTs: $F = 40.080$, $p < 0.001$) and Stimulus (accuracy: $F = 71.592$, $p < 0.001$; RTs: $F = 136.074$, $p < 0.001$). Participants were less accurate for relevant stimuli compared to categorized and irrelevant stimuli and were also less accurate for categorized stimuli compared to irrelevant stimuli. Participants were slower for relevant stimuli compared to categorized and irrelevant stimuli. Participants were more accurate and faster for face stimuli compared to scene stimuli.

There was also an interaction between Relevance and Stimulus for accuracy ($F = 7.123$, $p = 0.001$) and RTs ($F = 49.898$, $p < 0.001$), suggesting that the Stimulus effects depended on Relevance condition. For accuracy, participants were more accurate for faces in Categorize and Irrelevant conditions ($p < 0.001$; $p = 0.001$), but had equivalent accuracy for faces and scenes in the Relevant condition ($p = 0.679$). For RTs, participants were faster for faces in Categorize and Irrelevant conditions ($p < 0.001$), but were slower for faces in the Relevant condition ($p < 0.001$).

Table 2.1. Task performance (mean \pm SEM)

	Scenes			Faces		
	Categorize	Irrelevant	Relevant	Categorize	Irrelevant	Relevant
Accuracy (%)	95.0 \pm 0.6	97.6 \pm 0.4	93.4 \pm 0.7	97.6 \pm 0.4	98.8 \pm 0.4	93.2 \pm 0.7
RT (ms)	652.2 \pm 15.0	632.0 \pm 16.5	746.1 \pm 22.0	591.4 \pm 13.6	591.6 \pm 15.0	777.5 \pm 22.5
No. of betas	45.3 \pm 0.5	46.6 \pm 0.5	44.6 \pm 0.6	46.6 \pm 0.5	47.2 \pm 0.5	44.5 \pm 0.6

2.4.2 Reconfiguration of modular network organization due to attention condition

We first asked how the modular network structure of the brain was modulated by the task condition. We quantified task-related connectivity throughout the duration of the Categorize, Select Scene, and Select Faces conditions. The attention condition affected global brain modularity ($F = 5.733$, $p = 0.004$), in which modularity was lower for Select Scenes and Select Faces conditions compared to the Categorize condition (Figure 2.2A; $p = 0.007$; $p = 0.003$).

2.4.3 Reconfiguration of modular network organization due to stimulus relevance

We next investigated how brain network structure changed during the duration of the task condition depending on the relevance of the stimuli being encoded. Stimulus relevance altered global brain modularity (Figure 2.2B; main effect of Relevance: $F = 19.035$, $p < 0.001$). Modularity was selectively reduced during the processing of relevant stimuli in Select Scenes and Select Faces compared to both irrelevant stimuli and categorized stimuli ($p < 0.001$). The Stimulus type (Face, Scene) did not affect modularity (main effect of Stimulus: $F = 0.010$, $p = 0.922$) and the effect of Relevance on modularity was consistent for both Face and Scene stimuli (Relevance x Stimulus interaction: $F = 0.101$, $p = 0.891$).

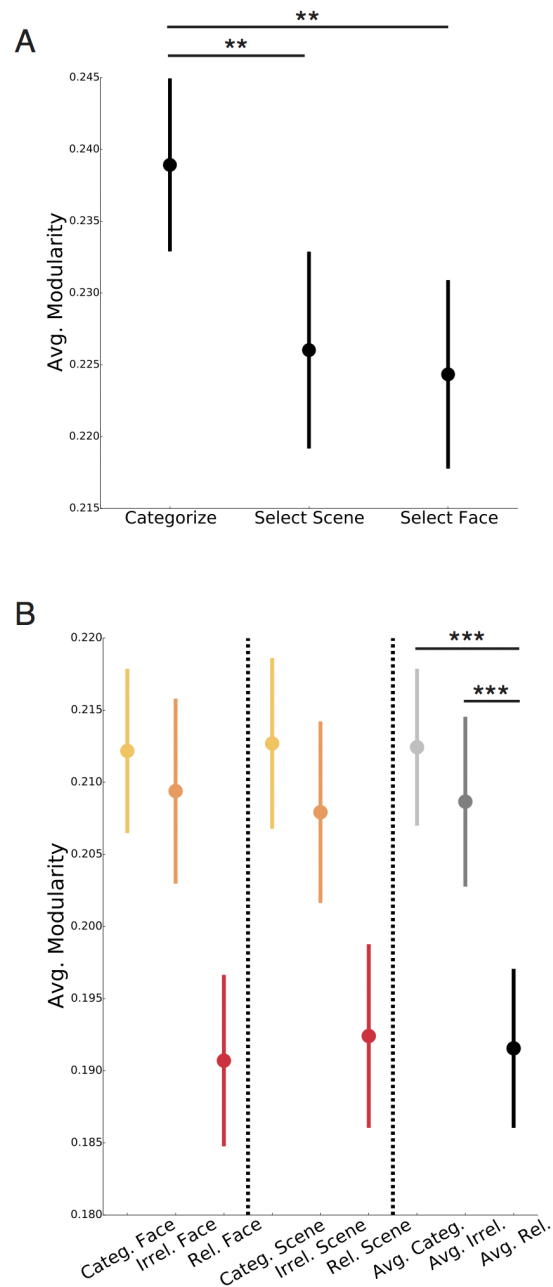


Figure 2.2. Network modularity for differing attention and relevance conditions. (A) Network modularity was lower during task conditions requiring working memory (1-back task) and had varying attention demands (i.e., both relevant and irrelevant stimuli in the Select Scenes and Select Faces conditions) compared to the Categorize condition. (B) Within the three task conditions, network modularity was selectively reduced for relevant stimulus processing compared to both irrelevant and categorized stimuli. Data are presented as mean \pm SEM. *** $P < 0.001$; ** $P < 0.01$.

We examined whether the effect of stimulus relevance on global modularity (the sum across all modules) was driven by particular brain sub-networks or modules by conducting an ANOVA with within-subject factors of Relevance (Categorize, Irrelevant, Relevant) and Module (N = 13). For this analysis, the modularity for face and scene stimuli were first averaged for each Relevance factor, as there was no main effect of Stimulus type for global modularity. Note that coverage of our functional data did not include the cerebellum, thus only permitting analysis of 13 of the 14 brain modules described in Power et al. (2011). A Relevance x Module interaction ($F = 6.750$, $p < 0.001$) suggested that the Relevance effect on modularity differed across modules (Figure 2.3). We then conducted separate ANOVAs for each module with a factor of Relevance to identify modules with effects that mirrored the global modularity effects (i.e., reduced modularity for relevant stimuli compared to irrelevant and categorized stimuli). Effects of stimulus relevance were pronounced in default mode ($F = 12.384$, $p < 0.001$) and visual ($F = 4.938$, $p = 0.008$) modules (Figure 2.4). In both the default and visual modules, modularity was reduced during processing relevant stimuli compared to irrelevant (default: $p < 0.001$; visual: $p = 0.001$) and categorized stimuli (default: $p < 0.001$; visual $p = 0.020$).

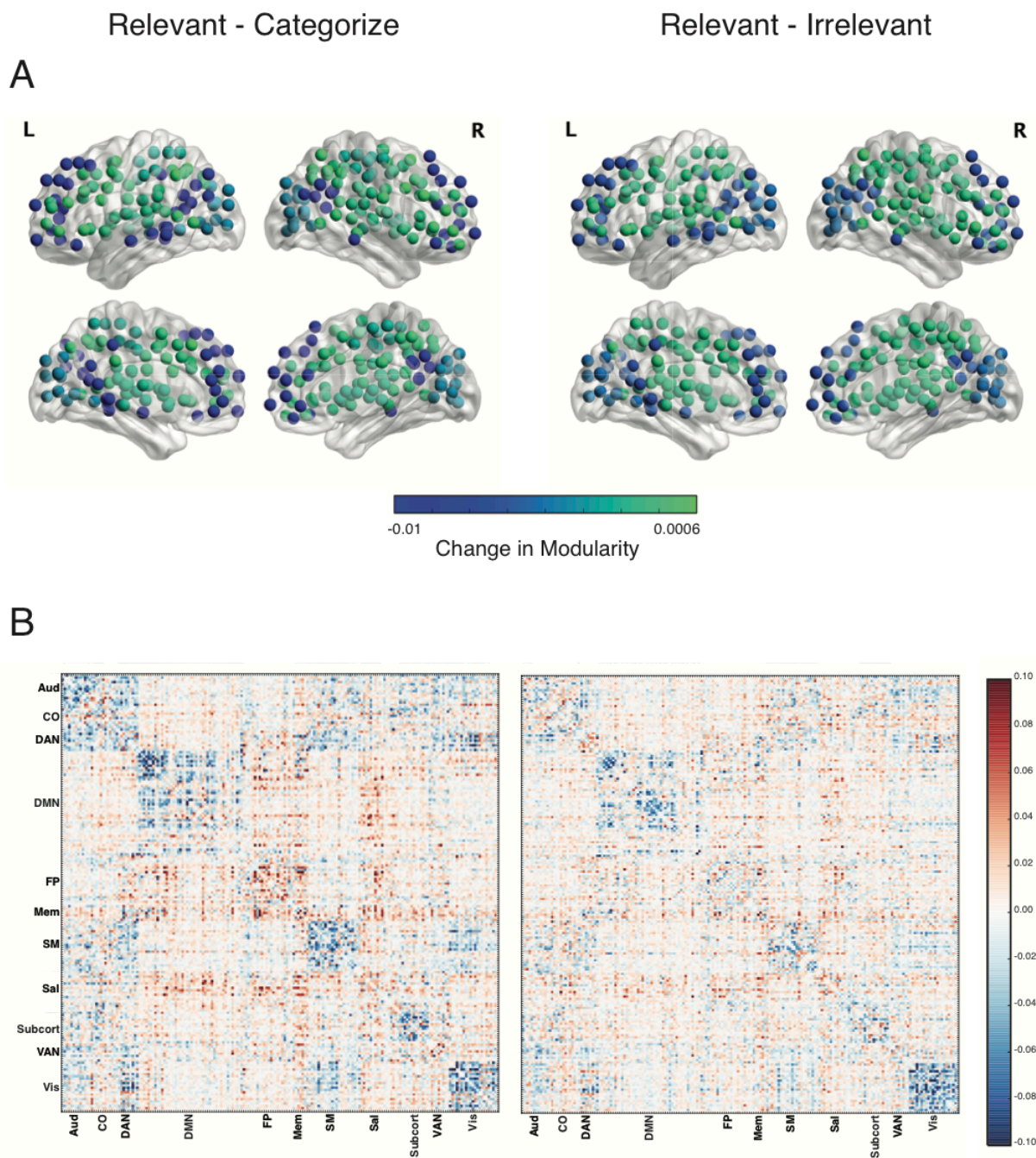


Figure 2.3. Module-specific changes in network organization. (A) Changes in network modularity between relevant stimulus processing and categorize (left) and irrelevant (right) stimulus conditions. Nodes are grouped according to the module definitions from Power et al. (2011) and are colored according to the change in modularity between the respective conditions. (B) Changes in within- and between-module network connections between relevant stimuli and categorize (left) and irrelevant (right) stimulus conditions. Binarized matrices were averaged across subjects and edge-density thresholds for each condition to examine changes in network connections. The resulting plots suggest that there are differences in the modularity decreases for relevant stimuli across the 13 network modules.

We replicated these effects after equating the length of the beta-series, or number of beta values used correlate between ROIs, across task conditions within each subject (Table 2.1). We also confirmed these results after using a spectral partitioning algorithm to identify ‘optimal’ network modules (those with the maximum modularity) for each subject and condition, rather than using the Power et al. (2011) module definition for all networks.

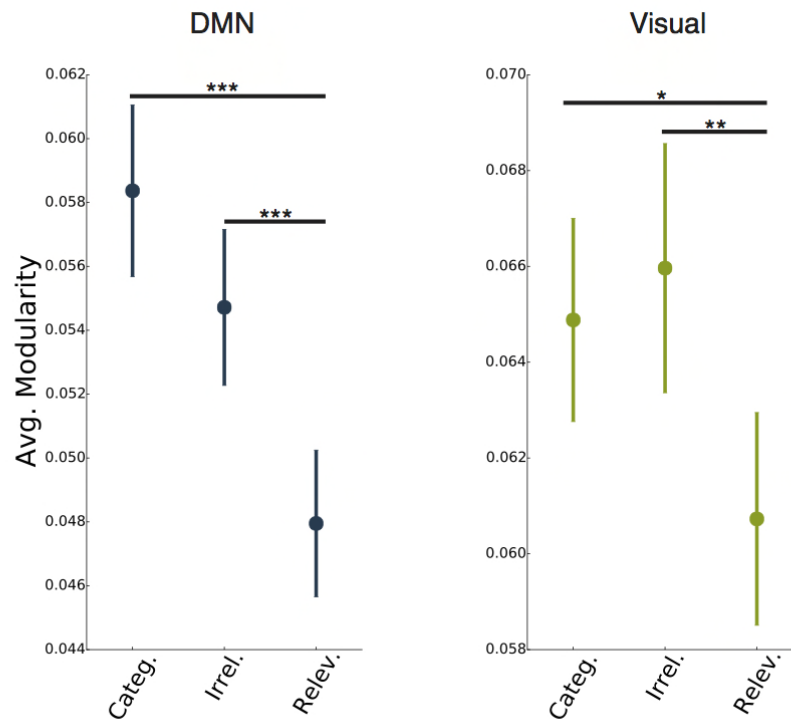


Figure 2.4. Network modularity for default mode and visual modules. Decreases in network modularity for relevant stimuli were most pronounced for default mode and visual modules. Data are presented as mean \pm SEM. *** $P < 0.001$; ** $P < 0.01$; * $P < 0.05$.

2.4.4 Relationship between network reorganization and task performance

We next examined how the changes in network modularity were related to task performance. We focused on RTs for relevant stimuli (quantified as the mean RT across relevant face and relevant scene stimuli) as our metric of task performance, as it assesses the speed of performance on correct trials during a 1-back task. We first examined how the change in global network modularity for relevant stimuli (compared to both categorize and irrelevant) was related to performance. A greater decrease in modularity for relevant stimuli compared to irrelevant stimuli was related to faster task performance for relevant stimuli (Figure 2.5A; $r = 0.337$, $p = 0.003$), while there was no

relationship between performance and the change in modularity between relevant and categorized stimuli ($r = 0.042$, $p = 0.719$).

We also examined the contribution of default and visual modularity in predicting task performance. To do so, we quantified the change between relevant and irrelevant modularity for each module and averaged these values across (1) default and visual modules and (2) all other network modules ($N = 11$). Greater decreases in modularity for relevant compared to irrelevant stimuli were related to RTs for relevant stimuli in default and visual modules (Figure 2.5B; $r = 0.326$, $p = 0.004$) but not across the remaining modules (Figure 2.5C; $r = 0.161$, $p = 0.167$). Further, examining correlations between modularity and performance separately for default and visual modules showed a similar relationship for both modules ($r = 0.228$, $p = 0.049$; $r = 0.212$, $p = 0.068$; respectively).

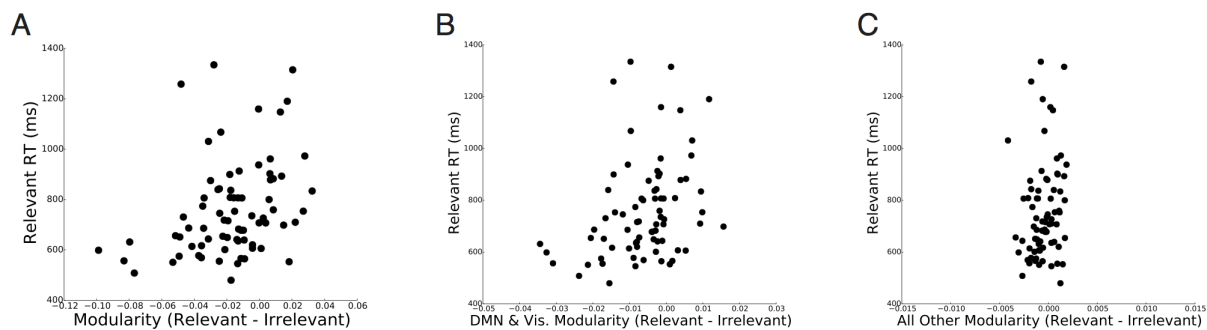


Figure 2.5. Relationship between changes in network modularity and behavior. (A) Correlation between the change in global modularity from irrelevant to relevant stimulus processing and reaction time for relevant stimuli. Greater decreases in modularity for relevant stimuli were related to faster performance on relevant trials. (B) Correlation between the change in default and visual modularity (average of two modules) and relevant stimulus reaction time. (C) Correlation between the change in modularity for all other modules ($N = 11$) and relevant stimulus reaction time. Changes in modularity for relevant stimuli were related to behavior for default and visual modules but not the remaining modules. Data points represent individual subjects.

Finally, to account for overall differences in performance across subjects, we also examined correlations between network reconfiguration between relevant and irrelevant stimulus processing and changes in RT between relevant and irrelevant stimuli. Note that here we assessed correlations with Spearman's rho to account for two potential outliers in the performance difference between relevant and irrelevant stimuli. Examining the correlation between whole-brain modularity and performance changes showed that subjects who exhibited greater network reconfiguration (i.e., decrease in modularity for relevant stimulus processing) were those with less of a performance deficit for relevant compared to irrelevant stimuli ($\rho = 0.194$; $p = 0.100$). Examining the correlation between default and visual network reconfiguration and performance changes showed a similar relationship for these modules ($\rho = 0.208$, $p = 0.073$), while this relationship was not present for all other modules ($\rho = 0.145$, $p = 0.215$).

2.5 Discussion

Here, we provide evidence that selective attention demands alter the modular network organization of the brain during working memory performance. We first show that modularity is lower during performance of a more demanding 1-back task with varying attention demands compared to a 0-back task. Further, we show that modularity changes throughout the duration of the 1-back task depend on the relevance of the stimuli. Network modularity was selectively reduced during the encoding of relevant stimuli used for the 1-back task compared to irrelevant stimuli that were ignored. These effects were pronounced in default and visual sub-networks or modules. Finally, we show that the changes in modularity for relevant stimulus processing are related to faster task performance, both in terms of global modularity and default and visual sub-network modularity.

Using all face and scene stimuli encoded throughout the duration of each task condition, we observed that network modularity was reduced during the performance of 1-back tasks that had varying attention and working memory components (Select Scenes and Select Faces) compared to the 0-back task (Categorize). This finding is in line with a growing literature that shows the modularity of the brain is influenced by working memory demands. Previous work has shown that network modularity is reduced during more demanding (i.e., higher load) N-back task conditions (Kitzbichler et al., 2011; Vatansever et al., 2015; Wen et al., 2015), suggesting that the brain adopts a more integrated network organization when more cognitive effort is required. Other network properties have also been shown to be modulated by n-back load, such as increases in long-range connectivity (Kitzbichler et al., 2011), lower local clustering (Kitzbichler et al., 2011), and higher global efficiency (Kitzbichler et al., 2011; Wen et al., 2015) in more demanding N-back conditions. These studies point to a global 'workspace' configuration (Dehaene et al., 1998) of the brain during increased cognitive effort.

Importantly, however, the majority of these previous studies have used block designs to assess the reconfiguration of brain networks during working memory performance (i.e., examine gross network changes between 1- and 2-back conditions). We expand on these observations by providing new evidence that brain networks dynamically reconfigure trial-by-trial during the 1-back task, depending on the relevance of the stimuli. By quantifying task-related connectivity separately for face and scene stimuli during the 1-back and 0-back tasks, we observed that network modularity was specifically reduced during the encoding of relevant face and scene stimuli that were used to guide working memory performance. Modularity quantified during the processing of irrelevant stimuli during the same 1-back task conditions was similar to that of the stimuli in the Categorize condition. These observations show that lower modularity during the 1-back task blocks may be driven by selective decreases in network modularity during the processing of relevant stimuli. Further, during these task blocks, brain networks are able to reconfigure on a trial-wise basis, as evident by increased modularity for irrelevant stimulus processing.

Examining the individual module contributions to the global modularity findings, we observed that decreases in modularity for relevant stimulus processing were

pronounced in default mode and visual modules. These findings provide evidence that particular modules may become less segregated from the rest of the brain network during the processing of relevant information. Previous studies examining brain network properties have also reported decreased within-module (Liang et al., 2015) and increased between-module (Stanley et al., 2014) connectivity in default mode regions in the context of increasing n-back demands. We expand on this and other work that examined goal-related connectivity of visual regions (Chadick and Gazzaley, 2011), by showing that the balance of within- and between-module connections in these modules is affected by varying attention demands during an n-back task. Interestingly, these network modules have also been shown to underlie behaviorally-relevant changes in global modularity during an auditory detection task (Sadaghiani et al., 2015).

Finally, our findings point to the behavioral importance of alterations in brain network modularity depending on stimulus relevance. Greater decreases in global modularity for relevant compared to irrelevant stimulus processing were related to faster performance on working memory trials. This behavioral relationship was not present when we quantified the change in modularity between stimuli in the Relevant and Categorize condition, potentially pointing to the significance of changes in modularity that occur on a trial-wise basis within a single task block. We further showed that these decreases in modularity were related to behavior for default mode and visual modules and not for the remaining modules. These results expand on previous graph theoretical analyses that have been limited to n-back block designs and showed that lower modularity at higher demands is beneficial for performance (Kitzbichler et al., 2011; Stanley et al., 2014; Vatansever et al., 2015).

In conclusion, we find that the modular organization of the brain reconfigures during working memory performance depending on whether stimuli are attended or ignored as distractors. Modularity was selectively decreased when encoding relevant stimuli, suggesting that increased integration between brain network modules is important for subsequent behavior. These observations support theories of attention that posit goal-directed behavior emerges from interactions between distributed large-scale networks of the brain (Buschman and Kastner, 2015). Further characterization of how brain networks reconfigure during other critical stages of working memory performance (e.g., maintenance and retrieval) are important questions for future work.

Chapter 3

RECONFIGURATION OF BRAIN NETWORK ARCHITECTURE TO SUPPORT EXECUTIVE CONTROL IN AGING

3.1 Abstract

Aging is accompanied by declines in executive control abilities and changes in underlying brain network architecture. Here, we examined brain networks in young and older adults during a task-free resting state and an N-back task and investigated age-related changes in the modular network organization of the brain. Compared with young adults, older adults showed larger changes in network organization between resting state and task. Although young adults exhibited increased connectivity between lateral frontal regions and other network modules during the most difficult task condition, older adults also exhibited this pattern of increased connectivity during less-demanding task conditions. Moreover, the increase in between-module connectivity in older adults was related to faster task performance and greater fractional anisotropy of the superior longitudinal fasciculus. These results demonstrate that older adults who exhibit more pronounced network changes between a resting state and task have better executive control performance and greater structural connectivity of a core frontal-posterior white matter pathway.

3.2 Introduction

Cognitive decline is pervasive in older adulthood, notably in executive control processes thought to be subserved by the frontal cortex (Park et al., 2002; Grady, 2008; 2012). Extensive alterations in brain structure and function are also observed in older adults. Functional changes in aging have been documented in the activation of individual brain regions and in the functional connectivity between brain regions (Spreng et al., 2010; Grady, 2012; Turner and Spreng, 2012; 2015). Alterations in functional connectivity are thought to be related, in part, to a decline in structural connectivity, such as through long-range white matter fiber tracts (Bennett and Madden, 2014).

Further work in older adults has examined the functional communication among groups of brain regions by quantifying the connectivity of brain subnetworks (Andrews-Hanna et al., 2007; Damoiseaux et al., 2008; Ferreira and Busatto, 2013), such as the default-mode and fronto-parietal networks. However, executive control processes rely on the integration of signals from frontal cortex to widely distributed brain regions, likely not limited to specific subnetworks as has been examined thus far (Fuster et al., 1985; Chao and Knight, 1998; Knight et al., 1999; Barceló et al., 2000; Miller and D'Esposito, 2005; Lee and D'Esposito, 2012). Thus, changes in executive control processing in aging may be better examined by methods that quantify the large-scale (e.g., whole brain) network organization of the brain. Graph theoretical methods describe the brain

as a complex network, comprised of functionally separable subnetworks or modules. This type of organization is critical for supporting both local processing within and global processing between modules. Using graph theory, the modularity of network organization can be quantified (Meunier et al., 2009b; 2010), where networks with high modularity have dense connections within modules and sparser connections between modules.

Studies examining modular network organization during working memory have shown that increasing executive control demands (i.e., increasing N-back load) are supported by a more integrated network organization, manifested in decreased modularity (Kitzbichler et al., 2011; Vatansever et al., 2015; Wen et al., 2015) and increased connectivity between network modules (Stanley et al., 2014; Liang et al., 2015). This reconfiguration of brain networks has also been observed when comparing networks from a task-free 'resting state' to those during the performance of tasks with increasing demands (Wen et al., 2015).

In older adults, analyses of structural MRI and resting-state fMRI data have demonstrated that aging is associated with declines in modularity (Meunier et al., 2009a; Chen et al., 2011b; Onoda and Yamaguchi, 2013; Chan et al., 2014; Geerligs et al., 2014a). Importantly, these studies have not examined how networks reconfigure during the performance of a task in older adults. To understand how network-level changes contribute to age-related alterations in executive control, it is critical to investigate changes in brain network properties during cognitive processing.

In this study, we examine how the modular organization of the brain reconfigures between the absence of a task (e.g., a resting state) and the performance of an N-back task in older and young adults. We first quantify the topological overlap of modules identified during resting state and task. We next examine changes in between-module connectivity with increasing cognitive demands, both across the entire brain (i.e., modularity) and in a subset of lateral frontal regions. We also examine how changes in between-module connectivity from a resting state to task are related to behavioral performance. Finally, as aging is associated with declines in white matter pathways (Bennett and Madden, 2014), we investigate how frontal-posterior structural connectivity is related to functional reconfiguration of brain networks in older adults.

3.3 Materials and Methods

3.3.1 Participants

Eighteen young (10 females; mean age = 21.08, range = 18-26) and 38 older (24 females; mean age = 66.97, range = 60-80) adults were included in this analysis. Young and older participants were matched on distribution of gender ($X^2(1, N = 56) = 0.30, p = 0.59$). Older participants had greater years of education compared with young participants (mean \pm standard error of the mean, older: 17.42 ± 0.49 ; young: 14.53 ± 0.48 ; $t(54) = 3.67, p = 0.001$). Participants were prescreened for the presence of

medical, neurological, or psychiatric illness (e.g., stroke, traumatic brain injury) and the use of prescribed drugs with known effects on cognition (e.g., benzodiazepines). Older participants were recruited through the Berkeley Aging Cohort and through the community (e.g., fliers, senior residences). Older participants were normal on cognitive screening (i.e., no score less than 1.5 standard deviations below expected performance in more than one cognitive domain for neuropsychological assessments of memory, concentration, verbal fluency, and visuospatial function). A complete neuropsychological evaluation was not available for one subject; however, this subject had a Mini-Mental State Examination score of 28. Young participants were recruited after the collection of older subject data through research study postings at the University of California, Berkeley. Informed consent was obtained from all participants in accordance with the Committee for Protection of Human Subjects at the University of California, Berkeley.

3.3.2 Cognitive task

The cognitive task performed during fMRI scanning was an N-back task that consisted of 20 runs lasting approximately 2 minutes each (Chen et al., 2011a; Lee and D'Esposito, 2012). Each run contained a series of pseudo-randomly interleaved face and natural scene stimuli (10 of each) during which participants were instructed to either attend to and maintain images from the relevant stimulus category, while ignoring images from the irrelevant category, or to attend both categories. Each stimulus was presented for 600 ms, with a 2.4, 4.4, or 6.4 second jittered delay (randomly ordered) between each stimulus presentation. The 4 conditions varied in executive control demands and were referred to as: "CATEGORIZE," "SCENES," "FACES," and "BOTH." In CATEGORIZE, participants indicated with a button press whether the current image was a face or a scene, with no attempt to remember the image. In SCENES and FACES, participants were instructed to selectively attend to and maintain images from the relevant category (i.e., scenes or faces, respectively) and ignore images from the irrelevant category (i.e., faces or scenes, respectively). Participants indicated if the current-attended image matched the previous image in the same category. Participants responded to all unattended items in SCENES and FACES with the "no-match" button. Finally, in BOTH, participants were instructed to attend to and maintain both the face and scene stimuli. If the current image matched the previous image of the same category, participants pressed the "match" button. Participants completed 5 blocks of each condition during fMRI scanning.

3.3.3 MRI acquisition and preprocessing

MRI scans were collected with a 12-channel head coil on a 3T Siemens Trio scanner at the University of California, Berkeley. A high-resolution T1-weighted MP-RAGE sequence was used to acquire 3D anatomical images (repetition time [TR] = 2300 ms, echo time [TE] = 2.98 ms, flip angle = 9°, 1.00-mm³ voxels). A T2*-weighted echoplanar imaging (EPI) sequence was used to acquire resting state and task functional data (TR = 1000 ms, TE = 27 ms for older participants; 24 ms for young participants, 5.00-mm thick interleaved (descending for young participants) axial slices (0.50- mm gap), in-plane resolution = 3.50 mm²). Functional data for older adults were collected using GRAPPA with an acceleration factor of 2. For the N-back task scans, five 114-volume

runs of each task condition were collected. For the resting state scans, one 300-volume run was collected for all young and 35 older adults. We collected the resting state scans for the remaining 3 older adults with the following parameters: 435 volumes, TR = 1370 ms, TE = 26 ms, 3.50-mm thick interleaved axial slices (0.35-mm gap), in-plane resolution = 2.34 mm².

Standard preprocessing of EPI data was carried out with AFNI, versions 2.61-4.21 (Cox, 1996). EPI volumes were slice-time and motion corrected, coregistered to the T1-weighted structural image using a 12-parameter affine transformation, and scaled to have each voxel's run mean be equal to 100. Structural scans were segmented into cerebrospinal fluid and gray and white matter components using SPM8 (Wellcome Department of Cognitive Neurology, London, UK). Functional data were spatially smoothed to a 6-mm full width at half maximum Gaussian kernel and signals (mean and temporal derivative) from white matter, cerebrospinal fluid, and motion were regressed out.

Diffusion-weighted images were acquired for 32 older participants along 30 noncollinear diffusion-encoding directions (50 slices, TR = 6400 ms, TE = 87 ms, field of view: 256 x 256 mm², 128 x 128 matrix, 2-mm thick axial slices, in-plane resolution = 2.2 mm²). The data were preprocessed using the functional magnetic resonance imaging in the brain software library (FSL; (Smith et al., 2004; Woolrich et al., 2009)). First, the digital imaging and communications in medicine files of each acquisition were converted to a single multivolume 4D format in the MRICron software (Rorden et al., 2007). Next, they were corrected for any effects of head movement and eddy current distortion using the eddy correct tool in functional magnetic resonance imaging in the brain's diffusion toolbox (FDT). This tool conducts an affine registration of each individual volume to a specified b0 volume. Brain tissue was segmented using the Brain Extraction Tool (Smith, 2002) in FSL, and a brain mask was created at a threshold of 0.3 as recommended by FSL. Diffusion-weighted images were also collected for 16 young adults but not analyzed here.

3.3.4 Functional connectivity analyses

Participants' T1-weighted anatomical scans were parcellated into 90 cortical and subcortical regions of interest (ROIs) from the automated anatomical labeling (AAL) atlas (Tzourio-Mazoyer et al., 2002). ROIs were reverse-normalized to each participant's native space using the parameters from SPM segmentation (i.e., a reverse normalization from the warping to Montreal Neurological Institute (MNI) template space that was computed during segmentation). Individual time-series from each resting state and task run were averaged over the voxels in each ROI and bandpass filtered (0.009 – 0.08 Hz) to remove physiological artifacts. Six ROIs were excluded from subsequent analyses because they were missing coverage in the EPI volumes in some scanning runs in either young or older participants (bilateral inferior occipital gyrus, left fusiform gyrus, right superior parietal gyrus, left middle temporal pole, left inferior temporal gyrus). Finally, functional connectivity matrices for resting state and task were created for each participant by correlating the time-series between each pair of ROIs using Pearson's correlation coefficient and applying a Fisher z-transform. As there are

multiple methods for parcellating the brain into ROIs for network analyses, we also repeated our analyses with a commonly used atlas that is composed of functionally, rather than anatomically, defined regions from healthy young subjects (Power et al., 2011).

We matched whether resting state scans were acquired before or after the N-back task in the young and older groups. Resting- state scans were collected after the task for 26 older and 13 young adults; the remaining participants had resting-state scans collected before the task (12 older and 5 young). The distribution of pre-task and post-task resting-state scans across participants was equivalent between the 2 age groups ($\chi^2(1, N = 56) = 0.08, p = 0.77$). Additional follow-up analyses in Section 3.4.4 address the potential effects of pre-task and post-task resting-state scans on our results.

To have similar numbers of volumes for resting state and task correlation analyses, 5.7 minutes (342 volumes) of each task condition were analyzed, by demeaning and concatenating 3 of the 5 blocks for each condition before computing correlations between each ROI pair. Concatenating task volumes allows for additional task data to be used to more reliably estimate functional connectivity between ROIs. Furthermore, it makes the amount of data for correlation analyses similar between resting state and task conditions. For 11 young and 29 older adults, we used the first 3 runs of each task condition to generate the task time-series. In a portion of the first 3 runs for the remaining 9 older adults, there were suspected artifacts from movement during the GRAPPA reference scan (autocalibrating signal scan); we therefore used 1 or 2 of the subsequent runs to generate task time-series (12 total time-series across participants and task conditions). We matched the composition of the task time-series for these older participants in a set of 7 young adults. Furthermore, the distribution of whether task time-series were generated from the first 3 runs was matched between the age groups ($\chi^2(1, N = 56) = 1.38, p = 0.24$). Additional follow-up analyses in Section 3.4.4 address the potential effects of task-run selection on our results.

3.3.5 Module-based network metrics

The functional connectivity matrices were binarized to create adjacency matrices that indicate the presence or absence of a connection between a pair of regions. Matrices were binarized over a range of connection density thresholds, where thresholding of the matrices was achieved by matching the number of network connections across participants (here, the top 5%e25% of all possible connections in the network in 5% increments). Each of these thresholded matrices was used to create unweighted, undirected whole-brain graphs (defined as a set of nodes or ROIs and the edges or connections between them) with which network metrics were examined. Unless otherwise noted, network metrics were created separately for each connection threshold and are presented as the average across all 5 connection density thresholds.

Each brain graph was then subdivided into modules using a simulated annealing algorithm (Kirkpatrick et al., 1983). We subsequently refer to the collection of modules as a “partition.” For each graph, we identified its “optimal” modular organization by choosing the partition with the highest modularity value across the algorithm iterations

(Newman and Girvan, 2004). Highly modular graphs have dense connections within modules and sparser connections between modules. We then investigated the reconfiguration of modular network structure between a resting state and task in the 2 age groups.

First, as our module-detection procedure allows for different partitions (groupings of nodes into modules) across individuals and task conditions, we investigated the overlap of modules between a resting state and task using mutual information (MI). MI quantifies the similarity of 2 partitions (Danon et al., 2005) with 1 representing identical partitions, and low values indicating that nodes tend to group together into different modules. We compared each subject's resting-state network organization to those created from the 4 task conditions to examine the differences in modules between a resting state and task.

Next, we investigated changes in network connections between resting state and task. We first quantified modularity, a whole-brain network measure that compares the number of connections within to the number of connections between modules (Newman and Girvan, 2004). Modularity will be 1 if all connections fall within modules, and it will be 0 if there are no more connections within modules than would be expected by chance.

Although modularity quantifies the balance of within- and between-module connections across the whole-brain network, there may also be changes in particular network connections in the brain. Thus, we also examined the properties of specific between-module connections that provide communication across network modules. To do so, we quantified the participation coefficient (PC) of individual brain regions, a measure of the distribution of a node's connections across modules (Guimera and Amaral, 2005; Guimera et al., 2006). A node's PC will be 1 if its connections are uniformly distributed across all network modules and it will be 0 if its connections are concentrated within its own module. In other words, a higher PC value suggests that a node's connections are more distributed among network modules, whereas a lower PC value indicates that a node's connections are more concentrated in its own module. We focused on examining PC of lateral frontal regions, as they play a critical role in top-down modulation of sensory cortices (Gazzaley and Nobre, 2012) to support executive control functions such as attention and working memory (Funahashi et al., 1993a; 1993b; Chao and Knight, 1998; Lee and D'Esposito, 2012). Furthermore, older adults exhibit notable impairments in these functions (Gazzaley et al., 2005b; Clapp et al., 2011). We calculated PC for 10 lateral frontal regions in the AAL atlas: bilateral precentral, middle frontal, superior frontal, and pars opercularis and pars triangularis of the inferior frontal gyrus. PC was averaged across lateral frontal regions to examine general changes that occur in lateral frontal cortex with aging. To examine the specificity of lateral frontal changes, we also examined PC for 10 control regions in the occipital cortex: bilateral superior occipital, middle occipital, cuneus, calcarine, and lingual gyrus. We restricted our analyses to one set of control regions to limit the number of statistical tests conducted.

3.3.6 White matter connectivity analyses

We were also interested in investigating the relationship between functional network changes and connectivity of long-range white matter association fiber tracts. We focused on the superior longitudinal fasciculus (SLF), as it has been shown to provide critical anatomical connections between frontal and posterior cortical regions (Makris et al., 2005), putative targets of frontal regions implicated in executive control (Mori et al., 2008). After pre-processing, the FDT tool in FSL was used to fit a diffusion tensor model at each voxel in the brain-extracted images created with Brain Extraction Tool. Fractional anisotropy (FA) maps were derived for each participant. Voxel-wise statistical analysis of the FA data was carried out using tract-based spatial statistics (Smith et al., 2006) in FSL. ROI masks for the left and right SLF were created using the JHU-ICBM-DTI-81 Atlas. These masks were then used to extract the average FA value for the tract across hemispheres in each participant, which we speculate reflects variability in underlying structural connectivity or white matter architecture across participants.

3.3.7 Statistical analysis

Effects of aging on task performance (i.e., accuracy and reaction time) were assessed with a repeated-measures ANOVA with a within-subjects factor of task condition (CATEGORIZE, SCENES, FACES, BOTH) and a between-subjects factor of age group (OLDER, YOUNG). MI between a resting state and the 4 task network partitions was assessed with a repeated-measures ANOVA with a within-subjects factor of task condition (CATEGORIZE, SCENES, FACES, BOTH) and a between-subjects factor of age group (OLDER, YOUNG). Modularity and PC were assessed with repeated-measures ANOVAs with a within-subjects factor of task condition (RESTING-STATE, CATEGORIZE, SCENES, FACES, BOTH) and a between-subjects factor of age group (OLDER, YOUNG). For ANOVAs that only include the 4 task conditions as factors (i.e., do not include resting state), we report both the overall within-subjects effects of task condition and the linear within-subjects contrasts, as we hypothesized that the task conditions would modulate outcome measures in a parametric fashion. We present descriptive statistics (mean and standard deviation) for these measures in Table 3.1.

We set a significance threshold of $p < 0.05$ and also report nonsignificant trends at $p < 0.10$. To ensure maximal transparency, we report uncorrected p-values and interpret results with caution when they do not pass a Bonferroni-corrected threshold for 3 tests (MI, modularity, and lateral frontal PC). For all ANOVAs, we also report estimates of effect size for each contrast as partial eta-squared (η_p^2). Significant interactions between age group and task condition were subsequently investigated with post hoc comparisons, focusing on age group differences across resting state and task conditions.

Recent work has shown that in-scanner motion can spuriously affect measures of functional connectivity (Power et al., 2012; Van Dijk et al., 2012; Power et al., 2013; Satterthwaite et al., 2013). We took several steps to ensure that the reconfiguration of modular network structure was not related to motion. First, we examined age and task differences in head motion, quantified as the Euclidean norm of the derivatives of

motion parameters. Second, we conducted all network analyses with motion as a covariate of no interest.

Finally, we examined behavioral and structural correlates of network reconfiguration in older adults. We quantified network reconfiguration as the change in lateral frontal PC between resting state and task (averaged across all task conditions). Correlations were quantified with Spearman's rho instead of Pearson's correlation coefficient to reduce the influence of extreme values. To examine the relationship between network reconfiguration and executive control, we conducted correlations between the change in lateral frontal PC and behavioral performance (reaction time) from the task. Differences in correlation values between older and young groups were evaluated using the formula described by Cohen (Cohen et al., 2003) after using the conversion from Spearman's to Pearson's coefficients described by Myers and Sirois (Myers and Sirois, 2004). To examine the relationship between white matter architecture and network reconfiguration in older adults, we conducted correlations between FA of the SLF (average of left and right hemispheres) and the change in lateral frontal PC.

Plots were created with the Matplotlib package ([http:// matplotlib.org/](http://matplotlib.org/)) in IPython (<http://ipython.org/>) and brain network graphs were visualized with BrainNet Viewer ([http://www.nitrc.org/ projects/bnv/](http://www.nitrc.org/projects/bnv/)).

3.4 Results

3.4.1 Task performance

Accuracy and reaction time (RT) analyses revealed main effects of age group (accuracy: $F(1,54) = 5.74$, $p = 0.02$, $\eta_p^2 = 0.10$; RT: $F(1,54) = 5.03$, $p = 0.03$, $\eta_p^2 = 0.09$) and task condition (accuracy: overall effect, $F(3,162) = 28.50$, $p < 0.001$, $\eta_p^2 = 0.35$ and linear contrast, $F(1,54) = 60.04$, $p < 0.001$, $\eta_p^2 = 0.53$; RT: overall effect, $F(3,162) = 141.90$, $p < 0.001$, $\eta_p^2 = 0.72$ and linear contrast, $F(1,54) = 200.92$, $p < 0.001$, $\eta_p^2 = 0.79$). Across all conditions, older adults had lower accuracy and longer RTs than young adults. Across all participants, accuracy was highest and RTs were shortest in the CATEGORIZE and SCENES conditions, followed by FACES and BOTH.

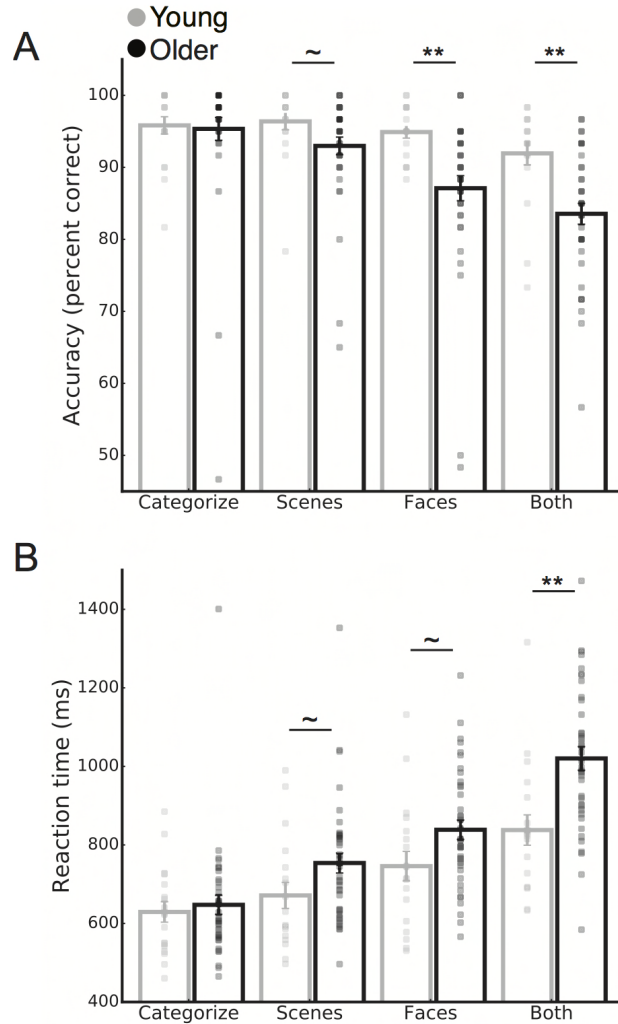


Figure 3.1. Task accuracy (A) and reaction time (B) for young and older adults. Data are presented as mean \pm standard error of the mean. Pairwise comparisons between young and older groups across the task conditions were conducted for metrics showing significant age group by task condition interactions. ** $p < 0.01$; $\sim p < 0.1$.

The age group by task condition interaction was also significant for both accuracy and RT (accuracy: $F(3,162) = 7.75$, $p < 0.001$, $\eta_p^2 = 0.13$; RT: $F(3,162) = 10.47$, $p < 0.001$, $\eta_p^2 = 0.16$), indicating that older adults performed worse than young adults, but not equally in all conditions. Older and young adults had equivalent accuracy and RT in the CATEGORIZE condition (accuracy: $p = 0.85$; RT: $p = 0.65$) but older adults had lower accuracy (Figure 3.1A) and longer RTs (Figure 3.1B) than young adults in the SCENES, FACES, and BOTH conditions (accuracy: $p = 0.09$, $p = 0.005$, $p = 0.001$; RT: $p = 0.07$, $p = 0.05$, $p = 0.001$). We also conducted non-parametric tests (Mann-Whitney U test) between the age groups for each task condition. These results confirmed that older adults performed less accurately and slower on all conditions except for CATEGORIZE (accuracy: CATEGORIZE, $p = 0.85$; SCENES, $p = 0.02$; FACES, $p < 0.001$; BOTH, $p <$

0.001; RT: CATEGORIZE, $p = 0.66$; SCENES, $p = 0.03$; FACES, $p = 0.04$; BOTH, $p = 0.001$)

3.4.2 Reconfiguration of modular network organization during executive control processing

Mutual information between network partitions during resting-state and task performance. We first examined changes in modules between resting-state and task in young and older adults. More specifically, we quantified the mutual information (MI) between each subject's resting network partition and those derived from the four task conditions, thus producing four MI values (each task condition compared to resting-state) for each subject. A repeated-measures ANOVA on MI revealed main effects of age group and task condition (Figure 3.2A; age group: $F(1,54) = 33.22$, $p < 0.001$, $\eta_p^2 = 0.38$; task condition: overall effect, $F(3,162) = 2.11$, $p = 0.10$, $\eta_p^2 = 0.04$ and linear contrast, $F(1,54) = 4.33$, $p = 0.04$, $\eta_p^2 = 0.07$). Across all task conditions, older adults had lower MI between resting-state and task than young adults. The significant linear contrast suggests that MI was modulated parametrically across the task conditions. Across all participants, MI between resting-state and task was higher for CATEGORIZE and SCENES compared to BOTH and higher in SCENES compared to FACES. The main effect of task condition on MI should be interpreted with caution, as it does not pass a Bonferroni-corrected significance threshold of $p < 0.05$. There was no significant age group by task condition interaction ($F(3,162) = 0.56$, $p = 0.64$, $\eta_p^2 = 0.01$)

Modularity of the brain during resting-state and task performance. We next examined changes in the balance of within- and between-module connections across the whole brain by quantifying the modularity of the network. ANOVAs on modularity revealed a main effect of age group ($F(1,54) = 43.38$, $p < 0.001$, $\eta_p^2 = 0.45$) and task condition ($F(4,216) = 2.59$, $p = 0.04$, $\eta_p^2 = 0.05$). Across all task conditions, older adults had lower modularity than young adults. Across all participants, RESTING-STATE, CATEGORIZE, SCENES, and FACES conditions were associated with higher modularity than the BOTH condition (Figure 3.2B). While the main effect of task condition on modularity using the AAL atlas does not pass a Bonferroni-corrected significance threshold of $p < 0.05$, we replicated this result using the Power et al. (2011) atlas (main effect of task condition, corrected $p < 0.05$; see Supplementary Material). There was no significant age group by task condition interaction ($F(4,216) = 1.12$, $p = 0.35$, $\eta_p^2 = 0.02$).

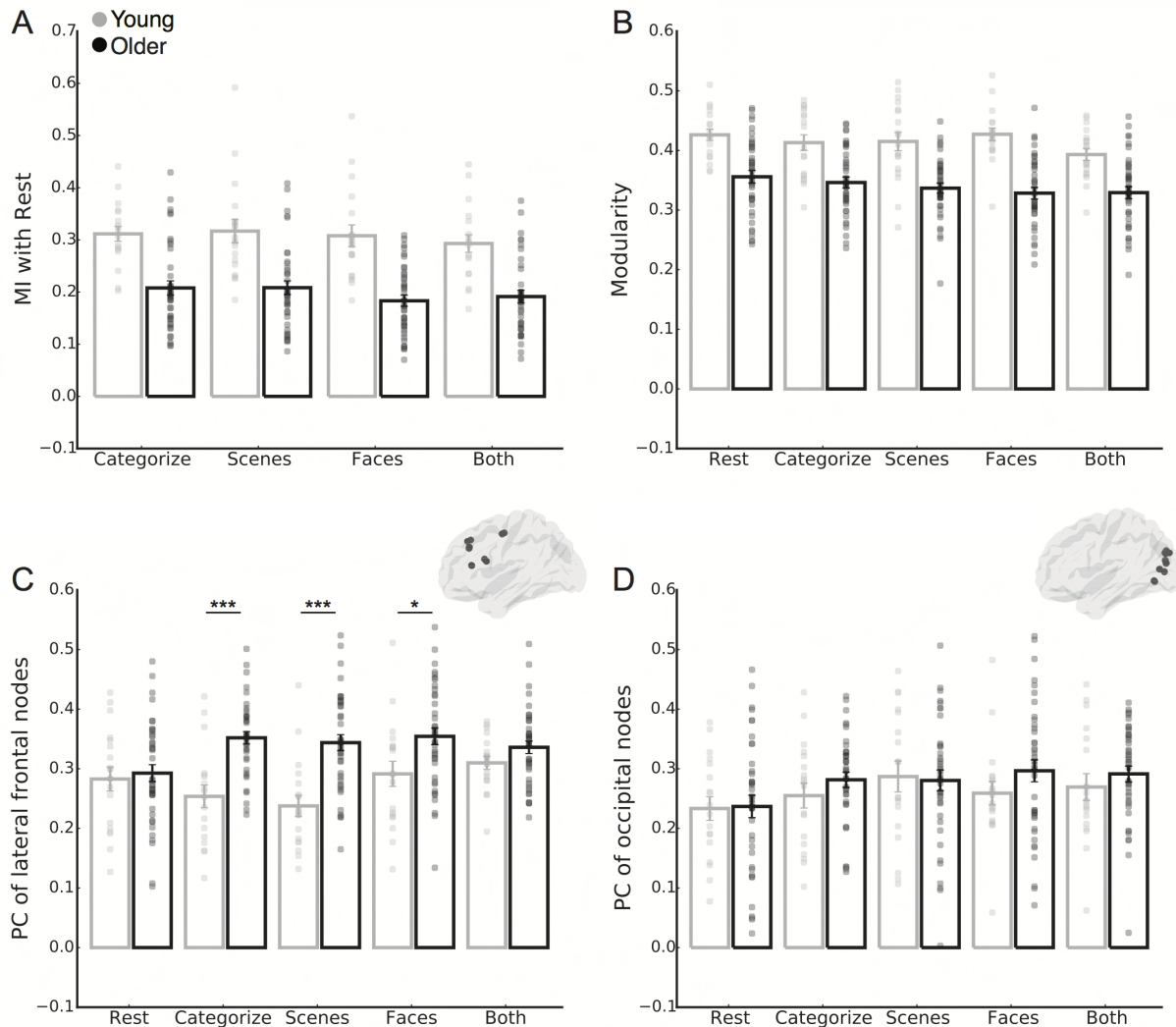


Figure 3.2. Module-based network metrics during resting state and task. (A) Mutual information (MI) between resting state network partitions and those derived from the task conditions. Note that we quantified the MI between each subject's resting network partition to those derived from the 4 task conditions. In this manner, MI during resting state would be equal to 1 because it is the network used for comparison and is therefore not plotted in (A). Modularity (B) and lateral frontal (C) and occipital (D) participation coefficient (PC) for resting state and task conditions. Centers of mass for lateral frontal and occipital AAL atlas nodes used to calculate PC are plotted on a sagittal view of the brain in C and D, respectively. Data are presented as mean \pm standard error of the mean. Pairwise comparisons between young and older groups across the task conditions were conducted for metrics showing significant age group by task condition interactions. *** $p < 0.001$; * $p < 0.05$.

Participation coefficient of lateral frontal regions during resting-state and task performance. To examine the specific contribution of lateral frontal connections to network reconfiguration, we quantified the distribution of between-module connections (i.e., participation coefficient, PC) from ten lateral frontal regions in the AAL atlas (Figure 3.2C). An ANOVA on lateral frontal PC revealed main effects of age group ($F(1,54) =$

18.26, $p < 0.001$, $\eta_p^2 = 0.25$) and task condition ($F(4,216) = 2.96$, $p = 0.02$, $\eta_p^2 = 0.05$). Across all task conditions, older adults had higher frontal PC than young adults. Across all participants, frontal PC was lower during RESTING-STATE and SCENES compared to FACES and BOTH. The main effect of task condition on lateral frontal PC passes a marginal Bonferroni-corrected significance threshold of $p < 0.1$.

There was also a significant age group by task condition interaction ($F(4,216) = 4.68$, $p = 0.001$, $\eta_p^2 = 0.08$), indicating that the increased frontal PC in older adults was not equivalent across all task conditions (Figure 3.3). Specifically, while there were no differences in lateral frontal PC between older and young adults during a RESTING-STATE condition ($p = 0.70$), older adults showed increased frontal PC compared to young adults during the three less demanding task conditions (CATEGORIZE, $p < 0.001$; SCENES, $p < 0.001$; FACES, $p = 0.02$). Further, there were no significant differences between older and young adults in the BOTH condition ($p = 0.14$). This suggests that older adults exhibited a task-related increase in lateral frontal PC during all conditions, while young adults only exhibited an increase during the most demanding condition. Importantly, this age group by task condition interaction was not present in 10 control regions from the occipital cortex (Figure 3.2D; $F(4,216) = 0.55$, $p = 0.70$, $\eta_p^2 = 0.01$), suggesting that the age-related reconfiguration of between-module connections may be specific to the lateral frontal cortex.

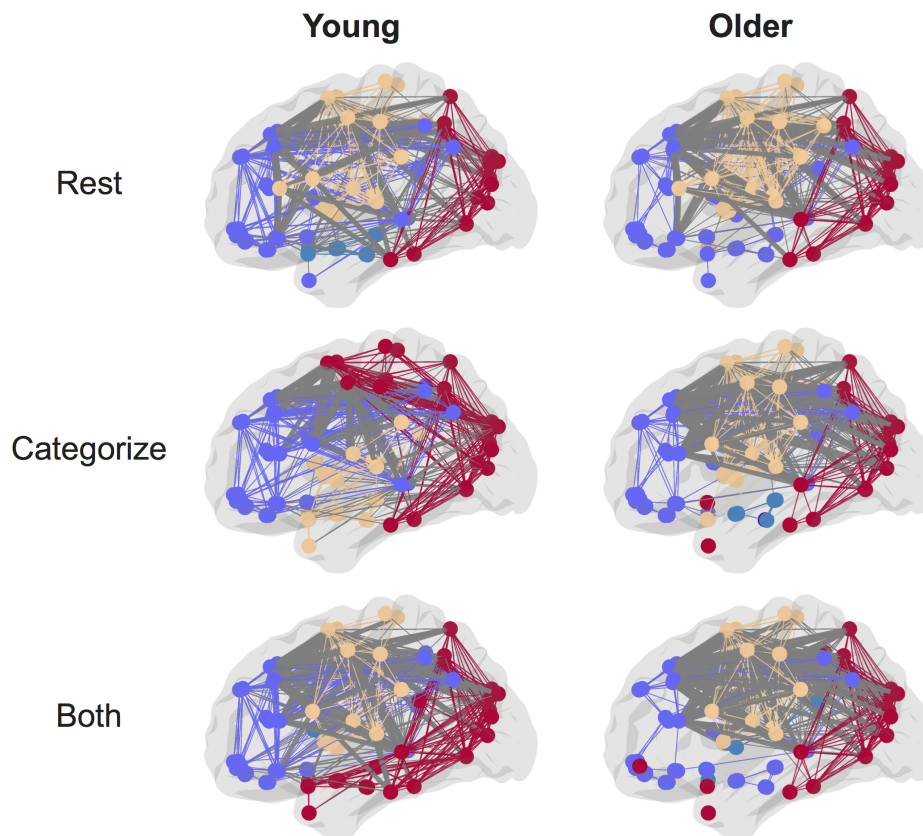


Figure 3.3. Sagittal views of group partitions during resting state (top) and the least and most demanding task conditions (middle and bottom, respectively) for young and older adults. For visualization purposes,

group consensus partitions were created by averaging the AAL atlas correlation matrices across subjects in each group and thresholding at 20% of possible network connections (although note that all analyses presented in the results were done at the individual subject level at multiple connection thresholds as described in the methods). Within-module edges are colored to match that of nodes in their own module and between-module edges are colored gray, with lateral frontal between-module connections bolded. Older adults show more between-module lateral frontal connections at lower levels of demand (CATEGORIZE) compared with young adults. Young and older adults have similar amounts of lateral frontal connections during resting state and the more demanding task condition (BOTH).

Behavioral correlates of network reconfiguration in older adults. To investigate how changes in between-module connections in lateral frontal cortex during task performance are related to individual differences in behavior, we correlated task-based reconfiguration of lateral frontal PC (i.e., difference between task and resting-state) and mean task RT. We averaged PC for each task condition given that older adults exhibited increases in PC across all task conditions. Older adults who exhibited greater task-based increases in lateral frontal PC had faster task performance (Figure 3.4A; $\rho(36) = -0.32$, $p = 0.05$), while this relationship was not present in young adults ($\rho(16) = 0.31$, $p = 0.21$). The difference in correlations between older and young groups was statistically significant ($p = 0.03$). Critically, the correlation in older adults was only present when quantifying the difference in lateral frontal PC between resting-state and task; there was no correlation between task performance and lateral frontal PC during resting-state or task alone in older adults (RESTING-STATE, $p = 0.14$; TASK, $p = 0.76$).

Replication analyses of changes in network reconfiguration. We reproduced the results of this study using a different brain parcellation scheme comprised of functionally defined ROIs (Power et al., 2011), with two separate approaches. First, we used spectral clustering to identify network modules for each subject and task condition. While simulated annealing is one of the most accurate methods to identify modules (Guimera and Amaral, 2005), it is computationally intensive. Thus, for this larger set of ROIs, we identified modules using a spectral clustering algorithm (Newman, 2006) that provides a tradeoff between accuracy and expediency, after thresholding the correlation matrices similarly to previous reports (Power et al., 2011): the top 2-10% of connections in 5% increments. This is an approach we have taken previously (Sadaghiani et al., 2015). Second, we used predefined modules previously identified in a group of individuals (Power et al., 2011), thus applying the same modular partition across all individuals rather than identifying modules with a clustering algorithm. This approach allowed us to examine changes in the connections between modules that are not influenced by changes in the grouping of nodes into modules themselves. In other words, the modules were fixed for all subjects and we then examined changes in the connectivity between modules (i.e., modularity and lateral frontal PC). Using these two approaches, we reproduced our previous results for changes in module-based network metrics and correlations with task performance (see Supplementary Material).

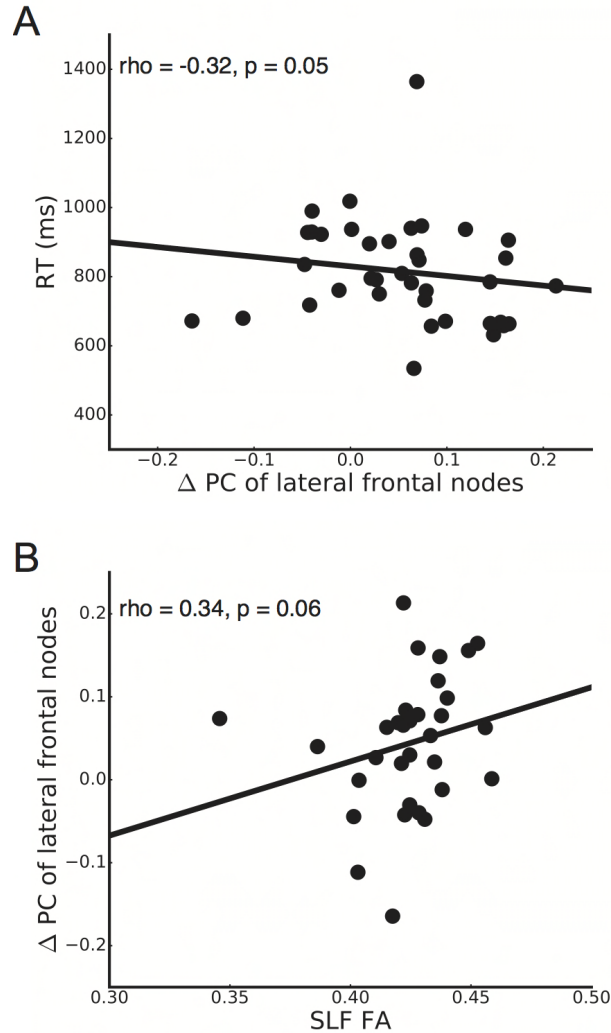


Figure 3.4. Relationship between change in lateral frontal PC from resting state to task and executive control task performance (RT; A) and fractional anisotropy (FA) of the superior longitudinal fasciculus (SLF; B) in older adults. Abbreviations: PC, participation coefficient; RT, reaction time.

3.4.3 Structural correlates of network reconfiguration in older adults

To investigate how the age-related functional reconfiguration of between-module connections in lateral frontal cortex is related to structural connectivity, we correlated task-based reconfiguration of lateral frontal PC and FA of the SLF in older adults (mean \pm SD, 0.42 ± 0.02). Older adults who exhibited greater task-based increases in lateral frontal PC had marginally greater FA of the SLF (Figure 3.4B; $\rho(30) = 0.34$, $p = 0.06$). While the correlation with 10 lateral frontal ROIs from the AAL atlas was marginally significant, we replicated this result using the 30 lateral frontal ROIs from the Power et al. (2011) atlas when modules were identified with spectral clustering. Using this atlas, greater task-based increases in lateral frontal PC were significantly related to greater SLF FA ($p = 0.02$; see Supplementary Material).

3.4.4 Consideration of confounds on network reconfiguration in older adults

We first examined the effects of head motion on measurements of network organization. While head motion was higher in older adults across all task conditions ($F(1,54) = 13.37$, $p = 0.001$), there was no effect of task condition or age group by task condition interaction on motion ($F(4,216) = 0.22$, $p = 0.83$; $F(4,216) = 0.80$, $p = 0.46$). Importantly, head motion did not differ *between* resting-state and task in either the older or young groups ($p = 0.91$; $p = 0.98$), suggesting that the age differences in network reconfiguration between resting-state and task were not driven by differences in head motion between conditions in the age groups. Further, including head motion as a covariate in the AAL network analyses did not substantially change any results.

We also examined effects of the time period of resting data collection on measurements of network organization. While the proportion of resting-state scans pre- or post-task was matched in the older and young groups, it is possible that there were group differences (i.e., an age group by resting-state position interaction). To test this, we repeated all AAL network analyses with resting-state position (i.e., pre- or post-task) as an additional between-subjects factor. There was no significant two-way interaction between age group and resting-state position or three-way interaction between age group, resting-state position, and task condition for mutual information, modularity, or lateral frontal PC. This suggests that the effects reported are not differentially present whether the resting-state scan was collected pre- or post-task.

Finally, we examined the effect of task run selection on measurements of network organization. We repeated all AAL network analyses with task-position (i.e., first three runs or containing some subsequent runs) as an additional between-subjects factor. There was no significant two-way interaction between age group and task-position or three-way interaction between age group, task-position, and task condition for mutual information, modularity, or lateral frontal PC. These results suggest that the results reported are not differentially present whether the task time-series were composed of the first three runs or subsequent runs.

3.5 Discussion

Here, we analyzed resting state and task-based fMRI data to characterize brain network reconfiguration that supports executive control functioning (i.e., performance of an N-back task) in older adults. Recent studies have shown that older adults have a less-modular brain network organization in a resting state compared with young adults (Onoda and Yamaguchi, 2013; Chan et al., 2014; Geerligs et al., 2014a). However, the extent to which this organization reconfigures during a cognitive task in older adults remains underspecified. We provide evidence that older adults exhibit larger changes in network organization at lower levels of N-back task demands compared with young adults. More specifically, older adults showed greater between-module connectivity of lateral frontal regions compared with young adults at low levels of executive control demands. In older adults, greater network reconfiguration (i.e., increased between-

module connections of lateral frontal regions) from resting state to task was related to better task performance, suggesting that greater between-module integration during task performance is critical for successful executive control in aging. Finally, network reconfiguration from resting state to task in older adults was related to individual variability in white matter microstructure of the SLF, the main tract connecting frontal and posterior brain regions.

3.5.1 Changes in topological overlap of modules between resting state and task

We found that older adults had less overlap between modules present during a task-free resting state and those present during the performance of an N-back task. In other words, the composition of modules identified during a resting state changed more during the task in older adults compared with young adults. This finding suggests that older adults exhibited greater reconfiguration of network modules detected during a resting state while performing a task.

Furthermore, across both young and older adults, we found that modules identified during the more challenging task conditions had less overlap with resting-state modules, suggesting that resting modular organization changed more during higher task demands. This latter finding is consistent with a previous study in young participants showing that there was less overlap of modules across subjects (e.g., more variability in the modules across subjects) during a more difficult N-back condition (Stanley et al., 2014). This result and ours adds to a growing literature suggesting that the modular organization of the brain shows more pronounced reconfigurations with increasing cognitive demands.

3.5.2 Reconfiguration of modular brain network organization during resting state and task

We found that older adults exhibited lower modularity than young adults during a resting state, which supports accumulating evidence that aging reduces the segregation of networks into distinct modules when measured in the absence of a task (Onoda and Yamaguchi, 2013; Chan et al., 2014; Geerligts et al., 2014a). Decreased modularity in older adults has been hypothesized to reflect reduced functional integrity of brain network modules, in which brain subnetworks are less segregated in older adults compared with young adults. We further found that older adults had lower modularity than young adults during the N-back task, suggesting that such global age differences in brain network organization are also present throughout task performance.

In addition, across both young and older adults, we found that modularity decreased with increasing task demands. This is consistent with previous findings in young adults examining network changes during task performance. First, prior work has shown that within-module connections decrease and between-module connections increase from resting state to task (Cole et al., 2014). Second, studies have shown that modularity decreases with increasing working memory load and that this reconfiguration is related to better task performance (Kitzbichler et al., 2011; Stanley et al., 2014; Vatansever et al., 2015). We found a similar pattern of results, in which the most demanding

conditions of the N-back task were associated with the lowest modularity and extend this work by showing similar effects across both young and older adults. Changes in modularity due to increasing cognitive demands are proposed to reflect increased integration between brain network modules to support higher processing demands. Furthermore, it has been proposed that reductions in modularity with increasing cognitive effort represent the formation of a neuronal “workspace” (Dehaene et al., 1998) that supports more efficient communication across the brain (Kitzbichler et al., 2011).

3.5.3 Alterations in between-module connections with increasing task demands

Although we found that modularity was reduced in older adults during a resting state and task performance, we also examined how specific between-module connections reconfigured during these conditions in young and older adults. We found that young and older adults had similar between-module connectivity (PC) of lateral frontal regions during a resting state, and that older adults exhibited increased connectivity during all task conditions. Specifically, older adults had greater between-module connectivity than young adults during the less-demanding conditions, but similar between-module connectivity in the most demanding condition (i.e., BOTH). These results suggest that older adults recruited additional between-module connections at all levels of task demand, whereas young adults only did so when task demands were highest. Furthermore, in older adults, greater network reconfiguration from a resting state to task was associated with better task performance. Not surprisingly, this relationship was not present in young adults, given that they did not show an increase in lateral frontal PC for most of the task conditions. Finally, we found that greater network reconfiguration from a resting state to task in older adults was associated with greater FA of the SLF, a core frontal-posterior white matter tract. Our results support the “workspace” hypothesis: increased cognitive effort is associated with increased between-module integration that is related to better task performance (Kitzbichler et al., 2011; Stanley et al., 2014; Vatansever et al., 2015). Here, we provide new evidence that older adults exhibit increased between-module integration at lower levels of cognitive demand than young adults and also show a relationship between structural connectivity and functional network changes in older adults. It should be noted that older adults showed this reconfiguration even when performance was equivalent to young adults in terms of accuracy and reaction time (e.g., during CATEGORIZE), suggesting that network changes were not merely due to the differences in performance between the older and young groups.

Most studies examining age-related changes in brain function due to specific cognitive demands have examined the activation of individual brain regions, rather than using a large-scale network approach. In particular, numerous studies have shown that older adults exhibit increased frontal activity during less-demanding cognitive tasks compared with young adults (Mattay et al., 2006; Spreng et al., 2010; Turner and Spreng, 2012; 2015). Together, these studies have been interpreted to reflect the recruitment of additional neural resources that support cognition at lower levels of cognitive demand (Reuter-Lorenz and Cappell, 2008). Our results further support the idea of compensatory recruitment and, importantly, suggest a large-scale network-level

mechanism by which the aging brain reorganizes to support executive control processing. Although our correlation analyses cannot provide information about directionality, we propose that greater structural connectivity of frontal-posterior white matter pathways enables older adults to appropriately reconfigure brain networks between a resting state and task performance, depending on the task demands. Specifically, older adults showed greater increases in lateral frontal between-module connections at lower levels of demand compared with young adults. We postulate that this pattern of increased connectivity between frontal regions and other modules is reflective of a more integrated network architecture that is important for successful executive control processing in aging.

Future work should investigate how other changes that occur with aging (e.g., reductions in cerebral gray matter) are related to functional network reconfiguration. Furthermore, as aging is associated with cognitive changes in other domains, such as long-term memory, an important future step would be to quantify network changes during other cognitive tasks. There is some evidence that older adults show larger connectivity changes in nonfrontal regions (i.e., parietal and somatosensory cortex) with increasing task demands compared with young adults (Geerligts et al., 2014b). The network reconfiguration reported here could be a domain-general response to increasing cognitive demands or there could be unique changes for the processing of specific cognitive functions.

3.5.4 Methodological considerations

There are many valid approaches to examine brain network properties with fMRI data. Regarding methods for parcellating the brain into ROIs, we demonstrated that our results are reproducible for both anatomically (Tzourio-Mazoyer et al., 2002) and functionally (Power et al., 2011) defined ROIs. Although the larger ROIs in the AAL atlas may encompass multiple functional regions, there may also be drawbacks to using a functionally defined atlas when comparing groups of young and older adults. Specifically, most functionally defined atlases have been created using data from young subjects. Thus, differences in functional boundaries in older adults could bias network measures in a way that an anatomically defined atlas would not. Given this, the replication of our results using an anatomical and functional atlas demonstrates the robustness of our findings. Future work should examine how potential changes in the functional boundaries of brain regions in older adults influence network measures.

Regarding methods for identifying brain network modules, subject-level modular networks may be noisier than those derived at the group level (e.g., identifying modules after averaging correlation matrices across subjects). Furthermore, if the modules are different across subjects, changes in network connections could arise from differences in the modules themselves and/or changes in connectivity. Although we examined the overlap in modules with MI, we also replicated our results after imposing the same modular organization across all subjects.

Finally, although our primary findings demonstrated an interaction between age group and task condition, we reported several main effects of age group on network

organization (e.g., MI and modularity). We cannot rule out the possibility that these effects are due to age-related changes in vasculature that may impact the BOLD signal, anatomical changes in gray and white matter (D'Esposito et al., 2003), or differences in functional image acquisition between older and young adults.

Table 3.1. Mean (SD) of task performance and network metrics (AAL atlas) for young and older adults

	Resting-state		Categorize		Scenes		Faces		Both	
	Young	Older	Young	Older	Young	Older	Young	Older	Young	Older
Accuracy (%)	N/A	N/A	95.83 (5.25)	95.35 (9.92)	96.39 (5.12)	92.98 (7.66)	94.91 (3.68)	87.11 (10.88)	91.94 (6.94)	83.55 (9.05)
RT (ms)	N/A	N/A	629.33 (113.74)	647.47 (150.86)	671.40 (144.62)	753.98 (159.79)	745.98 (163.99)	838.63 (154.67)	837.89 (168.70)	1,020.22 (187.76)
MI	N/A	N/A	0.31 (0.06)	0.21 (0.08)	0.32 (0.09)	0.21 (0.08)	0.31 (0.09)	0.18 (0.07)	0.29 (0.07)	0.19 (0.07)
Mod	0.43 (0.04)	0.36 (0.07)	0.41 (0.06)	0.35 (0.06)	0.42 (0.07)	0.34 (0.05)	0.43 (0.04)	0.33 (0.06)	0.39 (0.04)	0.33 (0.06)
Frontal PC	0.28 (0.09)	0.29 (0.09)	0.25 (0.08)	0.35 (0.06)	0.24 (0.08)	0.34 (0.08)	0.29 (0.09)	0.35 (0.09)	0.31 (0.05)	0.34 (0.07)
Occipital PC	0.23 (0.08)	0.24 (0.11)	0.25 (0.09)	0.28 (0.08)	0.29 (0.11)	0.28 (0.11)	0.26 (0.08)	0.30 (0.11)	0.27 (0.10)	0.29 (0.08)

Key: AAL, automated anatomical labeling; MI, mutual information; Mod, Modularity; PC, participation coefficient; RT, reaction time; SD, standard deviation

3.6 Supplemental Material

3.6.1 Replication analyses of changes in network reconfiguration using a functionally defined brain atlas.

We reproduced the results from Section 3.4.2 using a different brain parcellation scheme comprised of functionally defined ROIs (Power et al., 2011), with two separate approaches. First, we used spectral clustering (Newman, 2006) to identify network modules for each subject and task condition. MI between resting-state and task conditions revealed a main effect of age group (older less than young; $F(1,54) = 106.66$, $p < 0.001$) and a marginal effect of task condition (CATEGORIZE and SCENES greater than BOTH; linear effect, $F(1,54) = 3.22$, $p = 0.08$). There were also main effects of age group ($F(1,54) = 54.23$, $p < 0.001$) and task condition ($F(4,216) = 4.43$, $p = 0.003$) on modularity. Across all task conditions, modularity was lower in older adults. Across all participants, modularity was highest during RESTING-STATE and higher in CATEGORIZE, SCENES, and FACES compared to BOTH. We identified 30 lateral frontal ROIs in this atlas to examine the changes in PC between resting-state and task as in Section 3.4.2 Comparing lateral frontal PC between older and young adults, older and young adults had similar lateral frontal PC during RESTING-STATE ($p = 0.78$). Older adults exhibited greater lateral frontal PC than young adults during all task conditions but BOTH (CATEGORIZE, $p = 0.03$; SCENES, $p = 0.03$; FACES, $p = 0.03$; BOTH, $p = 0.41$). Increases in lateral frontal PC from resting-state to task in these 30 regions was marginally associated with faster task performance in older but not young adults (older, $\rho(36) = -0.30$, $p = 0.06$; young, $\rho(18) = 0.30$, $p = 0.23$), with the difference in correlations between older and young groups being statistically significant ($p = 0.04$).

Second, we used predefined modules previously identified in a group of individuals (Power et al., 2011), thus applying the same modular partition across all individuals rather than identifying modules at the subject-level with a clustering algorithm. We reproduced our previous results for both modularity and lateral frontal PC (note that MI between resting-state and task is equal to 1 for this analysis, as the modules are identical for all subjects and task conditions). Modularity was lower in older adults compared to young adults (main effect of age group, $F(1,54) = 75.95$, $p < 0.001$). Further, modularity during RESTING-STATE was higher than FACES and BOTH and modularity was lowest in BOTH compared to all other conditions (main effect of task condition, $F(4,216) = 6.31$, $p = 0.001$). Comparing lateral frontal PC between young and older adults, older and young adults had similar PC for the 30 lateral frontal regions during RESTING-STATE ($p = 0.77$). Older adults exhibited greater lateral frontal PC than young adults during all task conditions but BOTH where there was only a marginal difference between the groups (CATEGORIZE, $p = 0.005$; SCENES, $p = 0.01$; FACES, $p = 0.02$; BOTH, $p = 0.08$). The increase in lateral frontal PC from resting-state to task in these 30 regions was not significantly associated with faster task performance in older or young adults (older, $\rho(36) = -0.25$, $p = 0.13$; young, $\rho(18) = 0.13$, $p = 0.60$). However, while the relationship between lateral frontal PC and reaction time was not significant after imposing a predefined partition in older adults, the correlation magnitude was not significantly different than what we observed using the Power et al.

(2011) atlas with modules identified by spectral clustering (i.e., $\rho = -0.25$ compared to $\rho = -0.30$, respectively; $p = 0.82$).

3.6.2 Replication analyses of structural correlates of network reconfiguration using a functionally defined brain atlas.

We replicated the results in Section 3.4.3 using the 30 lateral frontal ROIs from the Power et al. (2011) atlas when modules were identified with spectral clustering at the subject level ($\rho(30) = 0.43$, $p = 0.02$). This correlation was not significant when predefined modules were applied to all subjects ($\rho(30) = 0.15$, $p = 0.42$). While the relationship between lateral frontal PC and SLF FA was not significant after imposing a predefined partition in older adults, the correlation magnitude was not significantly different than what we observed using the Power et al. (2011) atlas with modules identified by spectral clustering (i.e., $\rho = 0.15$ compared to $\rho = 0.43$, respectively; $p = 0.19$).

Chapter 4

MODULAR BRAIN NETWORK ORGANIZATION PREDICTS RESPONSE TO COGNITIVE TRAINING IN OLDER ADULTS

4.1 Abstract

Although cognitive deficits are common in aging, cognitive training interventions can mitigate these deficits to improve functioning in older adults. Baseline neural factors, such as properties of brain networks, may predict training outcomes. Here, we investigated the relationship between pre-training network modularity, a measure of the segregation of brain sub-networks, and training-related gains in cognition in older adults. We found that older adults with more segregated brain sub-networks (i.e., more modular networks) at baseline during a task-free resting-state exhibited greater training improvements in the ability to synthesize complex information. Further, the relationship between modularity and training-related gains was pronounced in modules mediating “associative” functions compared with those involved in sensory-motor processing. These results suggest that assessments of brain networks are a useful biomarker that can be used to guide the implementation of cognitive interventions and improve outcomes across individuals. More broadly, properties of brain networks may also capture individual differences in capacity for learning and neuroplasticity.

4.2 Introduction

Aging is associated with declines in various cognitive functions, such as attention, cognitive control, and memory (Grady, 2012). There is emerging evidence that characterization of large-scale brain network properties provides an important framework for understanding such complex behaviors, by examining the interactions of sub-networks, or modules, that span the whole brain (Mattar et al., 2015; Medaglia et al., 2015). Previous work has shown that brain networks exhibit a modular organization in that they are comprised of sub-networks, or modules. The extent of segregation and integration of brain network modules can be quantified with a modularity metric (Newman and Girvan, 2004), in which highly modular networks have many connections within modules and fewer connections to other modules. Studies examining changes in modularity with aging have shown that older adults have less modular networks than young adults (Onoda and Yamaguchi, 2013; Geerligs et al., 2014a), particularly in sub-networks thought to mediate “associative” functions, such as fronto-parietal control and dorsal and ventral attention modules (Chan et al., 2014).

Although cognitive declines are common in older adulthood, growing evidence suggests that cognitive training can induce neural plasticity and improve aspects of cognition (Lustig et al., 2009; Brehmer et al., 2011; Kelly et al., 2014; Ballesteros et al., 2015; Bherer, 2015) and underlying connectivity within brain sub-networks (Chapman et al.,

2015; Cao et al., 2016) in older adults, although changes in network modularity associated with training have not been directly assessed. For example, we have shown that strategy-based gist reasoning training alters functional connectivity of default mode and executive sub-networks and improves abstract thinking, concept formation, and other executive functions in a group of healthy older adults (Chapman et al., 2015). Despite previous work showing that cognitive training can alter network connectivity in older adults, there has been little focus on identifying baseline neural factors that can predict training-related improvements in cognition. In a study with traumatic brain injury (TBI) patients, we found that brain network organization assessed at baseline predicted training-related gains. Specifically, individuals with higher brain network modularity showed greater improvements on tests of executive functioning after goal-oriented attention self-regulation training (Arnemann et al., 2015). These findings suggest that brain network modularity can be used as a biomarker to guide cognitive interventions. However, the utility of modularity as a predictor of training outcomes has not yet been tested in healthy individuals.

In the present study, we examined the relationship between baseline brain network modularity and cognitive improvements in healthy older adults who participated in a previously published cognitive training protocol (Chapman et al., 2015). We hypothesized that older adults with higher baseline modularity would show greater training-related gains compared to those with lower modularity.

4.3 Materials and Methods

4.3.1 Participants

A total of 29 cognitively normal older adults (age range: 57-70) were included in this study. Participants were randomized to wait-list control (N = 14; mean \pm SD age: 64.36 \pm 3.30; 9 females; mean \pm SD IQ: 120.43 \pm 11.67) or cognitive training (N = 15; mean \pm SD age: 63.07 \pm 2.87; 9 females; mean \pm SD IQ: 122.13 \pm 8.30). The groups were matched on age ($t(27) = 1.13, p = 0.27$), distribution of gender ($\chi^2(1, N = 29) = 0.06, p = 0.81$), and WASI IQ ($t(27) = -0.46, p = 0.65$). Participants were screened for dementia (Telephone Interview of Cognitive Status-Modified, TICS-M), early cognitive impairment (Montreal Cognitive Assessment, MoCA), and depressive symptoms (Beck Depression Inventory-II, BDI) and underwent a complete medical assessment by a physician to ensure good health. Criteria for inclusion were: right-handed, native English speaker, no history of neurological or psychiatric conditions, normal IQ range, normal cognitive status (TICS-M \geq 28, MoCA \geq 26, BDI \leq 14), minimum of high school diploma, no MR scanning contraindications, and normal body mass (BMI \leq 40). Informed consent was obtained from all subjects in accordance with the Institutional Review Boards of The University of Texas at Dallas, the University of Texas Southwestern Medical Center, and the Cooper Institute.

4.3.2 Cognitive training (SMART)

The cognitive training group engaged in a 12-week course of Strategic Memory and Reasoning Training (SMART) (Vas et al., 2011). SMART is a strategy-based gist reasoning training that focuses on the use of strategic attention, integrated reasoning, and innovation to improve cognitive control processes related to gist reasoning. Each week, participants completed one-hour of small group training ($n \leq 5$ in each group) and two one-hour sessions of home practice (Chapman et al., 2015). To examine cognitive changes specifically associated with SMART, these participants were compared to a group of wait-list control subjects.

4.3.3 Neurocognitive measures

A battery of neurocognitive measures was collected as described in Chapman et al. (2015). In this study, we focused on pre- and post-training assessments of gist reasoning and concept abstraction measures (Test of Strategic Learning (TOSL; (Vas et al., 2011)) and WAIS-III Similarities, respectively) that were previously shown to improve following SMART training (Chapman et al., 2015). Gist reasoning refers to synthesizing abstracted meanings from lengthy textual information (e.g., global ideas conveyed in an article) and concept abstraction refers to identifying categorical abstraction between two items (e.g., how a fly and an airplane are alike).

4.3.4 MRI acquisition and preprocessing

At baseline, MRI scans were collected with an 8-channel head coil on a 3T Philips scanner. A T1-weighted sequence was used to acquire anatomical images (in-plane resolution = 1 mm^2 , 160 1-mm thick sagittal slices, TR/TE = 8.3/3.8 ms). A T2*-weighted echoplanar imaging (EPI) sequence was used to acquire a four-minute resting-state scan (in-plane resolution = 3.44 mm^2 , 36 4-mm thick ascending axial slices, TR/TE = 2000/30 ms).

Standard preprocessing of MRI data was carried out with Configurable Pipeline for the Analysis of Connectomes (CPAC). Briefly, EPI data was slice-time and motion corrected and co-registered to the T1-weighted structural image. Then, signals from motion (Friston 24-parameter model), the top five principal components from white matter and CSF voxels (Behzadi et al., 2007), and linear and quadratic trends were regressed out. Lastly, EPI data was bandpass filtered (0.009 – 0.08 Hz), scaled to a whole-brain mode value of 1000, and warped to MNI space.

4.3.5 Functional connectivity and network analyses

Participants' T1-weighted anatomical scans were registered to MNI space and parcellated into 264 regions of interest (ROIs) (Power et al., 2011). Time-series from EPI data were averaged over the voxels in each ROI. Nine ROIs were excluded from subsequent analyses due to incomplete EPI coverage in at least one subject (i.e., no ROI voxels remained). Correlation matrices were created for each participant by correlating the time-series between each pair of ROIs using Pearson's correlation coefficient and applying a Fisher z-transform. Adjacency matrices were created by

thresholding each correlation matrix over a range of thresholds (the top 2-10% of connections in 2% increments), resulting in unweighted, undirected graphs. We then assigned each ROI to a module as defined in Power et al. (2011) and quantified each participant's network modularity, a measure that compares the number of connections within to the number of connections between modules (Newman and Girvan, 2004). Modularity will be 1 if all connections fall within modules and it will be 0 if there are no more connections within modules than would be expected by chance. We also repeated these analyses using spectral clustering (Newman, 2006) to group ROIs into subject-specific modules before quantifying modularity. Unless otherwise noted, modularity values are presented as the average across connection density thresholds.

4.3.6 Statistical analysis

To quantify the relationships between baseline modularity and training-related cognitive gains, we examined the correlation between pre-training modularity and cognitive gains in TOSL and Similarities, computed as the difference in post-training and pre-training scores, separately in the control and SMART groups. Due to the relatively small sample size in each group, we conducted non-parametric Spearman correlations to reduce the influence from extreme values.

As aging has been shown to have a more pronounced effect on the modularity of association modules compared with sensory-motor modules (Chan et al., 2014), we also examined the differential contribution of the modularity of these sub-networks on predicting cognitive gains in older adults. The whole-brain modularity metric is computed as the sum of the modularity values for each module. Using the modules defined in Power et al. (2011), we computed the baseline modularity of sensory-motor and association modules as described in Chan et al. (2014). For sensory-motor network modularity, we computed the average modularity of the auditory, somato-motor (hand and mouth), and visual modules. For association network modularity, we computed the average modularity of the cingulo-opercular, default mode, dorsal attention, fronto-parietal, salience, and ventral attention modules. We then examined the relationships between cognitive training gains and sensory-motor and association modularity in each group.

4.4 Results

4.4.1 Cognitive changes after SMART training

As previously reported (Chapman et al., 2015), there were no group differences in baseline TOSL ($p = 0.30$) or Similarities ($p = 0.82$); however, the SMART group performance on TOSL (complex abstraction) and Similarities (simple concept abstraction) improved (group by time Interaction: $F(1,27) = 5.82$, $p = 0.02$; $F(1,27) = 4.03$, $p = 0.06$). Within the SMART group, participants improved in TOSL (Figure 4.1A; $p = 0.05$) and Similarities (Figure 4.1B; $p = 0.001$), whereas control participants' scores did not change ($p = 0.15$; $p = 0.10$, respectively).

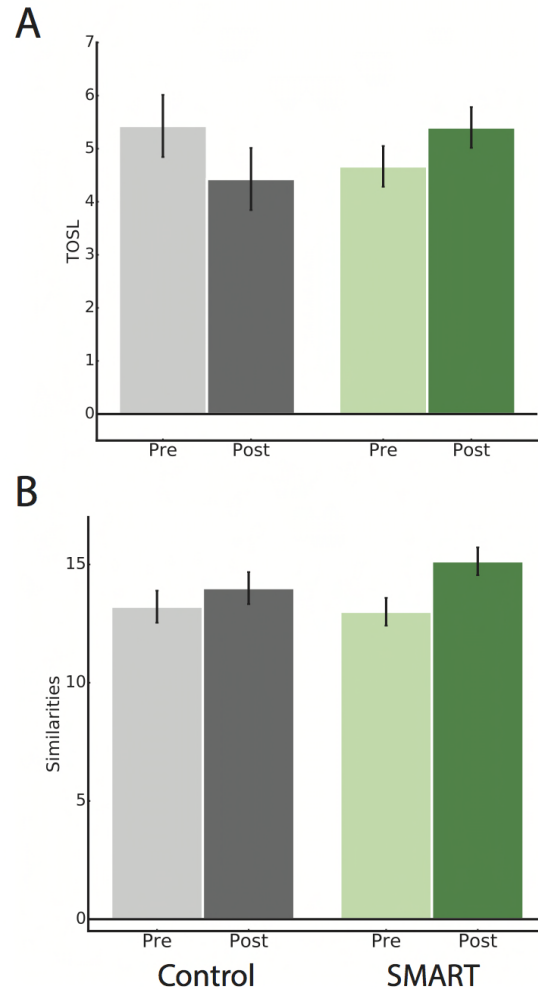


Figure 4.1. Performance on Test of Strategic Learning (TOSL, A) and WAIS-III Similarities (B) for control and SMART groups pre- and post-training. Scores are presented as in Chapman et al. (2015), where TOSL is presented as raw scores and Similarities is presented as standard scores. Data are presented as mean \pm SEM.

4.4.2 Relationship between baseline whole-brain modularity and cognitive changes

Baseline modularity was similar in the SMART and control groups ($t(27) = 0.39$, $p = 0.70$) and was not related to participant age in either group (control: $\rho(13) = -0.29$, $p = 0.31$; SMART: $\rho(14) = -0.14$, $p = 0.62$). In the SMART group, baseline modularity was positively correlated with training-related gains on TOSL ($\rho(13) = 0.65$, $p = 0.01$), but not on Similarities ($\rho(13) = 0.03$, $p = 0.90$). There was no relationship in the control group between baseline modularity and TOSL ($\rho(12) = -0.12$, $p = 0.68$) or Similarities ($\rho(12) = -0.26$, $p = 0.37$). As the correlation between baseline modularity and training gains was not significant for Similarities, we focus on training-related TOSL gains for the remaining analyses.

The modularity-TOSL gain correlations were significantly different between the control and SMART groups (Figure 4.2A; $p = 0.03$). While pre-training TOSL was related to TOSL gains in both groups when they were combined ($p < 0.001$), there was no relationship between baseline TOSL and modularity in either group ($p > 0.23$). We further confirmed the modularity-TOSL gain relationship was significant in the SMART group, but not control group, when controlling for pre-training TOSL ($p = 0.03$; $p = 0.22$).

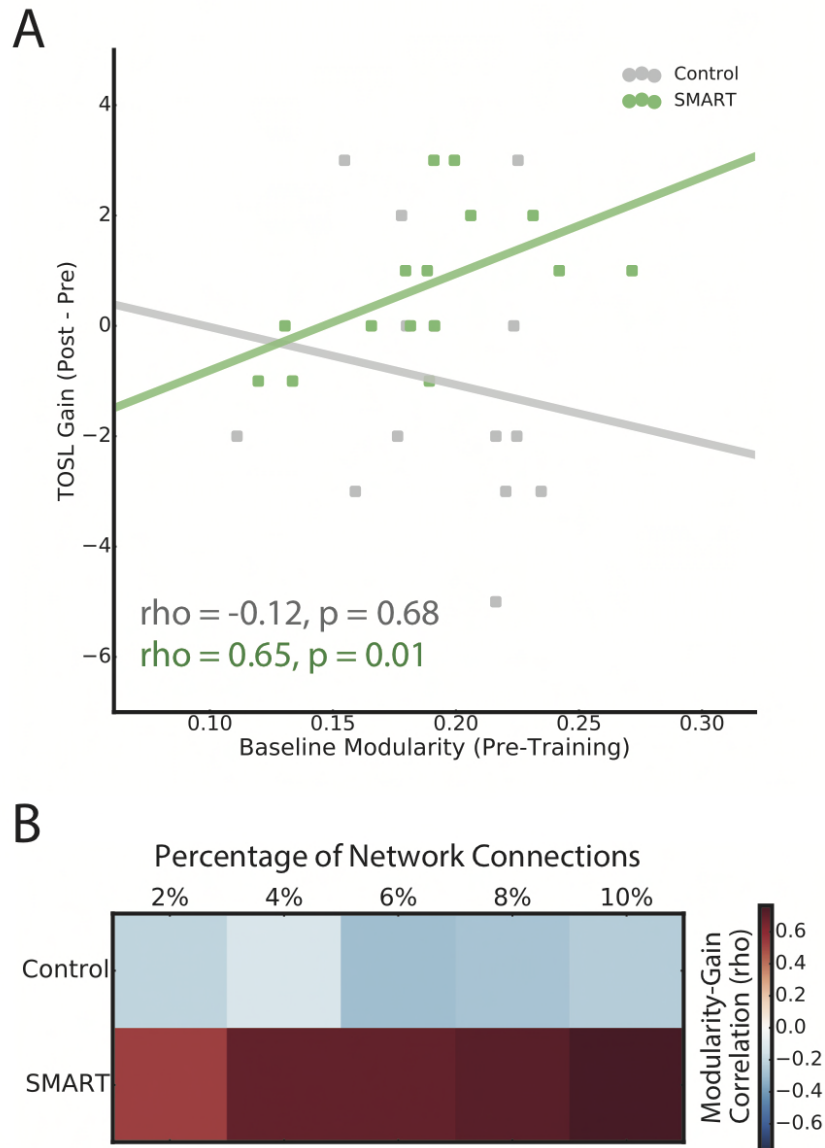


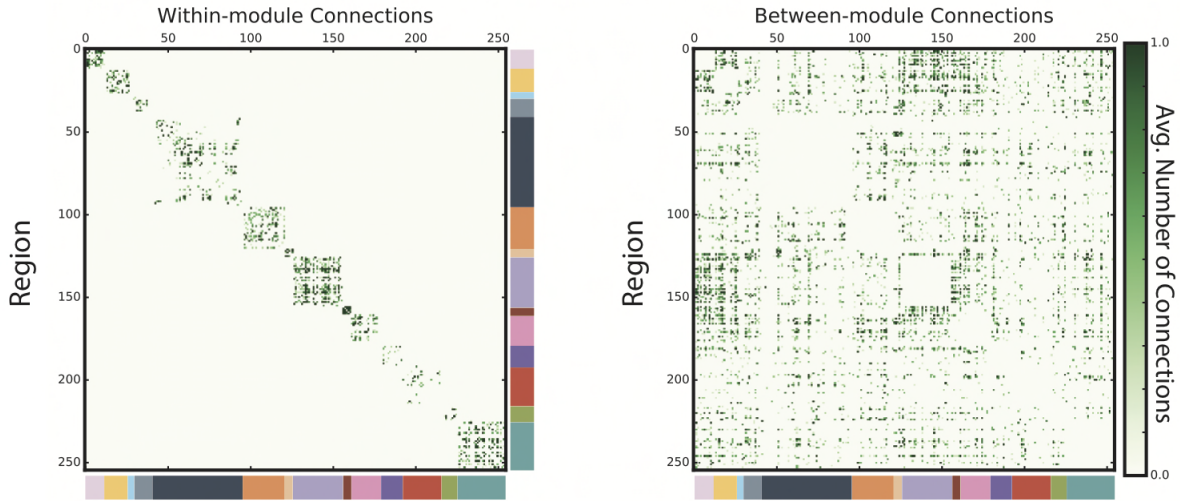
Figure 4.2. Relationship between baseline modularity (pre-training) and change in TOSL (difference of post-training and pre-training) in control and SMART groups (A). Here, modularity values were calculated for each connection threshold and averaged for each participant. Relationship between baseline modularity and change in TOSL at each connection threshold for each group (B).

We conducted several additional analyses to examine the robustness of our findings. First, to ensure that the relationship between modularity and cognitive gains was not significantly affected by a particular choice of connection density threshold, we examined the modularity-TOSL gain for each threshold separately in the two groups. The correlations between modularity and TOSL changes were consistent across the connection thresholds (Figure 4.2B). Second, as there are multiple methods for identifying network modules, we also identified subject-specific modules using a spectral clustering algorithm (Newman, 2006) instead of imposing the same modules for all subjects as defined in Power et al. (2011). In each group, the correlations between modularity and TOSL changes were similar when using the spectral method (control: $\rho(13) = -0.38$, $p = 0.18$; SMART: $\rho(14) = 0.76$, $p = 0.001$). Finally, as in-scanner motion can spuriously affect functional connectivity estimates (Power et al., 2012; Satterthwaite et al., 2012; Van Dijk et al., 2012), we confirmed that motion (framewise displacement (Power et al., 2012)) was similar between the groups (mean \pm SD FD: control: 0.16 ± 0.10 ; SMART: 0.15 ± 0.05 ; $p = 0.80$) and was not related to modularity in either group ($p > 0.13$). Controlling for motion did not substantially alter any of the modularity-TOSL gain correlations (control: $r(11) = -0.16$, $p = 0.60$; SMART: $r(12) = 0.55$, $p = 0.04$).

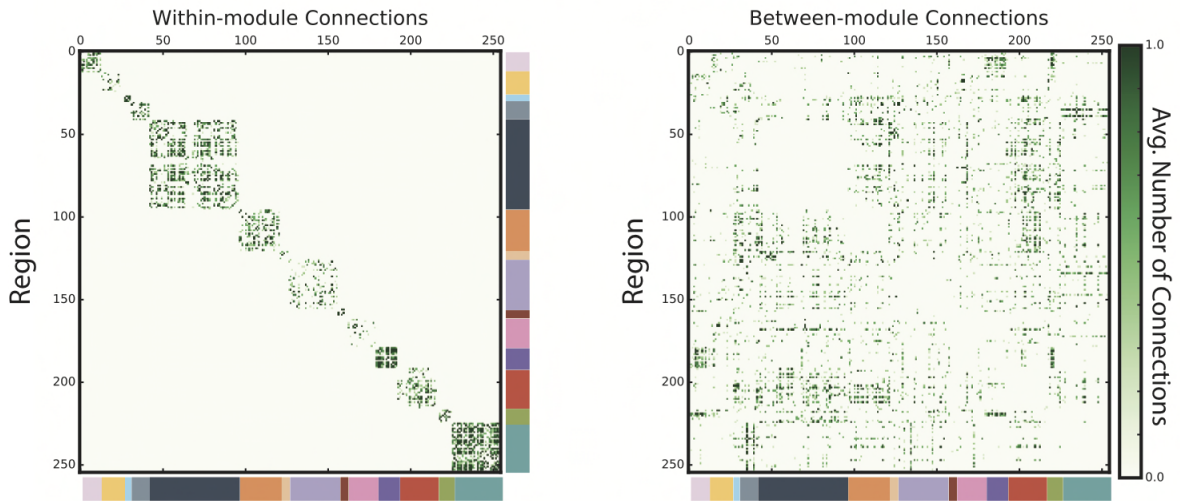
4.4.3 Relationship between sensory-motor and association modularity and cognitive changes

As expected, examination of the adjacency matrices for SMART participants with the lowest and highest modularity showed that brain networks of subjects with high modularity were characterized by modules with many connections between regions belonging to the same module and relatively few connections between regions belonging to different modules (Figure 4.3). Further, the concentration of connections within and between modules varied across the modules themselves. We next examined the differential contribution of sensory-motor and association modularity on predicting TOSL changes, as there is evidence that association modules show more pronounced aging effects (Chan et al., 2014). Comparisons of baseline sensory-motor and association modularity in each group showed that modularity was greater in sensory-motor compared with association sub-networks in control ($t(13) = 8.52$, $p < 0.001$) and SMART ($t(14) = 5.71$, $p < 0.001$) groups. Further, sensory-motor and association modularity were not significantly correlated in either group (control: $\rho(12) = -0.24$, $p = 0.42$; SMART: $\rho(13) = 0.04$, $p = 0.90$).

SMART Subject with Lowest Modularity



SMART Subject with Highest Modularity



- | | | |
|---|---|--|
| <p>Sensory-Motor Modules</p> <ul style="list-style-type: none"> Auditory Somatomotor (hand) Somatomotor (mouth) Visual | <p>Association Modules</p> <ul style="list-style-type: none"> Cingulo-Opercular Default Mode Dorsal Attention Fronto-Parietal Salience Ventral Attention | <p>Other Modules</p> <ul style="list-style-type: none"> Cerebellum Memory Retrieval Subcortical Unknown |
|---|---|--|

Figure 4.3. Depictions of within- (left) and between- (right) module connections for SMART participants with lowest (top) and highest (bottom) brain network modularity. The presence or absence of a connection was calculated for each connection density threshold (i.e., an adjacency matrix) and averaged over thresholds for each subject. Brain regions are colored according to their module assignments in Power et al. (2011) and are grouped into sensory-motor and association modules as defined in Chan et al. (2014). SMART subjects with high modularity have many connections within modules and fewer connections between modules compared with subjects with low modularity.

Separate correlations of sensory-motor and association modularity and TOSL gains showed that the modularity-TOSL gain relationship in the SMART group was significant for association ($\rho(13) = 0.60$, $p = 0.02$) but not sensory-motor ($\rho(13) = 0.19$, $p = 0.49$) modularity (Figure 4.4). There was no relationship between TOSL gains and either sensory-motor or association modularity in the control group ($p = 0.45$ and 0.94 , respectively). To further examine how association and sensory-motor modularity contribute to the whole-brain modularity-TOSL gain correlation in the SMART group, we conducted the whole-brain modularity and TOSL gain correlation controlling for either association or sensory-motor modularity. Controlling for sensory-motor modularity did not substantially alter the relationship between whole-brain modularity and TOSL gain ($r(12) = 0.58$, $p = 0.03$), while controlling for association modularity reduced the relationship between whole-brain modularity and TOSL gain ($r(12) = 0.12$, $p = 0.69$).

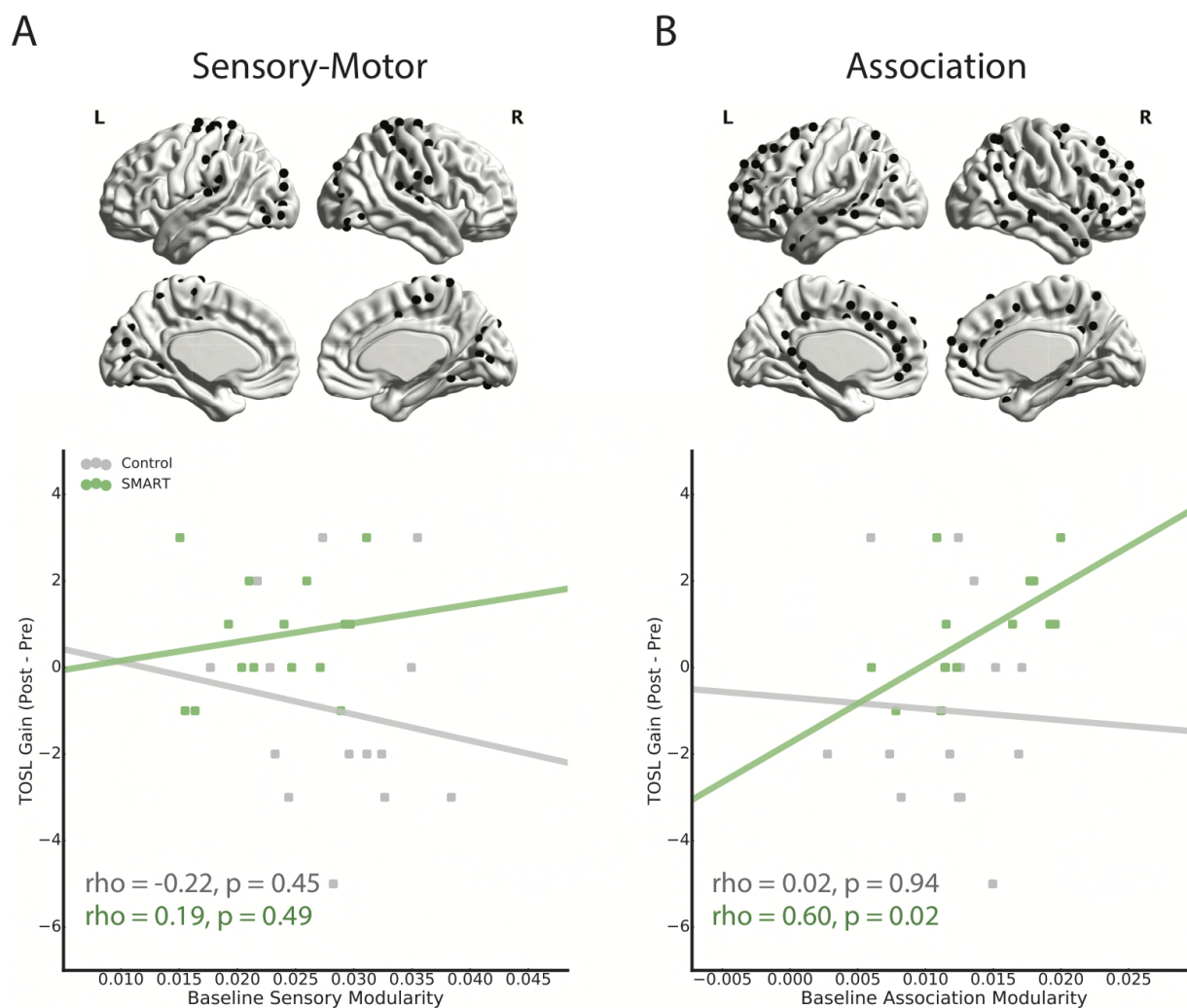


Figure 4.4. Relationship between sensory-motor (A) and association (B) modularity and TOSL gain in control and SMART groups. Cerebral cortex regions belonging to sensory-motor and association modules are plotted on on sagittal views of the brain in A and B, respectively.

4.5 Discussion

Our findings demonstrate that older adults with more modular brain networks at baseline show greater improvements after cognitive training. Critically, this relationship was not present in a control group and remained significant when accounting for baseline cognitive functioning on measures that improved with training. These results are directly in-line with previous work showing that TBI patients with higher brain network modularity exhibited greater improvements in executive functioning after training (Arneemann et al., 2015). We also expand on this work by showing that the relationship between modularity and training-related cognitive gains in cognitively normal older adults was stronger for modularity of association cortex sub-networks compared with sensory-motor sub-networks. Together, these findings suggest that individuals who had a more modular brain network organization during a 'resting-state' were more likely to benefit from cognitive training.

Modular brain network organization is thought to enable complex behavior by supporting both specialized functions through communication within network modules and globally-integrated functions through communication between network modules (Meunier et al., 2009b; 2010). Previous studies have provided support for the importance of this global network property by showing that resting-state modularity is related to aspects of memory (Stevens et al., 2010; Alavash et al., 2015), predicts perception (Sadaghiani et al., 2015), and dynamically reconfigures depending on task demands (Wen et al., 2015). In addition to whole-brain network modularity, specific network modules important for associative functions, such as the default mode network, have been shown to be related to memory (Power et al., 2011; Chan et al., 2014), exhibit reorganization during working memory performance (Stanley et al., 2014; Liang et al., 2015; Vatansever et al., 2015), and show pronounced changes with aging (Onoda and Yamaguchi, 2013; Chan et al., 2014; Geerligns et al., 2014a). Here, we add to this previous work by showing that network modularity, particularly that of associative systems, may represent a beneficial brain organization for improving cognitive functioning in older adults with training.

More generally, our results also suggest that brain network properties may be related to learning, such that individuals with a more modular brain may have a greater learning capacity and, thus, ability to benefit from training. While previous studies have shown that neural factors (e.g., frontal alpha power and striatal volume) are related to skill learning (Erickson et al., 2010; Basak et al., 2011; Power et al., 2011; Vo et al., 2011; Mathewson et al., 2012), the aspects of brain structure and function that predicted learning are variable across studies. Given that we have found that brain network modularity is predictive of cognitive training gains in two types of training paradigms and populations, network modularity may provide a unifying framework that predicts training outcomes across a variety of interventions and groups.

We propose that brain network modularity is a valuable biomarker that can inform the implementation of cognitive interventions, as assessments of modularity could be used to personalize interventions to maximize outcomes across individuals. For example, individuals with low network modularity might require a longer or repeated training

intervention. Although we have demonstrated that modularity is predictive of training gains in older adults and TBI patients (Arneemann et al., 2015), future work should also examine this relationship in healthy young subjects and other patient populations to further address the generalization of these findings. More broadly, our results also imply that modularity may index individual differences in neuroplasticity. To more directly address this, an important area of future research should be to examine the relationship between modularity and underlying training-related neural changes.

There are several limitations to the present study. First, lack of an active control group limited full examination of the specificity of our results to SMART training. However, previous work showed that an active control group did not exhibit cognitive changes compared to SMART (Vas et al., 2011). In this study, TBI patients in the active control group participated in an 8-week information-based program (Brain Health Workshop, BHW)(Binder et al., 2008) in small groups. The content of BHW covered topics such as brain anatomy and function and brain health. Further, modularity has previously been shown to not be predictive of cognitive changes after BHW in TBI patients (Arneemann et al., 2015). Second, each group had a relatively small sample size. This may have limited our power to detect a relationship between modularity and Similarities gains, where the effect of training was smaller than that of TOSL. Future studies with larger samples may allow for examination of other relationships between modularity and training-related neural and cognitive changes.

Chapter 5

BRAIN NETWORK PREDICTORS OF COGNITIVE TRAINING-RELATED GAINS IN YOUNG ADULTS

5.1 Abstract

The brain operates via networked activity in separable groups of regions called modules. The quantification of modularity compares the number of connections within and between modules, thus characterizing the balance of segregation and integration in a network. Previous work has demonstrated that baseline brain network modularity positively predicts cognitive training outcomes in older adults and in patients with traumatic brain injury. In healthy young adults, however, the functional significance of modularity in predicting training-related cognitive improvements is not yet known. Here, we quantified brain network modularity in young adults who underwent cognitive training with working memory and reasoning (WM-REAS) casual video games (e.g., games that are relatively easy to learn and freely available on the internet or handheld devices). After training, WM-REAS participants improved in divided attention measures relative to control groups. Network modularity assessed at baseline was positively correlated with this improvement in divided attention following training, even after controlling for baseline behavioral measures. The modularity-gain relationship was especially evident in individuals with lower baseline scores in fluid intelligence and divided attention. Finally, we assessed individual module contributions to predicting cognitive training gains and found that greater modularity of the default mode (DMN) sub-network was related to larger gains in divided attention. These results show that a more modular brain network organization may allow for greater adaptive reconfiguration during cognitive training. On a broader scale, these findings suggest that, in low-performing individuals, global network properties can capture aspects of brain function that are important in understanding individual differences in learning.

5.2 Introduction

Computer-based cognitive training in the form of video games and laboratory exercises is an increasingly popular approach to improve cognitive function, yet training-related benefits can vary greatly across studies and individuals (Boot and Kramer, 2014). To better inform the implementation of such interventions, it is important to examine individual differences that can predict training effectiveness. Pre-training patterns of neural activity (Vo et al., 2011; Mathewson et al., 2012) and brain volume (Erickson et al., 2010; Basak et al., 2011; Verghese et al., 2016) have been found to correlate with improvements after cognitive training, although these brain measures have often been limited to a single region or to a small group of regions which vary across studies. Since complex cognitive functions likely involve widespread interactions between groups of brain regions (Cole et al., 2013; Medaglia et al., 2015) or sub-networks, it is critical to

consider whether baseline global brain network properties can serve as a useful biomarker in assessing training outcomes.

Graph theoretical tools can be used to describe the brain as a complex network, where individual brain regions represent network nodes and the structural or functional connections between them represent network edges. Previous work using structural and functional MRI has shown that brain networks exhibit a modular organization, comprised of separable sub-networks or modules, with dense connections within modules and sparser connections between modules (Newman and Girvan, 2004; Newman, 2006; Chen et al., 2008; Bullmore and Sporns, 2009; Meunier et al., 2010). Using graph theory, the extent of segregation of network modules can be quantified with a modularity metric.

More generally, modularity has been found to be disrupted in patients with mental disorders (Alexander-Bloch et al., 2010; 2012; Fornito et al., 2015) and with damage to highly connected brain areas (Gratton et al., 2012). In healthy adults, lower modularity is also observed with increasing age (Meunier et al., 2009a; Betzel et al., 2014; Chan et al., 2014; Geerligs et al., 2014a). Across individuals, modularity predicts variability in working memory capacity (Stevens et al., 2012; Stanley et al., 2014) and has been observed to change during working memory task performance, showing a decrease in more cognitive-demanding conditions (Kitzbichler et al., 2011). Taken together, these results suggest that modularity is a critical component of learning, with a more modular structure potentially allowing for more efficient and greater adaptive reorganization in response to changing demands (Bassett et al., 2011; Russo et al., 2014).

Recent work has shown that higher modularity at baseline predicts greater training-related cognitive improvements in healthy older adults (Gallen et al., Submitted) and in patients with traumatic brain injury (TBI; Arnemann et al., 2015), above and beyond baseline behavioral measures. Previous studies also suggest that cognitive interventions can improve aspects of cognition in healthy young adults (Boot et al., 2008; Strobach et al., 2012; Au et al., 2014; Karbach and Verhaeghen, 2014), but see (Melby-Lervåg and Hulme, 2013; Redick et al., 2013; Boot and Kramer, 2014; Dougherty et al., 2016). However, the functional significance of modularity in predicting training outcomes in young adults has not yet been examined.

In the present study, we sought to test whether modularity is a useful predictor of training effectiveness in a healthy young, relatively high-functioning population. In a large sample of young adults (N = 68) who displayed improvements in divided attention after 15 hours of training with working memory and reasoning (WM-REAS) casual video games compared to an active control group (N = 37) and a no-contact control group (N = 38) (Baniqued et al., 2014), we examined whether pre-training modularity as measured during a task-free "resting state" can predict the observed training-related gains in divided attention. We hypothesized that, in line with previous findings, higher modularity will predict greater training-related gains in the WM-REAS group, but not in the control groups.

5.3 Materials and Methods

5.3.1 Participants

209 right-handed adults aged 18-30 participated in a multi-session study (see (Baniqued et al., 2014) and (Nikolaidis et al., 2016) for behavioral data and MR spectroscopy data published from this same cohort). Individuals were recruited from the University of Illinois at Urbana-Champaign and surrounding communities through paper and web-based announcements advertising a “cognitive training study.” Eligible applicants had normal or corrected-to-normal vision, no major medical, psychiatric or psychological conditions, and must have reported playing video and board games for 3 hours or less per week in the last 6 months. Participants were compensated \$15/hour if they completed all required sessions. To encourage study completion, individuals who discontinued study participation were paid \$7.50/hr for every completed session. The University of Illinois Institutional Review Board approved study procedures and all participants provided written informed consent. Additional details about recruitment procedures (e.g., initial e-mail survey, phone screening) are provided in the original training report (Baniqued et al., 2014). In the publication of the behavioral training effects, participants were excluded from analysis if they reported in a post-experiment questionnaire that they 1) played any of the games used for training or testing and/or 2) were active video game players as defined by game play of more than 3 hours in the last 6 months, leaving 170 participants for analysis. We follow this procedure and other exclusionary criteria in the original study (including excluding behavioral measures greater than 4 standard deviations (SD) from the mean), and exclude more participants from analysis based on MRI data quality (N = 26, see MRI Preprocessing). Summary demographics for the remaining participants are presented in Table 5.1.

Table 5.1. Demographics

	WM-REAS 1	WM-REAS 2	Active Control	No- Contact	Group Effect (4 groups)	Group Effect (2 groups)
Dropped due to video game play outside lab	10	12	9	8	$\chi^2(3)=1.07$, $p=.79$	$\chi^2(1)=0.73$, $p=.39$
Dropped due to poor MRI data quality	9	6	7	5	$\chi^2(3)=1.60$, $p=.66$	$\chi^2(1)=0.97$, $p=.33$
Final N	34	34	37	38	-	-
Age (SD)	21.32 (2.21)	21.5 (2.49)	20.70 (1.87)	20.71 (2.17)	$F(3,139)=1.27$ $p=.29$	$t(141)=1.94$, $p=.06$
Years of education (SD)	14.87 (1.24)	15.25 (1.72)	14.66 (1.30)	14.86 (1.56)	$F(3,139)=0.98$, $p=.40$	$t(141)=1.21$, $p=.23$
Females / Males	26 / 8	25 / 9	25 / 12	29 / 9	$\chi^2(1)=0.98$, $p=.81$	$\chi^2(1)=0.17$, $p=.69$

5.3.2 Behavioral Methods

Protocol Summary. Participants completed four baseline testing sessions in a fixed session and task order (three behavioral sessions followed by one MRI session). For the training groups, participants then completed 10 sessions of casual game play. After training or after a comparable amount of time (3-4 weeks) elapsed for the no-contact control group, participants completed four testing sessions in reverse session order (MRI session followed by three behavioral sessions in reverse order as baseline testing).

Training Games. Participants assigned to the training groups completed 10 sessions at a rate of two to three sessions per week. During each session, participants played four games in pseudo-random order for 20 minutes each. Training games were selected based on results from a study that correlated performance on casual games with performance on various tests of cognitive abilities (Baniqued et al., 2014). The WM-REAS groups played casual games that were highly correlated with performance on working memory and reasoning tests, while the active control group played games that were not highly correlated with working memory and reasoning tests. As previously reported (Baniqued et al., 2014), the groups were comparable in their experience of the

games as assessed by feedback questions of enjoyment, motivation, and engagement. Table 5.2 contains brief descriptions of each game. The WM-REAS 1 and WM-REAS 2 groups differed primarily in the adaptiveness of the training games, such that all WM-REAS 2 games were adaptive across sessions. Since the two WM-REAS groups showed similar effects of training (Baniqued et al., 2014), they are analyzed together in this study. The no-contact group did not undergo any training and only completed pre- and post-testing.

Table 5.2. Training games

Games	Group	Description	Source
Silversphere	WM-REAS 1, WM-REAS 2	Move a sphere to a blue vortex by creating a path using blocks of different features and avoiding obstacles along the path.	miniclip.com
Digital Switch	WM-REAS 1	Switch “digibot” positions to collect falling coins corresponding to the same “digibot” color.	miniclip.com
TwoThree	WM-REAS 1	Target rapidly presented numbers by pointing the mouse to the numbers and subtracting the numbers down to exactly zero in units of 2 or 3.	armorgames.com
Sushi Go Round	WM-REAS 1	Serve customers in the allotted time by learning and preparing recipes correctly, cleaning tables, and ordering ingredients.	miniclip.com
Aengie Quest	WM-REAS 2	Move across the board and exit each level by pushing switches and boxes, finding keys, and opening doors.	freegamesjungle.com
Gude Balls	WM-REAS 2	Remove all plates by filling a plate with four of the same colored balls and switching balls to other plates while navigating around obstacles.	bigfishgames.com
Block Drop	WM-REAS 2	Move around a gem on three-dimensional blocks of varying shapes to remove all blocks except the checkered block.	miniclip.com
Alphattack	Active Control	Prevent bombs from landing by typing characters presented on approaching bombs.	miniclip.com
Crashdown	Active Control	Prevent the wall from reaching the top of the screen by clicking on groups of three or more same colored blocks.	miniclip.com
Music Catch 2	Active Control	Earn points by mousing over streams of colored shapes and avoiding contiguously appearing red shapes.	reflexive.com

Enigmata	Active Control	Navigate a ship while avoiding and destroying enemies, and collecting objects that provide armor or power.	maxgames.com
----------	-------------------	--	--------------

Cognitive Tests. Here, we focused on the behavioral measures that demonstrated training-related effects, although additional details about other behavioral measures assessed can be found in the original training report (Baniqued et al., 2014). Significant group by time interactions were found in three tests that tap aspects of divided attention: Attention Blink, Trail Making, and Dodge, with the WM-REAS groups showing better performance after training. Moreover, improvement in divided attention was negatively correlated with baseline fluid intelligence scores as assessed by six tests: Form Boards, Spatial Relations, Matrix Reasoning, Paper Folding, Shipley Abstraction, and Letter Sets. We re-analyzed these measures using the subset of participants with usable MRI data. In the next section are brief descriptions of each test and the measures used for analyses. All tests were completed before and after training (baseline cognitive testing was performed before baseline MRI testing), but here we focus on pre-test and post-test performance in the divided attention tests, and on pre-training performance in the fluid intelligence tests. We computed a composite measure of divided attention improvement for each participant by averaging standardized gain scores for each task. Standardized gain scores were computed by taking the difference between post-test and pre-test performance and dividing this gain measure by the standard deviation of pre-test performance (collapsed across all groups). To reduce the influence of remaining extreme values in the correlation analyses, the composite scores were then winsorized (Tukey, 1962; Wilcox, 2005): any value 3 SD away from the mean was replaced with the 3 SD cut-off value (we replaced the scores of only one subject with divided attention gain score > 3 SD from the mean and baseline divided attention gain score < 3 SD from mean).

Attentional Blink (Shapiro et al., 1997). Participants were tasked to identify the white letter (target 1) in a sequence of rapidly presented black letters, and identify whether the white letter was followed by a black “X” (target 2). The attentional blink was computed from trials when target 1 was accurately detected, as the difference in target 2 accuracy when detection is easiest (lag 8 after target 1) and when detection is most difficult (lag 2 after target 1).

Trail Making (Reitan, 1958). In “Trails A”, participants connected numbered circles as quickly as possible by drawing a line between them in numerical order. In “Trails B,” participants connected both numbered and lettered circles by drawing a line between them, alternating between numbers and letters in numerical and alphabetical order. The trail-making cost was computed by taking the difference in Trails B and Trails A completion time.

Dodge (Armor Games). In this game, participants were directed to avoid enemy missiles and destroy enemy ships by guiding enemy missiles (directed at the participant’s ship) into other enemies. Participants pressed four buttons to navigate around the screen,

which was increasingly populated with enemy ships and their missiles. Participants completed the first two levels on a laboratory computer, and practiced the same two levels in an MRI environment. Data used for analysis was the highest level reached after eight minutes of game play in an fMRI environment.

Shipley Abstraction (Zachary and Shipley, 1986). Participants were given a list of 20 word, letter, or number sequences and instructed to fill in the missing letters or numbers in each sequence. We analyzed the total number of correctly answered items within five minutes.

Matrix Reasoning (Ravens, 1962; Crone et al., 2009). Participants were shown a 3 x 3 matrix of abstract patterns with one cell missing, and instructed to select which among three options best completes the matrix along both the rows and columns. We analyzed the total number of correctly answered items.

Paper Folding (Ekstrom et al., 1976). Participants were asked to select the pattern of holes that would result from a punch through a sheet of paper folded in a certain sequence. We analyzed the total number of correctly answered items within 10 minutes.

Spatial Relations (Bennett, Seashore and Wesman, 1997). Participants were instructed to identify that 3-dimensional object that would match a 2-dimensional object when folded. We analyzed the total number of correctly answered items in 10 minutes.

Form Boards (Ekstrom et al., 1976). Participants were instructed to choose pieces that will exactly fill a certain shape. We analyzed the total number of correctly answered items in 8 minutes.

Letter Sets (Ekstrom et al., 1976). Participants were presented with five sets of letter strings and asked to determine which letter set was different from the other four. We analyzed the total number of correctly answered items within 10 minutes.

5.3.3 MRI Acquisition and Preprocessing

During the fourth session of baseline testing, participants underwent MRI scanning on a 3 Tesla Siemens Trio MR scanner with a 12-channel head array receive coil. Anatomical data consisting of T1-weighted MPRAGE images were acquired with the following parameters: GRAPPA acceleration factor 2, voxel size = 0.9 x 0.9 x 0.9 mm, TR = 1900 ms, TI = 900 ms, TE = 2.32 ms, flip angle = 9°, FoV = 230 mm). Functional data during a six-minute resting state scan were obtained using a T2*-weighted echoplanar imaging (EPI) pulse sequence with the following parameters: GRAPPA acceleration factor 2, 180 volumes, in-plane resolution = 2.4 mm², TR = 2000 ms, TE = 25 ms, flip angle = 80°, FoV = 220 mm; 38 3.5 mm ascending slices, no slice gap). Participants were instructed to close their eyes, stay awake, and remain as still as possible. The resting-state scan was performed after five MRI runs of the Attention Network Task (Fan et al., 2002), which lasted for six minutes each. We excluded three participants from analyses due to artifacts in the anatomical and functional scans (N=1 in WM-REAS 1 group, N=2 in no-contact group).

Brain extraction of anatomical images was performed with Advanced Normalization Tools (ANTs; (Avants et al., 2011)) using the LPBA40 template (Shattuck et al., 2008). Subjects with remaining non-brain tissue after this step were instead run through ANTs brain extraction using the Kirby/MMRR template (Landman et al., 2011). The skull-stripped structural images and raw functional images were preprocessed through the Configurable Pipeline for the Analysis of Connectomes (CPAC). Structural scans were registered to the MNI152 template using ANTs and segmented into grey matter (probability threshold = 0.7), white matter (probability threshold = 0.96) and CSF (probability threshold = 0.96) via FSL/FAST (Zhang et al., 2001). EPI scans were slice-time corrected, motion-corrected using the Friston 24-Parameter Model (Friston et al., 1996), and co-registered to the anatomical images. Nuisance signal correction was performed by regressing out the aforementioned motion parameters, signals from the first five principal components from white matter and CSF voxels (CompCor; (Behzadi et al., 2007)), and linear and quadratic trends. The functional data were then bandpass filtered from 0.009 to 0.08 Hz. Participants with maximum absolute displacement greater than 3.4 mm were excluded from analysis (N = 24, see Table 5.1 for group breakdown).

5.3.4 Functional Connectivity and Modularity Analyses

The functional scans were warped to the MNI template and parcellated into 264 regions of interest (Power et al., 2011). Time series were averaged for all voxels in an ROI. Due to uneven partial coverage of the cerebellum in the functional data, we excluded the four cerebellum module ROIs prior to running the network analyses. Nine additional ROIs were excluded due to lack of EPI coverage in at least one subject. For each participant, functional connectivity matrices were created by correlating the time-series between each pair of ROIs using Pearson's coefficient and applying a Fisher z-transformation.

In the remaining 143 participants, the 251 x 251 functional connectivity matrices were binarized to create adjacency matrices that indicate the presence or absence of a connection between a pair of regions. Matrices were binarized over a range of connection density thresholds or 'costs' (here, the top 2-10% of all possible connections in the network in 2% increments, following Power et al., 2011). Each of these thresholded matrices was used to create unweighted, undirected whole-brain graphs with which network metrics were examined. Network metrics were created separately for each connection threshold to determine the consistency of results. Unless otherwise noted, we report results both at a 6% connection threshold and as the average across connection density thresholds. The NetworkX Python package and custom Python scripts were used for network analyses.

To examine the role in modular network organization in predicting training-related gains, we quantified network modularity, a global network measure that compares the number of connections within to the number of connections between modules (Newman and Girvan, 2004). Modularity will be 1 if all connections fall within modules and it will be 0 if there are no more connections within modules than would be expected by chance.

As there are multiple methods for identifying network modules, we used several approaches. We first quantified modularity using a spectral algorithm (Newman, 2006) to identify the most optimal modular partition (i.e., maximal modularity) for each subject at each connection threshold. We also computed modularity by pre-defining modules by assigning each node to its module as identified in Power et al. (2011). Using this module definition, we also examined the contribution of each module to global modularity, which is the sum of the modularity across network modules.

5.3.5 Statistical Analysis

Training-related gains in divided attention measures were assessed at 1) a construct level using a one-way ANOVA with a between-subject factor of training group (WM-REAS 1, WM-REAS 2, active control, no-contact) and with a composite score of divided attention gain as the dependent measure (described in *Cognitive Tests*) and at 2) a task-level using repeated-measures ANOVAs with a within-subject factor of time (pre- and post-test score) and a between-subject factor of training group. Effect size for ANOVAs is provided as partial-eta squared (η^2p).

The relationships between whole-brain baseline modularity and training-related gains were assessed with correlations between modularity identified with spectral clustering (6% cost threshold and averaged across thresholds) and a divided attention composite gain score. Specific module contributions to the relationship between modularity (averaged across thresholds) and training gains were assessed with the modularity of each sub-network as defined in Power et al. (2011). The majority of correlations were assessed with two-tailed Pearson correlations (r). Partial correlations are presented as rp . Further, follow-up correlation analyses were assessed controlling for motion or baseline cognitive ability.

In the analysis of module contributions to global modularity in the WM-REAS group, we first tested if modularity values differed across the 12 modules using a repeated-measures ANOVA with a between-subject factor of baseline cognitive ability group (fluid intelligence (Gf) or divided attention) group and a within-subject factor of module. F-values and P-values in ANOVAs were corrected for sphericity using the Greenhouse-Geisser method (GG).

5.4 Results

5.4.1 Behavioral Results

Consistent with the previously published report (Baniqued et al., 2014), the WM-REAS groups showed greater gains in divided attention (Figure 5.1A) as assessed by a one-way ANOVA with a between-subject factor of the four training groups on the composite improvement score, ($F(3,139) = 5.253, p = 0.002, \eta^2p = 0.102$), and by repeated-measures ANOVAs of pre- and post-test performance on each task (Trail Making: $F(3,135) = 3.721, p = 0.013, \eta^2p = 0.076$; Attention Blink: $F(3,139) = 3.464, p = 0.018, \eta^2p = 0.070$; Dodge: $F(3,133) = 3.153, p = 0.027, \eta^2p = 0.066$).

Similarly to the previous study, baseline Gf was negatively correlated with divided attention gain (Figure 5.1B) in the WM-REAS groups (WM-REAS all: $r(66) = -0.296$, $p = 0.014$, two-tailed; WM-REAS 1: $r(32) = -0.307$, $p = 0.077$; WM-REAS 2: $r(32) = -0.280$, $p = 0.109$) but not in the control groups (Figure 5.1C; CONTROL all: $r(73) = 0.081$, $p = 0.490$, two-tailed; no-contact: $r(36) = 0.055$, $p = 0.743$; active: $r(35) = 0.137$, $p = 0.417$). Given their comparable training-related effects in divided attention and the reduced sample size after excluding participants with unusable MRI data, in the subsequent MRI analyses, we combined the two WM-REAS groups into one group and the active control group and no-contact control group into another group.

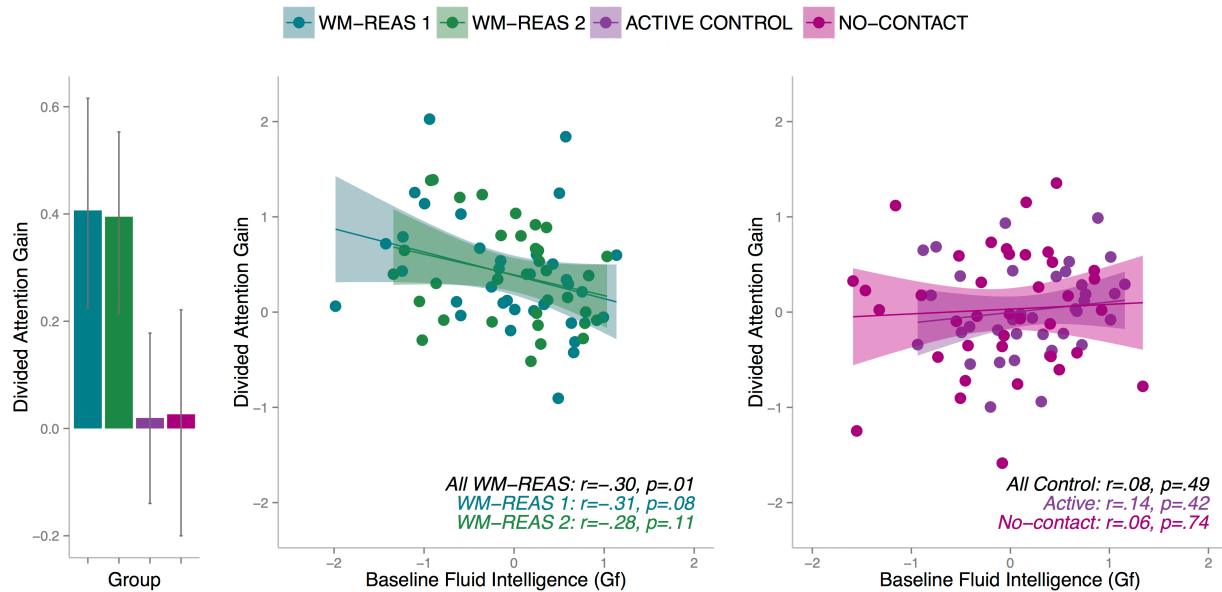


Figure 5.1. Behavioral training effects. A) Mean divided attention gain for all four groups. Error bars are 95% bootstrapped confidence intervals. The right panels (B, C) show the relationship between baseline fluid reasoning and divided attention gain in the WM-REAS groups (B) and control groups (C). The Pearson's coefficient (r) and the two-tailed p -value are shown. Shaded areas represent 95% confidence region of the regression line.

As a follow-up analysis, we probed the relationship between baseline divided attention and divided attention gain, finding that higher baseline performers showed smaller gains. A negative relationship was observed across all four groups ($r(141) = -0.620$, $p < 0.001$, two-tailed) and within each of the two combined groups (WM-REAS: $r(66) = -0.665$, $p < 0.001$, two-tailed; CONTROL: $r(73) = -0.579$, $p < 0.001$, two-tailed). Not surprisingly, across the whole sample, baseline divided attention was positively correlated with baseline Gf, $r(141) = 0.306$, $p < 0.001$, two-tailed. Including baseline Gf or baseline divided attention as a covariate in the analysis of group effects in divided attention improvement or post-training divided attention scores did not significantly alter the results.

5.4.2 Brain Network Modularity Results

Baseline modularity and divided attention gain. First, we determined whether the observed improvements in divided attention could be predicted by pre-training brain modularity (i.e., global modularity identified with spectral clustering). In the combined WM-REAS groups, we found a significant relationship between divided attention gain and baseline modularity (Figure 5.2A; 6% cost: $r(66) = 0.253$, $p = 0.037$, two-tailed; average: $r(66) = 0.215$, $p = 0.078$, two-tailed). In the combined control groups, there was no significant relationship between divided attention gain and baseline modularity (Figure 5.2A; 6% cost: $r(73) = -0.200$, $p = 0.086$, two-tailed; average: $r(73) = -0.207$, $p = 0.074$, two-tailed). We confirmed that this relationship was similar at different cost thresholds tested for the WM-REAS and control groups (Figure 5.2B). The correlations between baseline modularity and divided attention were significantly different between the two groups (6% cost: $Z = 2.70$, $p = 0.007$, two-tailed; average: $Z = 2.50$, $p = 0.012$, two-tailed).

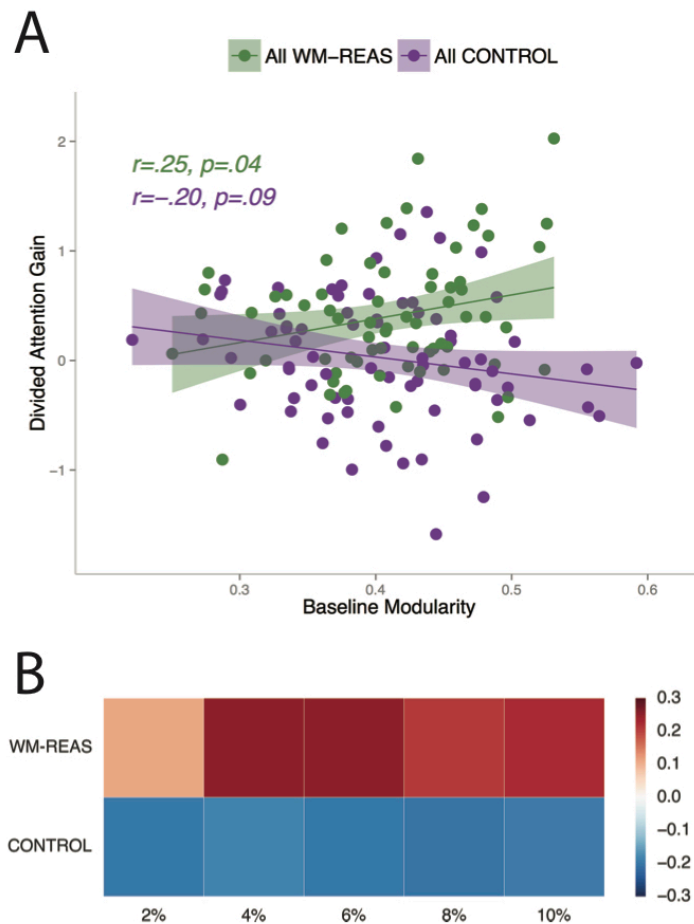


Figure 5.2. Baseline modularity effects. A) Relationship between baseline modularity (6% threshold) and divided attention gain. Pearson's coefficients (r) and two-tailed p -values are shown. Shaded areas represent 95% confidence region of the regression line. B) Correlation (Pearson's coefficient) between baseline modularity and divided attention gain for each tested threshold.

As in-scanner motion can spuriously affect functional connectivity estimates (Power et al., 2012; Satterthwaite et al., 2012; Van Dijk et al., 2012), we confirmed that the relationship between baseline modularity and training-related gains was not due to motion. Across the two groups, mean framewise displacement (FD; (Power et al., 2012)) was negatively correlated with baseline modularity (6% cost: $r(141) = -0.209$, $p = 0.012$, two-tailed; average: $r(141) = -0.205$, $p = 0.014$, two-tailed). To test whether our results were influenced by the relationship between modularity and motion, we re-analyzed the data while controlling for mean FD. Controlling for motion did not substantially change the relationship between baseline modularity and divided attention gain in the WM-REAS group (6% cost: $rp(65) = 0.230$, $p = 0.060$, two-tailed; average: $rp(65) = 0.195$, $p = 0.114$, two-tailed) or the control group (6% cost: $rp(72) = -0.196$, $p = 0.096$, two-tailed; average: $rp(72) = -0.203$, $p = 0.082$, two-tailed). Mean FD did not differ between the two groups, $F(1,141) = 0.084$, $p = 0.772$, $\eta^2p = 0.001$ (WM-REAS: $M = 0.141$, $SD = 0.047$; CONTROL: $M = 0.143$, $SD = 0.052$).

Baseline modularity and baseline cognition. As previous studies have shown that modularity is a better predictor of training-related cognitive gains than behavioral measures (Arneemann et al., 2015; Gallen et al, Submitted), we examined the relationships between baseline cognition and training-related gains in this sample of young adults. Across the two groups, baseline modularity was not significantly associated with baseline Gf (6% cost: $rp(141) = -0.074$, $p = 0.381$, two-tailed; average: $rp(141) = -0.083$, $p = 0.322$, two-tailed) or baseline divided attention (6% cost: $rp(141) = -0.133$, $p = 0.113$, two-tailed; average: $rp(141) = -0.125$, $p = 0.138$, two-tailed). This relationship was similar even after controlling for mean FD (6% cost, baseline Gf: $rp(140) = -0.075$, $p = 0.375$, two-tailed; baseline divided attention: $rp(140) = -0.133$, $p = 0.115$, two-tailed; average, baseline Gf: $rp(140) = -0.085$, $p = 0.317$, two-tailed; baseline divided attention: $rp(140) = -0.124$, $p = 0.140$, two-tailed).

As baseline Gf was strongly correlated with divided attention gain in the WM-REAS group (Figure 5.1B; (Baniqued et al., 2014)) and we have previously found a relationship between modularity and training-related gains in populations exhibiting cognitive declines (Arneemann et al., 2015), we examined the relationship between modularity and divided attention gain in the WM-REAS group while controlling for baseline Gf and re-examined this relationship within low and high Gf groups. Overall, the relationship between modularity and divided attention gain remained after controlling for baseline Gf (6% cost: $rp(65) = 0.236$, $p = 0.054$, two-tailed; average: $rp(65) = 0.197$, $p = 0.110$, two-tailed). A median split based on baseline Gf ($N = 34$ in each group) revealed that the correlation between baseline modularity and divided attention gain (controlling for baseline Gf) was more pronounced in the low Gf group (Figure 5.3A; 6% cost: $rp(31) = 0.299$, $p = 0.092$, two-tailed; average: $rp(31) = 0.268$, $p = 0.146$, two-tailed) than the high Gf group (Figure 5.3A; 6% cost: $rp(31) = 0.163$, $p = 0.364$, two-tailed; average: $rp(31) = 0.126$, $p = 0.484$, two-tailed), although the correlations did not significantly differ between the groups (6% cost: $Z = 0.57$, $p = 0.569$, two-tailed; average: $Z = 0.58$, $p = 0.562$, two-tailed). Further, baseline modularity did not significantly differ between Gf groups (6% cost: $F(1,66) = 1.041$, $p = 0.311$, $\eta^2p = 0.016$, low Gf: $M = 0.417$, $SD = 0.071$, high Gf: $M = 0.401$, $SD = 0.059$; average: $F(1,66) =$

0.909, $p = 0.344$, $\eta^2p = 0.014$, low Gf: $M = 0.432$, $SD = 0.070$, high Gf: $M = 0.417$, $SD = 0.059$).

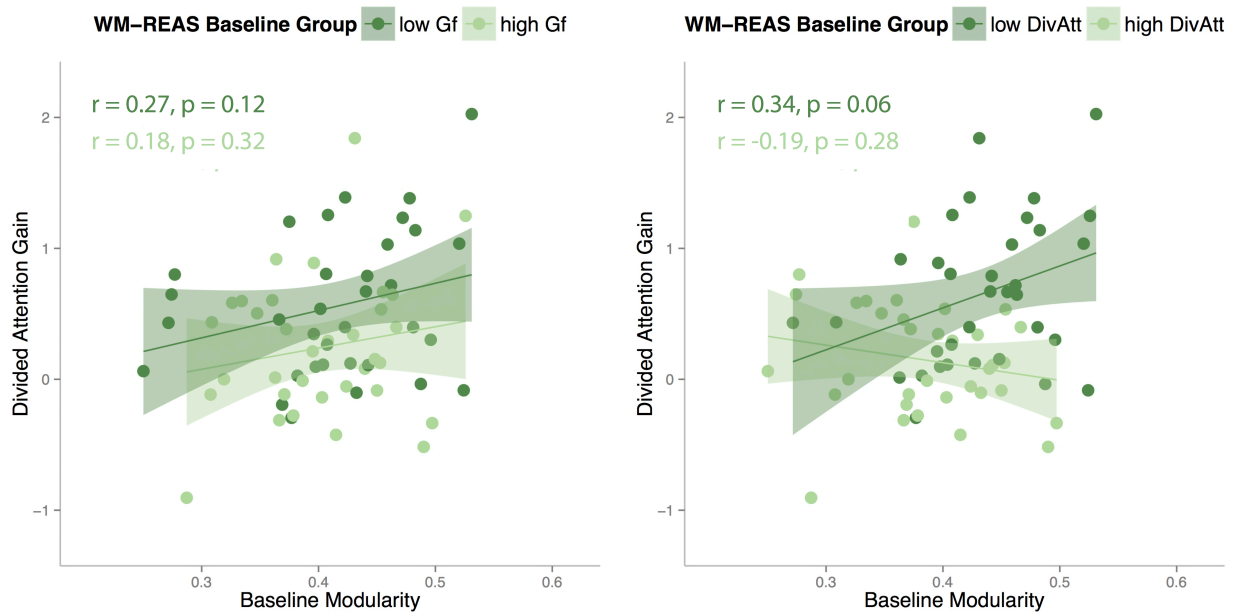


Figure 5.3. Baseline modularity (6% threshold) and divided attention gain relationships in the WM-REAS group based on a median split on baseline fluid intelligence (A) and baseline divided attention (B). Pearson's coefficients (r) and two-tailed p -values are shown. Correlations displayed do not control for any other factors. Shaded areas represent 95% confidence region of the regression line. Gf = fluid intelligence, DivAtt = Divided Attention.

Within the WM-REAS high and low Gf groups, the relationship between baseline modularity and divided attention remained the same when controlling for mean FD in addition to controlling for baseline Gf, with a numerically greater relationship between modularity and divided attention gain in the low Gf group (6% cost: $rp(30) = 0.250$, $p = 0.168$, two-tailed; average: $rp(30) = 0.215$, $p = 0.238$, two-tailed) compared to the high Gf group (6% cost: $rp(30) = 0.161$, $p = 0.378$, two-tailed; average: $r(p30) = 0.124$, $p = 0.498$, two-tailed), although these correlations were not significantly different from each other (6% cost: $Z = 0.354$, $p = 0.723$, two-tailed; average: $Z = 0.357$, $p = 0.721$, two-tailed). Mean FD did not differ between the Gf groups, $F(1,66) = 0.132$, $p = 0.718$, $\eta^2p = 0.002$ (low Gf: $M = 0.139$, $SD = 0.055$; high Gf: $M = 0.143$, $SD = 0.039$).

Since baseline divided attention was also correlated with divided attention gain, we examined the relationship between modularity and divided attention gain in the WM-REAS group while controlling for baseline divided attention and re-examined this relationship within low and high divided attention groups. Unlike controlling for baseline Gf, controlling for baseline divided attention attenuated the relationship between baseline modularity and divided attention gain (6% cost: $rp(65) = 0.038$, $p = 0.758$, two-tailed; average: $rp(65) = 0.002$, $p = 0.984$, two-tailed). These results may have been

driven by a potential behavioral ceiling effect in divided attention performance, where higher performers at baseline show smaller gains. To test this, we performed a median split on baseline divided attention in the WM-REAS group ($N = 34$ in each group). Examining the correlations between baseline modularity and divided attention gain within each group (controlling for baseline divided attention) revealed a positive, but not significant, correlation in the low divided attention group (Figure 5.3B; 6% cost: $rp(31) = 0.198$, $p = 0.268$, two-tailed; average: $rp(31) = 0.173$, $p = 0.334$, two-tailed) and a negative, but not significant, correlation in the high divided attention group (6% cost: $rp(31) = -0.147$, $p = 0.412$, two-tailed; average: $rp(31) = -0.150$, $p = 0.404$, two-tailed). The correlations were not significantly different from each other (6% cost: $Z = 1.35$, $p = 0.177$; average: $Z = 1.26$, $p = 0.208$). The groups significantly differed in baseline modularity (6% cost: $F(1,66) = 11.156$, $p = 0.001$, $\eta^2p = 0.145$; average: $F(1,66) = 13.367$, $p = 0.001$, $\eta^2p = 0.168$), with higher baseline modularity in the low performers (6% cost, low Gf: $M = 0.434$, $SD = 0.060$, high Gf: $M = 0.384$, $SD = 0.063$; average, low Gf: $M = 0.451$, $SD = 0.054$; high Gf: $M = 0.398$, $SD = 0.064$).

Controlling for FD, in addition to baseline divided attention, revealed a marginally positive correlation in the low divided attention group (Figure 5.3B; 6% cost: $rp(30) = 0.233$, $p = 0.198$, two-tailed; average: $rp(30) = 0.214$, $p = 0.240$, two-tailed) but not in the high divided attention group (6% cost: $rp(65) = -0.147$, $p = 0.422$, two-tailed; average: $rp(65) = -0.148$, $p = 0.418$, two-tailed), although the correlations were not significantly different from each other (6% cost: $Z = 1.517$, $p = 0.129$, two-tailed; average: $Z = 1.443$, $p = 0.149$, two-tailed). The high and low divided attention groups did not differ in mean FD, $F(1,66) = 1.214$, $p = 0.275$, $\eta^2p = 0.018$ (low divided attention: $M = 0.134$, $SD = 0.043$; high divided attention: $M = 0.147$, $SD = 0.052$).

Exploratory analyses: contributions of each module to the relationship between global modularity and divided attention gain. In the WM-REAS group, we examined the contribution of each module to global modularity, which is the sum of contributions from all modules. Here, instead of using the spectral algorithm to maximize modularity, we used 13 pre-defined modules (Power et al., 2011) to compute modularity. This approach yielded modularity measures that were highly correlated with the spectral maximization approach in the WM-REAS group ($r(66) = 0.884$, $p < 0.001$, two-tailed). A repeated measures ANOVA revealed that modularity differed across the 12 modules (excluding “Uncertain” module; $F(3.086,203.693) = 382.950$, $p(GG) < 0.001$, $\eta^2p = 0.853$), suggesting that there may be a differential contribution the modules to training-related gains. For each module, we examined the relationship between modularity and divided attention gain and found a positive correlation in the DMN (Figure 5.4A; $r(66) = 0.271$, $p = 0.026$, two-tailed).

To examine whether this relationship differed in high and low baseline cognition groups (i.e., Gf or divided attention), we next tested for an interaction between module and baseline cognitive ability group (Gf or divided attention). There was a marginally significant interaction between module and Gf group, $F(3.086,203.693) = 2.276$, $p(GG) = 0.079$, $\eta^2p=0.033$. Inspecting the DMN-gain relationship within each Gf group showed that the DMN-gain relationship was driven by the low Gf group (Figure 5.4A; $r(32) = 0.338$, $p = 0.050$, two-tailed; high Gf: $r(32) = 0.024$, $p = 0.894$, two-tailed), although the

correlations were not significantly different from each other ($Z = 1.29$, $p = 0.197$, two-tailed). There was also a significant interaction between module and divided attention group ($F(3.132, 206.688) = 4.162$, $p(\text{GG}) = 0.006$, $\eta^2 p = 0.069$). Similar to the Gf group analyses, the DMN-gain relationship was driven by the low divided attention group (Figure 5.4A; $r(32) = 0.265$, $p = 0.130$, two-tailed; high divided attention group: $r(32) = -0.075$, $p = 0.674$, two-tailed), although the correlations did not significantly differ from each other ($Z = 1.36$, $p = 0.174$, two-tailed).

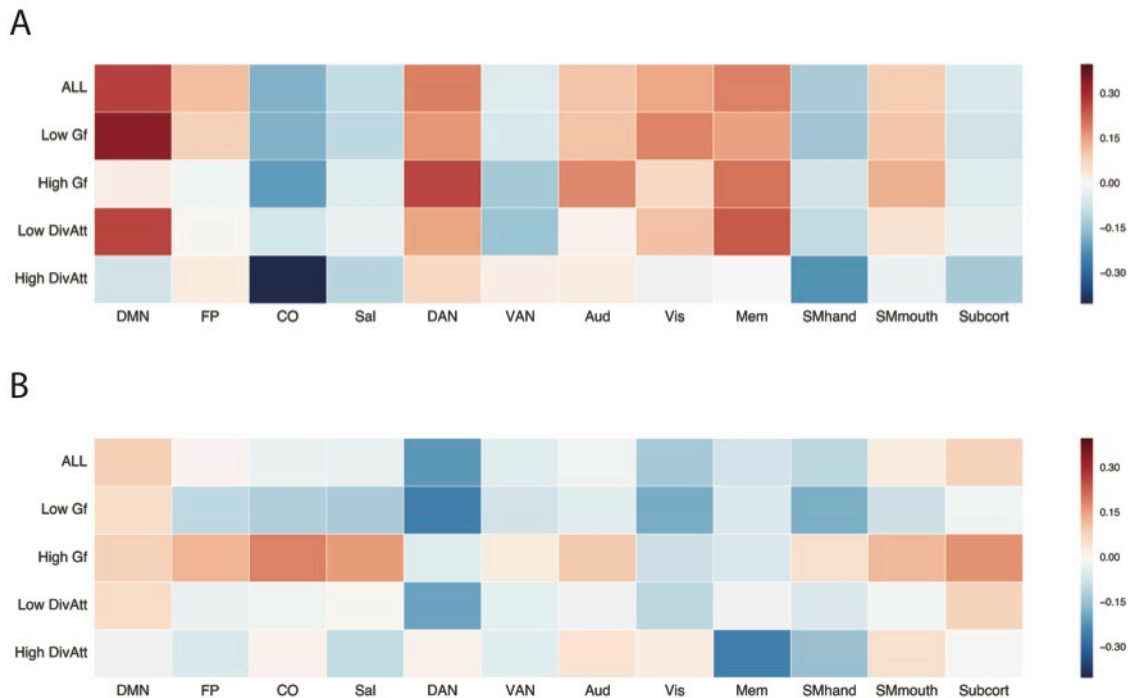


Figure 5.4. A) Module contributions to the relationship between global modularity and divided attention gain. Shown is the correlation between divided attention gain and the degree of within-to-between connectivity (averaged across thresholds) in each module. A high negative correlation between divided attention gain and CO connectivity was observed in the high DivAtt group ($r > 0.5$, $p < 0.001$), but this effect is not discussed since this effect was not present when collapsed across baseline cognitive ability groups, and because of the small training gains observed in the high DivAtt group. B) Shown is the correlation between divided attention gain and connectivity between DMN and all other modules. Gf = fluid intelligence, DivAtt = Divided Attention.

Although DMN modularity was predictive of training gains in the WM-REAS group, ‘modularity’ provides a summary measure of the balance of within-module and all between-module connections. Thus, we next separately examined how connectivity within DMN regions and connectivity between DMN regions and each individual other module ($N = 11$, excluding ‘Uncertain’) was related to divided attention gain. Across the entire WM-REAS group (Figure 5.4B), no significant associations between intra-module or between-module DMN connectivity and divided attention gain were found. Breaking down the analyses by baseline cognitive ability (i.e., Gf and divided attention), revealed

predominantly negative, but not statistically significant, associations between divided attention gain and DMN connectivity in the low Gf and low divided attention groups (Figure 5.4B). Controlling for mean FD in the aforementioned exploratory analyses yielded qualitatively similar results. It is important to note, however, that the correlations in these exploratory analyses are not statistically significant after Bonferroni correction for multiple comparisons across modules.

5.5 Discussion

Here, we demonstrate that higher baseline modularity predicts larger gains in divided attention after training with working memory and reasoning casual games in young adults. This modularity-gain relationship was more prominent in lower-performing individuals and remained significant after controlling for baseline cognitive ability. Critically, this relationship was not present in a control group. These results are consistent with previous findings in smaller samples of TBI patients (Arneemann et al., 2015) and cognitively normal older adults (Gallen et al., Submitted), and more importantly, demonstrate the predictive power of modularity for training intervention outcomes in a young, high-functioning population. On a broader scale, these findings suggest that global network properties can capture unique aspects of brain function that are important in understanding individual differences in learning and neuroplasticity.

5.5.1 Baseline Whole-Brain Modularity and Training-Related Gains

Considering individual differences is important for determining and maximizing intervention effectiveness. Here, we show that modularity provides useful information about training-related cognitive gains beyond those captured by behavioral measures. Specifically, controlling for baseline Gf, which also significantly predicted divided attention gain, still produced a positive relationship between modularity and divided attention gain in the WM-REAS group. Re-examining this relationship within high and low Gf groups showed that the modularity-gain relationship may be driven by low performers, although the correlations between the low and high groups were not significantly different. Further, modularity was not correlated with baseline Gf and was also comparable between Gf groups, suggesting that a relationship baseline between modularity and Gf was not driving the modularity-divided attention gain prediction in the WM-REAS group.

Moreover, although controlling for baseline divided attention, instead of baseline Gf, attenuated the modularity-gain relationship in the whole WM-REAS sample, this was likely due to a very high correlation between divided attention baseline scores and training-related divided attention gain. Re-evaluating this relationship within high and low divided attention groups also showed that the modularity-gain relationship may be driven by low performers. It is important to note, however, that we observed a ceiling effect in high-performing individuals (i.e., high performers tended to not improve in divided attention with training), which may have prevented us from detecting any potential relationships between modularity and cognitive improvement in this group.

Unlike the Gf groups, the divided attention groups significantly differed in baseline modularity, which suggests that modularity may be sensitive to more state-like aspects of cognition, as observed in previous work (Kitzbichler et al., 2011; Stevens et al., 2012). Baseline modularity and baseline divided attention were not significantly correlated, however, which indicates that baseline modularity only partly captures individual differences in baseline divided attention. Together with findings in TBI patients (Arnemann et al., 2015) and healthy older adults (Gallen et al., Submitted), these results suggest that modularity may be a useful biomarker for predicting training outcomes in lower-performing individuals and may be used to better inform interventions, for example, by increasing training intensity or duration in an individual with lower baseline modularity.

Modular brain network organization is thought to be critical for supporting a range of behaviors (Meunier et al., 2009b; Sporns and Betzel, 2015). In particular, modular organization has been hypothesized to support specialized functions, such as vision, through local processing within modules and complex functions, such as working memory, through global processing across modules (Meunier et al., 2009b; 2010). Such a configuration is also thought to allow for a system that is more adaptable to new environments (Kashtan and Alon, 2005; Clune et al., 2013). Previous work has shown that whole-brain modular organization is altered by increasing cognitive demands, such that there is more communication between network modules to support task performance (Kitzbichler et al., 2011; Cohen et al., 2014; Vatansever et al., 2015). In this sense, a more modular organization may also be able to more effectively reconfigure in response to complex task demands, such as those encountered during learning or cognitive training.

In previous functional connectivity studies, individual differences in brain network properties have been shown to be predictive of learning an artificial language (Sheppard et al., 2012) and learning a new motor skill (Bassett et al., 2011). Unlike these studies, however, the intervention in the current study involved more complex training that targeted cognitive control processes rather than a specific skill, similar to previous work from our group that also found a relationship between baseline modularity and training-related gains. Although other studies have examined how individual differences in neural measures predict training-related improvements in more complex tasks, these studies have often focused on a single brain region or small set of brain regions thought to be relevant to the training task (Erickson et al., 2010; Basak et al., 2011; Baldassarre et al., 2012). Our study goes a step further in examining how whole-brain network properties can predict training gains, which may better capture individual variations that support complex task processing. Overall, given that we have found similar relationships between modularity and training gains in previous studies, we speculate that network modularity may be generally useful, across interventions and populations, for characterizing individual differences in neuroplasticity and, consequently, training outcomes.

5.5.2 Baseline DMN Network Properties and Training-Related Gains

In addition to examining whole-brain modularity, we also examined each module's contribution to predicting training gains and found that individuals with greater modularity of DMN regions showed greater divided attention gains. The DMN's involvement is not surprising given the well-documented high connectivity within DMN regions during task-free 'resting' states (Fox et al., 2005; Raichle and Snyder, 2007). Despite being traditionally tied to resting states, DMN regions have also been found to play active roles during task performance. Previous studies examining the reconfiguration of brain network properties due to cognitive demands have reported decreased within-module (Liang et al., 2015) and increased between-module (Anon, 2014) connectivity in DMN regions with increasing n-back load. These findings suggest that the integrity of the DMN is reflected in a highly modular organization during resting states, but that this structure is also capable of adaptive reconfiguration, for example, during learning or training (Chapman et al., 2015).

Finally, we examined whether the connectivity within DMN or connectivity from DMN to other modules was also correlated with training-related gains. We found no significant relationships between divided attention gain and DMN connectivity within or to other modules. The lack of significant correlations may be partly due to statistical power, but it may also suggest that global network measures (i.e., modularity) are more predictive of individual differences in training responses than the connectivity of individual modules. Previous work has also suggested that network modularity is more predictive of behavior (i.e., working memory capacity) than the strength of individual network connections (Stevens et al., 2012). Although we did not find a similar relationship between baseline modularity and baseline cognition in the current study, we also find that modularity significantly accounted for training gain while measures of connectivity for individual modules did not, which may suggest that whole-brain modularity can capture critical aspects of cognitive function. Taken together, these results point to the importance of a baseline, intrinsic structure in enabling complex behavior.

5.5.3 Limitations and Future Directions

Although this study involved a fairly large sample, functional connectivity was assessed during a relatively short resting-state scan. It is possible that more information regarding network structure, particularly in higher performing individuals, could be gleaned from a longer scan period (Birn et al., 2013). Further, a larger sample size would allow for examination of a variety of demographic and lifestyle factors (e.g., income, physical health; (Smith et al., 2015)), that in addition to modularity, could provide more reliable and converging information regarding individual differences in training-related cognitive gains and, potentially, neuroplasticity. Here, we focused on training outcomes assessed immediately after completion of training; ultimately, it will also be important to determine if baseline network properties are predictive of longer-lasting benefits from training as well. It also remains to be seen whether the relationship between modularity and training outcomes is generalizable to other interventions (e.g., exercise) aimed to improve cognitive function (Hillman et al., 2008; Lustig et al., 2009; Voss et al., 2013). Finally, more research is needed to determine the neural changes that accompany the

observed behavioral outcomes and to examine the mechanisms by which pre-intervention modularity supports these neural alterations.

Chapter 6

Conclusions and Future Directions

In this dissertation, I have provided evidence for the importance of the modular organization of functional brain networks in supporting executive control processing and plasticity. First, I have shown that brain networks reconfigure during working memory performance and that this pattern of reconfiguration is altered by attention demands (**Ch. 2**) and aging (**Ch. 3**). Second, I have shown that individual differences in modular organization are predictive of training-related gains in aspects of executive control processing in older (**Ch. 4**) and young (**Ch. 5**) adults.

Several follow-up projects related to the findings in this dissertation are currently in progress or planned. First, the findings in Chapters 4 and 5 as well as those from Arnemann et al. (2015) suggest that network properties can predict training-related gains after cognitive interventions. In addition to cognitive training, there is also evidence that physical exercise plays an important role in cognitive functioning (Colcombe et al., 2004; Erickson et al., 2011; Esteban-Cornejo et al., 2014; Hartanto et al., 2015). We are currently examining the relationship between pre-intervention modularity and training-related gains after physical fitness interventions (e.g., aerobic exercise and walking, stretching, and toning) in a group of older adults. Preliminary analyses have shown that modularity is also predictive of executive control gains after physical fitness interventions, suggesting that network properties may be related to general individual differences in neuroplasticity.

A second line of work that follows from these findings is to examine whether network properties are also predictive of neural alterations that arise from more acute perturbations in addition to longer cognitive and physical fitness interventions. Previous work has shown that individual differences in TMS-induced changes in cerebral blood flow (CBF) are related to changes in resting-state functional connectivity after TMS (Gratton et al., 2014). I plan to examine whether network modularity prior to TMS is predictive of the neural changes associated with TMS (i.e., CBF and functional connectivity). This work would provide further evidence for the role of brain network organization in individual differences in neuroplasticity associated with stimulation.

In addition to these projects, the findings presented in this dissertation raise broad questions for future research. First, the predictive power of brain network modularity could be used to enhance the therapeutic effects of cognitive interventions. Two projects presented in this dissertation (**Ch. 4 and Ch. 5**) were retrospective assessments of the relationship between pre-training network modularity and training outcomes. These results suggest that subjects with lower modularity may require additional or modified training to show training-related cognitive gains. Along this line, subjects with low modularity could be identified prior to training and enrolled in a longer-duration or modified intervention that would enhance training gains. It would therefore be hypothesized that these subjects would ultimately show training-related gains similar to subjects with high modularity who participated in a standard intervention.

Second, a multimodal approach using fMRI and EEG could allow for further characterization of the mechanisms underlying individual differences in modularity. As in several of the analyses in this dissertation, investigation of fMRI-derived networks typically entails the examination of 'static' network organization assessed over an entire scanning run. The brain is a dynamic system (Deco et al., 2011) and there is evidence that the functional connectivity of brain networks reconfigures on shorter timescales (Hutchison et al., 2013) than can typically be assessed using fMRI. An important line of future research would be to combine higher temporal resolution neuroimaging (e.g., EEG) with fMRI to examine how fluctuations in EEG-derived connectivity over short timescales are related to 'static' fMRI network organization. It is possible that subjects with more modular fMRI-derived networks are more temporally stable (i.e., show fewer fluctuations as assessed with EEG), while those with lower modularity show have less stable connectivity over time.

These future directions could further our understanding of the role of modular brain network organization in supporting executive control functions as well as the neural mechanisms underlying individual differences in network modularity.

References

- Alavash M, Doebler P, Holling H, Thiel CM, Giessing C (2015) Is functional integration of resting state brain networks an unspecific biomarker for working memory performance? *NeuroImage* 108:182–193.
- Alexander-Bloch AF, Gogtay N, Meunier D, Birn R, Clasen L, Lalonde F, Lenroot R, Giedd J, Bullmore ET (2010) Disrupted Modularity and Local Connectivity of Brain Functional Networks in Childhood-Onset Schizophrenia. *Front Syst Neurosci* 4:1–16.
- Alexander-Bloch AF, Vértes PE, Stidd R, Lalonde F, Clasen L, Rapoport J, Giedd J, Bullmore ET, Gogtay N (2012) The Anatomical Distance of Functional Connections Predicts Brain Network Topology in Health and Schizophrenia. *Cerebral Cortex* 23:127–138.
- Andrews-Hanna JR, Snyder AZ, Vincent JL, Lustig C, Head D, Raichle ME, Buckner RL (2007) Disruption of Large-Scale Brain Systems in Advanced Aging. *Neuron* 56:924–935.
- Arnemann KL, Chen A, Novakovic-Agopian T, Gratton C, Nomura EM, D'Esposito M (2015) Functional brain network modularity predicts response to cognitive training after brain injury. *Neurology*.
- Au J, Sheehan E, Tsai N, Duncan GJ, Buschkuehl M, Jaeggi SM (2014) Improving fluid intelligence with training on working memory: a meta-analysis. *Psychon Bull Rev* 22:366–377.
- Avants BB, Tustison NJ, Song G, Cook PA, Klein A, Gee JC (2011) A reproducible evaluation of ANTs similarity metric performance in brain image registration. *NeuroImage* 54:2033–2044.
- Baldassarre A, Lewis CM, Committeri G, Snyder AZ, Romani GL, Corbetta M (2012) Individual variability in functional connectivity predicts performance of a perceptual task. *Proceedings of the National Academy of Sciences* 109:3516–3521.
- Ballesteros S, Kraft E, Santana S, Tziraki C (2015) Maintaining older brain functionality: A targeted review. *Neuroscience and Biobehavioral Reviews* 55:453–477.
- Baniqued PL, Kranz MB, Voss MW, Lee H, Cosman JD, Severson J, Kramer AF (2014) Cognitive training with casual video games: points to consider. *Frontiers in Psychology* 4:1–19.
- Barceló F, Suwazono S, Knight RT (2000) Prefrontal modulation of visual processing in humans. *Nature Neuroscience* 3:399–403.
- Basak C, Voss MW, Erickson KI, Boot WR, Kramer AF (2011) Regional differences in brain volume predict the acquisition of skill in a complex real-time strategy

- videogame. *Brain and Cognition* 76:407–414.
- Bassett DS, Wymbs NF, Porter MA, Mucha PJ, Carlson JM, Grafton ST (2011) Dynamic reconfiguration of human brain networks during learning. *Proceedings of the National Academy of Sciences* 108:7641–7646.
- Behzadi Y, Restom K, Liao J, Liu TT (2007) A component based noise correction method (CompCor) for BOLD and perfusion based fMRI. *NeuroImage* 37:90–101.
- Bennett G, Seashore H, Wesman A (1997). *Differential Aptitude Test*. San Antonio, TX: The Psychological Corporation.
- Bennett IJ, Madden DJ (2014) Disconnected aging: cerebral white matter integrity and age-related differences in cognition. *Neuroscience* 276:187–205.
- Betzler RF, Byrge L, He Y, Goñi J, Zuo X-N, Sporns O (2014) Changes in structural and functional connectivity among resting-state networks across the human lifespan. *NeuroImage* 102:345–357.
- Bherer L (2015) Cognitive plasticity in older adults: effects of cognitive training and physical exercise Bigand E, Tillmann B, Peretz I, Zatorre RJ, Lopez L, Majno M, eds. *Annals of the New York Academy of Sciences* 1337:1–6.
- Binder D, O'Connor C, Levine B (2008) *Brain Health Workshop*. Toronto, ON: Rotman Research Institute, Baycrest Center.
- Birn RM, Molloy EK, Patriat R, Parker T, Meier TB, Kirk GR, Nair VA, Meyerand ME, Prabhakaran V (2013) The effect of scan length on the reliability of resting-state fMRI connectivity estimates. *NeuroImage* 83:550–558.
- Boot WR, Kramer AF (2014) The Brain-Games Conundrum: Does Cognitive Training Really Sharpen the Mind? *Cerebrum: the Dana Forum on Brain Science* 2014.
- Boot WR, Kramer AF, Simons DJ, Fabiani M, Gratton G (2008) The effects of video game playing on attention, memory, and executive control. *Acta Psychologica* 129:387–398.
- Braun U, Schäfer A, Walter H, Erk S, Romanczuk-Seiferth N, Haddad L, Schweiger JI, Grimm O, Heinz A, Tost H, Meyer-Lindenberg A, Bassett DS (2015) Dynamic reconfiguration of frontal brain networks during executive cognition in humans. *Proceedings of the National Academy of Sciences*:1–6.
- Brehmer Y, Rieckmann A, Bellander M, Westerberg H, Fischer H, Bäckman L (2011) Neural correlates of training-related working-memory gains in old age. *NeuroImage* 58:1110–1120.
- Bullmore E, Sporns O (2009) Complex brain networks: graph theoretical analysis of structural and functional systems. *Nat Rev Neurosci* 10:186–198.

- Buschman TJ, Kastner S (2015) From Behavior to Neural Dynamics: An Integrated Theory of Attention. *Neuron* 88:127–144.
- Cao W, Cao X, Hou C, Li T, Cheng Y, Jiang L, Luo C, Li C, Yao D (2016) Effects of Cognitive Training on Resting-State Functional Connectivity of Default Mode, Salience, and Central Executive Networks. *Front Ag Neurosci* 8:1–11.
- Chadick JZ, Gazzaley A (2011) Differential coupling of visual cortex with default or frontal- parietal network based on goals. *Nature Neuroscience* 14:830–832.
- Chan MY, Park DC, Savalia NK, Petersen SE, Wig GS (2014) Decreased segregation of brain systems across the healthy adult lifespan. *Proceedings of the National Academy of Sciences*:E4997–E5006.
- Chao LL, Knight RT (1998) Contribution of human prefrontal cortex to delay performance. *Journal of Cognitive Neuroscience* 10:167–177.
- Chapman SB, Aslan S, Spence JS, Hart JJ, Bartz EK, Didehbani N, Keebler MW, Gardner CM, Strain JF, DeFina LF, Lu H (2015) Neural Mechanisms of Brain Plasticity with Complex Cognitive Training in Healthy Seniors. *Cerebral Cortex* 25:396–405.
- Chen AJW, Novakovic-Agopian T, Nycum TJ, Song S, Turner GR, Hills NK, Rome S, Abrams GM, D'Esposito M (2011a) Training of goal-directed attention regulation enhances control over neural processing for individuals with brain injury. *Brain* 134:1541–1554.
- Chen ZJ, He Y, Rosa-Neto P, Germann J, Evans AC (2008) Revealing Modular Architecture of Human Brain Structural Networks by Using Cortical Thickness from MRI. *Cerebral Cortex* 18:2374–2381.
- Chen ZJ, He Y, Rosa-Neto P, Gong G, Evans AC (2011b) Age-related alterations in the modular organization of structural cortical network by using cortical thickness from MRI. *NeuroImage* 56:235–245.
- Clapp WC, Rubens MT, Sabharwal J, Gazzaley A (2011) Deficit in switching between functional brain networks underlies the impact of multitasking on working memory in older adults. *Proceedings of the National Academy of Sciences* 108:7212–7217.
- Clune J, Mouret J-B, Lipson H (2013) The evolutionary origins of modularity. *Proc R Soc B* 280:1–9.
- Cohen J, Cohen P, West SG, Aiken LS (2003) *Applied Multiple Regression/ Correlation Analysis for the Behavioral Sciences*. Erlbaum, Mahwah, NJ.
- Cohen JR, Gallen CL, Jacobs EG, Lee TG (2014) Quantifying the Reconfiguration of Intrinsic Networks during Working Memory. *PLoS ONE* 9:1–8.

- Colcombe SJ, Kramer AF, Erickson KI, Scalf P, McAuley E, Cohen NJ, Webb A, Jerome GJ, Marquez DX, Elavsky S (2004) Cardiovascular fitness, cortical plasticity, and aging. *Proceedings of the National Academy of Sciences* 101:3316–3321.
- Cole MW, Bassett DS, Power JD, Braver TS, Petersen SE (2014) Intrinsic and Task-Evoked Network Architectures of the Human Brain. *Neuron* 83:238–251.
- Cole MW, Reynolds JR, Power JD, Repovs G, Anticevic A, Braver TS (2013) Multi-task connectivity reveals flexible hubs for adaptive task control. *Nature Publishing Group* 16:1348–1355.
- Crone EA, Wendelken C, van Leijenhorst L, Honomichl RD, Christoff K, Bunge SA (2009) Neurocognitive development of relational reasoning. *Developmental Science* 12:55–66.
- D'Esposito M, Deouell LY, Gazzaley A (2003) Alterations in the BOLD fMRI signal with ageing and disease: a challenge for neuroimaging. *Nat Rev Neurosci* 4:863–872.
- Damoiseaux JS, Beckmann CF, Arigita EJS, Barkhof F, Scheltens P, Stam CJ, Smith SM, Rombouts SARB (2008) Reduced resting-state brain activity in the “default network” in normal aging. *Cerebral Cortex* 18:1856–1864.
- Danon L, Díaz-Guilera A, Duch J, Arenas A (2005) Comparing community structure identification. *Journal of Statistical Mechanics: Theory and Experiment* 2005:P09008.
- Deco G, Jirsa VK, McIntosh AR (2011) Emerging concepts for the dynamical organization of resting-state activity in the brain. *Nat Rev Neurosci* 12:43–56.
- Dehaene S, Kerszberg M, Changeux JP (1998) A neuronal model of a global workspace in effortful cognitive tasks. *Proceedings of the National Academy of Sciences* 95:14529–14534.
- Dougherty MR, Hamovitz T, Tidwell JW (2016) Reevaluating the effectiveness of n-back training on transfer through the Bayesian lens: Support for the null. *Psychon Bull Rev* 23:306–316.
- Ekstrom RB, French JW, Harman HH (1976) Manual for kit of factor-referenced cognitive tests. Educational Testing Service, Princeton NJ.
- Erickson KI, Boot WR, Basak C, Neider MB, Prakash RS, Voss MW, Graybiel AM, Simons DJ, Fabiani M, Gratton G, Kramer AF (2010) Striatal Volume Predicts Level of Video Game Skill Acquisition. *Cerebral Cortex* 20:2522–2530.
- Erickson KI, Voss MW, Prakash RS, Basak C, Szabo A, Chaddock L, Kim JS, Heo S, Alves H, White SM (2011) Exercise training increases size of hippocampus and improves memory. *Proceedings of the National Academy of Sciences* 108:3017–

3022.

- Esteban-Cornejo I, Gómez-Martínez S, Tejero-González CM, Castillo R, Lanza-Saiz R, Vicente-Rodríguez G, Marcos A, Martínez-Gómez D (2014) Characteristics of extracurricular physical activity and cognitive performance in adolescents. The AVENA study. *Journal of Sports Sciences* 32:1596–1603.
- Ferreira LK, Busatto GF (2013) Resting-state functional connectivity in normal brain aging. *Neuroscience and Biobehavioral Reviews* 37:384–400.
- Fornito A, Zalesky A, Breakspear M (2015) The connectomics of brain disorders. *Nat Rev Neurosci* 16:159–172.
- Fox MD, Snyder AZ, Vincent JL, Corbetta M, Van Essen DC, Raichle ME (2005) The human brain is intrinsically organized into dynamic, anticorrelated functional networks. *Proceedings of the National Academy of Sciences* 102:9673–9678.
- Friston KJ, Williams S, Howard R, Frackowiak RSJ, Turner R (1996) Movement-Related effects in fMRI time-series. *Magn Reson Med* 35:346–355.
- Funahashi S, Bruce CJ, Goldman-Rakic PS (1993a) Dorsolateral prefrontal lesions and oculomotor delayed-response performance: evidence for mnemonic “scotomas.” *The Journal of Neuroscience* 13:1479–1497.
- Funahashi S, Chafee MV, Goldman-Rakic PS (1993b) Prefrontal neuronal activity in rhesus monkeys performing a delayed anti-saccade task. *Nature* 365:753–756.
- Fuster JM, Bauer RH, Jervey JP (1985) Functional interactions between inferotemporal and prefrontal cortex in a cognitive task. *Brain Research* 330:299–307.
- Gallen CL, Turner GR, Adnan A, D'Esposito M (2016) Reconfiguration of brain network architecture to support executive control in aging. *Neurobiology of Aging* 44:42–52.
- Gazzaley A (2011) Influence of early attentional modulation on working memory. *Neuropsychologia* 49:1410–1424.
- Gazzaley A, Cooney JW, McEvoy K, Knight RT, D'Esposito M (2005a) Top-down Enhancement and Suppression of the Magnitude and Speed of Neural Activity. *Journal of Cognitive Neuroscience* 17:507–517.
- Gazzaley A, Cooney JW, Rissman J, D'Esposito M (2005b) Top-down suppression deficit underlies working memory impairment in normal aging. *Nature Neuroscience* 8:1298–1300.
- Gazzaley A, Nobre AC (2012) Top-down modulation: bridging selective attention and working memory. *Trends in Cognitive Sciences* 16:128–134.
- Gazzaley A, Rissman J, Cooney J, Rutman A, Seibert T, Clapp W, D'Esposito M (2007)

- Functional Interactions between Prefrontal and Visual Association Cortex Contribute to Top-Down Modulation of Visual Processing. *Cerebral Cortex* 17:i125–i135.
- Geerligs L, Renken RJ, Saliassi E, Maurits NM, Lorist MM (2014a) A Brain-Wide Study of Age-Related Changes in Functional Connectivity. *Cerebral Cortex*:1–13.
- Geerligs L, Saliassi E, Renken RJ, Maurits NM, Lorist MM (2014b) Flexible connectivity in the aging brain revealed by task modulations. *Hum Brain Mapp* 35:3788–3804.
- Godwin D, Barry RL, Marois R (2015) Breakdown of the brain's functional network modularity with awareness. *Proceedings of the National Academy of Sciences* 112:3799–3804.
- Grady C (2012) The cognitive neuroscience of ageing. *Nat Rev Neurosci* 13:491–505.
- Grady CL (2008) Cognitive Neuroscience of Aging. *Annals of the New York Academy of Sciences* 1124:127–144.
- Gratton C, Lee TG, Nomura EM, D'Esposito M (2014) Perfusion MRI Indexes Variability in the Functional Brain Effects of Theta-Burst Transcranial Magnetic Stimulation. *PLoS ONE* 9:e101430.
- Gratton C, Nomura EM, Pérez F, D'Esposito M (2012) Focal brain lesions to critical locations cause widespread disruption of the modular organization of the brain. *Journal of Cognitive Neuroscience* 24:1275–1285.
- Guimera R, Amaral LAN (2005) Functional cartography of complex metabolic networks. *Nature* 433:895–900.
- Guimera R, Sales-Pardo M, Amaral LAN (2006) Classes of complex networks defined by role-to-role connectivity profiles. *Nat Phys* 3:63–69.
- Hartanto TA, Krafft CE, Iosif AM, Schweitzer JB (2015) A trial-by-trial analysis reveals more intense physical activity is associated with better cognitive control performance in attention-deficit/hyperactivity disorder. *Child Neuropsychology* 22:618–626.
- Hillman CH, Erickson KI, Kramer AF (2008) Be smart, exercise your heart: exercise effects on brain and cognition. *Nat Rev Neurosci* 9:58–65.
- Hutchison RM, Womelsdorf T, Allen EA, Bandettini PA, Calhoun VD, Corbetta M, Penna SD, Duyn JH, Glover GH, Gonzalez-Castillo J, Handwerker DA, Keilholz S, Kiviniemi V, Leopold DA, de Pasquale F, Sporns O, Walter M, Chang C (2013) Dynamic functional connectivity: promise, issues, and interpretations. *NeuroImage* 80:360–378.
- Karbach J, Verhaeghen P (2014) Making Working Memory Work: A Meta-Analysis of Executive-Control and Working Memory Training in Older Adults. *Psychological*

Science 25:2027–2037.

Kashtan N, Alon U (2005) Spontaneous evolution of modularity and network motifs. *Proceedings of the National Academy of Sciences* 102:13773–13778.

Kelly ME, Loughrey D, Lawlor BA, Robertson IH, Walsh C, Brennan S (2014) Ageing Research Reviews. *Ageing Research Reviews* 15:28–43.

Kirkpatrick S, Jr DG, Vecchi MP (1983) Optimization by simulated annealing. *Science* 220:671–680.

Kitzbichler MG, Henson RNA, Smith ML, Nathan PJ, Bullmore ET (2011) Cognitive Effort Drives Workspace Configuration of Human Brain Functional Networks. *Journal of Neuroscience* 31:8259–8270.

Knight RT, Staines WR, Swick D, Chao LL (1999) Prefrontal cortex regulates inhibition and excitation in distributed neural networks. *Acta Psychologica* 101:159–178.

Landman BA, Huang AJ, Gifford A, Vikram DS, Lim I, Farrell J, Bogovic JA, Hua J, Chen M, Jarso S, Smith SA, Joel S, Mori S, Pekar JJ, Barker PB, Prince JL, van Zijl PC (2011) Multi-parametric neuroimaging reproducibility: A 3-T resource study. *NeuroImage* 54:2854–2866.

Lee TG, D'Esposito M (2012) The Dynamic Nature of Top-Down Signals Originating from Prefrontal Cortex: A Combined fMRI-TMS Study. *Journal of Neuroscience* 32:15458–15466.

Liang X, Zou Q, He Y, Yang Y (2015) Topologically Reorganized Connectivity Architecture of Default-Mode, Executive-Control, and Salience Networks across Working Memory Task Loads. *Cerebral Cortex*:1–11.

Lustig C, Shah P, Seidler R, Reuter-Lorenz PA (2009) Aging, Training, and the Brain: A Review and Future Directions. *Neuropsychol Rev* 19:504–522.

Makris N, Kennedy DN, McInerney S, Sorensen AG, Wang R, Caviness VS, Pandya DN (2005) Segmentation of Subcomponents within the Superior Longitudinal Fascicle in Humans: A Quantitative, In Vivo, DT-MRI Study. *Cerebral Cortex* 15:854–869.

Mathewson KE, Basak C, Maclin EL, Low KA, Boot WR, Kramer AF, Fabiani M, Gratton G (2012) Different slopes for different folks: Alpha and delta EEG power predict subsequent video game learning rate and improvements in cognitive control tasks. *Psychophysiol* 49:1558–1570.

Mattar MG, Cole MW, Thompson-Schill SL, Bassett DS (2015) A Functional Cartography of Cognitive Systems. *PLoS Comput Biol* 11:e1004533.

Mattay VS, Fera F, Tessitore A, Hariri AR, Berman KF, Das S, Meyer-Lindenberg A,

- Goldberg TE, Callicott JH, Weinberger DR (2006) Neurophysiological correlates of age-related changes in working memory capacity. *Neuroscience Letters* 392:32–37.
- Medaglia JD, Lynall M-E, Bassett DS (2015) Cognitive Network Neuroscience. *Journal of Cognitive Neuroscience* 27:1471–1491.
- Melby-Lervåg M, Hulme C (2013) Is working memory training effective? A meta-analytic review. *Developmental Psychology* 49:270–291.
- Meunier D, Achard S, Morcom A, Bullmore E (2009a) Age-related changes in modular organization of human brain functional networks. *NeuroImage* 44:715–723.
- Meunier D, Lambiotte R, Bullmore ET (2010) Modular and Hierarchically Modular Organization of Brain Networks. *Front Neurosci* 4:1–11.
- Meunier D, Lambiotte R, Fornito A, Ersche KD, Bullmore ET (2009b) Hierarchical modularity in human brain functional networks. *Front Neuroinform* 3:1–12.
- Miller BT, D'Esposito M (2005) Searching for “the Top” in Top-Down Control. *Neuron* 48:535–538.
- Mori S, Oishi K, Jiang H, Jiang L, Li X, Akhter K, Hua K, Faria AV, Mahmood A, Woods R, Toga AW, Pike GB, Neto PR, Evans A, Zhang J, Huang H, Miller MI, van Zijl P, Mazziotta J (2008) Stereotaxic white matter atlas based on diffusion tensor imaging in an ICBM template. *NeuroImage* 40:570–582.
- Myers L, Sirois MJ (2006) Spearman Correlation Coefficients, Differences between. *Encyclopedia of Statistical Sciences*. John Wiley and Sons, New York.
- Newman ME (2006) Modularity and community structure in networks. *Proceedings of the National Academy of Sciences* 103:8577–8582.
- Newman ME, Girvan M (2004) Finding and evaluating community structure in networks. *Phys Rev E* 69:026113.
- Nikolaidis A, Baniqued PL, Kranz MB, Scavuzzo CJ, Barbey AK, Kramer AF, Larsen RJ (2016) Multivariate Associations of Fluid Intelligence and NAA. *Cerebral Cortex*:1–10.
- Onoda K, Yamaguchi S (2013) Small-worldness and modularity of the resting-state functional brain network decrease with aging. *Neuroscience Letters* 556:104–108.
- Park DC, Lautenschlager G, Hedden T, Davidson NS, Smith AD, Smith PK (2002) Models of visuospatial and verbal memory across the adult life span. *Psychology and Aging* 17:299–320.
- Power JD, Barnes KA, Snyder AZ, Schlaggar BL, Petersen SE (2012) Spurious but systematic correlations in functional connectivity MRI networks arise from subject

- motion. *NeuroImage* 59:2142–2154.
- Power JD, Cohen AL, Nelson SM, Wig GS, Barnes KA, Church JA, Vogel AC, Laumann TO, Miezin FM, Schlaggar BL, Petersen SE (2011) Functional Network Organization of the Human Brain. *Neuron* 72:665–678.
- Power JD, Mitra A, Laumann TO, Snyder AZ, Schlaggar BL, Petersen SE (2013) Methods to detect, characterize, and remove motion artifact in resting state fMRI. *NeuroImage* 84:1–22.
- Raichle ME, Snyder AZ (2007) A default mode of brain function: A brief history of an evolving idea. *NeuroImage* 37:1083–1090.
- Ravens J (1962) *Advanced progressive matrices*. London: HK Lewis.
- Redick TS, Shipstead Z, Harrison TL, Hicks KL, Fried DE, Hambrick DZ, Kane MJ, Engle RW (2013) No evidence of intelligence improvement after working memory training: A randomized, placebo-controlled study. *Journal of Experimental Psychology: General* 142:359–379.
- Reitan RM (1958) *Trail making manual for administration, scoring, and interpretation*. Department of Neurology, Section of Neuropsychology, Indiana University Medical Center, Indianapolis.
- Reuter-Lorenz PA, Cappell KA (2008) Neurocognitive Aging and the Compensation Hypothesis. *Current Directions in Psychol Sci* 17:177–182.
- Rissman J, Gazzaley A, D'Esposito M (2004) Measuring functional connectivity during distinct stages of a cognitive task. *NeuroImage* 23:752–763.
- Rorden C, Bonilha L, Nichols TE (2007) Rank-order versus mean based statistics for neuroimaging. *NeuroImage* 35:1531–1537.
- Russo R, Herrmann HJ, de Arcangelis L (2014) Brain modularity controls the critical behavior of spontaneous activity. *arXiv*.
- Sadaghiani S, Poline J-B, Kleinschmidt A, D'Esposito M (2015) Ongoing dynamics in large-scale functional connectivity predict perception. *Proceedings of the National Academy of Sciences* 112:8463–8468.
- Satterthwaite TD, Elliott MA, Gerraty RT, Ruparel K, Loughhead J, Calkins ME, Eickhoff SB, Hakonarson H, Gur RC, Gur RE, Wolf DH (2013) An improved framework for confound regression and filtering for control of motion artifact in the preprocessing of resting-state functional connectivity data. *NeuroImage* 64:240–256.
- Satterthwaite TD, Wolf DH, Loughhead J, Ruparel K, Elliott MA, Hakonarson H, Gur RC, Gur RE (2012) Impact of in-scanner head motion on multiple measures of functional connectivity: Relevance for studies of neurodevelopment in youth. *NeuroImage*

60:623–632.

Shapiro KL, Raymond JE, Arnell KM (1997) The attentional blink. *Trends in Cognitive Sciences* 1:291–296.

Shattuck DW, Mirza M, Adisetiyo V, Hojatkashani C, Salamon G, Narr KL, Poldrack RA, Bilder RM, Toga AW (2008) Construction of a 3D probabilistic atlas of human cortical structures. *NeuroImage* 39:1064–1080.

Sheppard JP, Wang J-P, Wong PC (2012) Large-scale cortical network properties predict future sound-to-word learning success. *Journal of Cognitive Neuroscience* 24:1087–1103.

Smith SM (2002) Fast robust automated brain extraction. *Hum Brain Mapp* 17:143–155.

Smith SM, Jenkinson M, Johansen-Berg H, Rueckert D, Nichols TE, Mackay CE, Watkins KE, Ciccarelli O, Cader MZ, Matthews PM, Behrens TEJ (2006) Tract-based spatial statistics: Voxelwise analysis of multi-subject diffusion data. *NeuroImage* 31:1487–1505.

Smith SM, Jenkinson M, Woolrich MW, Beckmann CF, Behrens TEJ, Johansen-Berg H, Bannister PR, De Luca M, Drobnjak I, Flitney DE, Niazy RK, Saunders J, Vickers J, Zhang Y, De Stefano N, Brady JM, Matthews PM (2004) Advances in functional and structural MR image analysis and implementation as FSL. *NeuroImage* 23:S208–S219.

Smith SM, Nichols TE, Vidaurre D, Winkler AM, Behrens TEJ, Glasser MF, Ugurbil K, Barch DM, Van Essen DC, Miller KL (2015) A positive-negative mode of population covariation links brain connectivity, demographics and behavior. *Nature Neuroscience* 18:1565–1567.

Sporns O, Betzel RF (2015) Modular Brain Networks. *Annu Rev Psychol* 67:1–28.

Spreng RN, Wojtowicz M, Grady CL (2010) Reliable differences in brain activity between young and old adults: A quantitative meta-analysis across multiple cognitive domains. *Neuroscience and Biobehavioral Reviews* 34:1178–1194.

Stanley ML, Dagenbach D, Lyday RG, Burdette JH, Laurienti PJ (2014) Changes in global and regional modularity associated with increasing working memory load. *Frontiers in Human Neuroscience* 8:1–14.

Stevens AA, Tappon SC, Garg A, Fair DA (2012) Functional Brain Network Modularity Captures Inter- and Intra-Individual Variation in Working Memory Capacity. *PLoS ONE* 7:1–10.

Stevens WD, Buckner RL, Schacter DL (2010) Correlated Low-Frequency BOLD Fluctuations in the Resting Human Brain Are Modulated by Recent Experience in Category-Preferential Visual Regions. *Cerebral Cortex* 20:1997–2006.

- Strobach T, Frensch PA, Schubert T (2012) Video game practice optimizes executive control skills in dual-task and task switching situations. *Acta Psychologica* 140:13–24.
- Tukey JW (1962) The future of data analysis. *The Annals of Mathematical Statistics* 33:1–67.
- Turner GR, Spreng RN (2012) Executive functions and neurocognitive aging: dissociable patterns of brain activity. *Neurobiology of Aging* 33:826.e1–826.e13.
- Turner GR, Spreng RN (2015) Prefrontal Engagement and Reduced Default Network Suppression Co-occur and Are Dynamically Coupled in Older Adults: The Default–Executive Coupling Hypothesis of Aging. *Journal of Cognitive Neuroscience* 27:2462–2476.
- Tzourio-Mazoyer N, Landeau B, Papathanassiou D, Crivello F, Etard O, Delcroix N, Mazoyer B, Joliot M (2002) Automated Anatomical Labeling of Activations in SPM Using a Macroscopic Anatomical Parcellation of the MNI MRI Single-Subject Brain. *NeuroImage* 15:273–289.
- Van Dijk KRA, Sabuncu MR, Buckner RL (2012) The influence of head motion on intrinsic functional connectivity MRI. *NeuroImage* 59:431–438.
- Vas AK, Chapman SB, Cook LG, Elliott AC, Keebler M (2011) Higher-Order Reasoning Training Years After Traumatic Brain Injury in Adults. *Journal of Head Trauma Rehabilitation* 26:224–239.
- Vatansver D, Menon DK, Manktelow AE, Sahakian BJ, Stamatakis EA (2015) Default Mode Dynamics for Global Functional Integration. *Journal of Neuroscience* 35:15254–15262.
- Verghese A, Garner KG, Mattingley JB, Dux PE (2016) Prefrontal Cortex Structure Predicts Training-Induced Improvements in Multitasking Performance. *Journal of Neuroscience* 36:2638–2645.
- Vo LTK, Walther DB, Kramer AF, Erickson KI, Boot WR, Voss MW, Prakash RS, Lee H, Fabiani M, Gratton G, Simons DJ, Sutton BP, Wang MY (2011) Predicting Individuals' Learning Success from Patterns of Pre-Learning MRI Activity. *PLoS ONE* 6:1–9.
- Voss MW, Vivar C, Kramer AF, van Praag H (2013) Bridging animal and human models of exercise-induced brain plasticity. *Trends in Cognitive Sciences* 17:525–544.
- Wen X, Zhang D, Liang B, Zhang R, Wang Z, Wang J, Liu M, Huang R (2015) Reconfiguration of the Brain Functional Network Associated with Visual Task Demands. *PLoS ONE* 10:1–16.
- Wilcox RR (2005) *Robust Testing Procedures*. Chichester, UK: John Wiley & Sons, Ltd.

Woolrich MW, Jbabdi S, Patenaude B, Chappell M, Makni S, Behrens T, Beckmann C, Jenkinson M, Smith SM (2009) Bayesian analysis of neuroimaging data in FSL. *NeuroImage* 45:S173–S186.

Zachary RA, Shipley WC (1986) Shipley institute of living scale: Revised manual. WPS, Western Psychological Services.

Zhang Y, Brady JM, Smith SM (2001) An HMRF-EM Algorithm for Partial Volume Segmentation of Brain MRI FMRIB Technical Report TR01YZ1. Technical report, Oxford Centre for Functional Magnetic Resonance Imaging of the Brain.